Carbon TerraVault V
Class VI Permit Application
Narrative Report

Submitted to:

U.S. Environmental Protection Agency Region 9
San Francisco, CA

Prepared by:

27200 Tourney Road, Suite 200
Santa Clarita, CA 91355
(888) 848-4754

ATTACHMENT A: NARRATIVE REPORT
[40 CFR 146.82(a)]
CTV V

Table of Contents

List of Attachments

List of Appendices

Document Version History

Version	Submission Date	File Name	Description of Change
1	7/12/2023	Att A – CTV V Narr_v1	Original Submission
2	9/12/2023	Att A – CTV V Narr_v2	Update Figure 2.2-11 and added references tables for Figure 2.2-11 in response to EPA comment letter dated 8/30/2023.
3	7/11/2023	Att A – CTV V Narr_v3	Updated in response to EPA comment letter dated 05/24/2024.
4	5/29/2025	Att A – CTV V Narr_v4	Updated in response to EPA comment letter dated 02/28/2025.

1. Project Background and Contact Information

Carbon TerraVault Holdings LLC (CTV), a wholly owned subsidiary of California Resources Corporation (CRC), proposes to construct and operate six carbon dioxide (CO_2) geologic sequestration wells at the project area located in San Joaquin County, California. This application was prepared in accordance with the U.S. Environmental Protection Agency's (EPA's) Class VI regulations in Title 40 of the Code of Federal Regulations (40 CFR 146.81). CTV is not requesting an injection depth waiver or aquifer exemption expansion.

CTV will obtain the required authorizations from applicable local and state agencies, including the associated environmental review process under the California Environmental Quality Act. **Appendix 1** outlines potential local, state, and federal permits and authorizations. The project wells and facilities will not be located on Indian Lands. Federal act considerations and additional consultation, which includes the Endangered Species Act, the National Historic Preservation Act and consultations with Tribes in the Area of Review (AoR), are presented in **Appendix 2**: Applicable Federal Acts and Consultation.

CTV forecasts the potential CO_2 stored in the Mokelumne River Formation (Upper Injection Zone) at 0.41 million metric tonnes (MMT) annually on average for 25 years for a total of 10.3 MMT, and in the Starkey Formation (Lower Injection Zone) at 0.43 MMT annually on average for 15 years for a total of 6.4 MMT. Taking both injection zones, the expected total storage for the site is up to 16.7 MMT at an average injection rate of up to 0.67 million metric tonnes per annum (MMTPA).

CTV is planning to construct a carbon capture and sequestration "hub" project (i.e., a project that collects CO_2 from multiple sources over time and injects the CO_2 stream(s) via Class VI Underground Injection Control (UIC)-permitted injection well(s)). Therefore, CTV is currently considering multiple sources of anthropogenic CO_2 for the project. Potential sources include capture from existing and potential future industrial sources in the Sacramento Valley area, as well as Direct Air Capture (DAC).

The Carbon TerraVault V (CTV V) storage site is located in the Sacramento Valley, nine miles east of the Rio Vista Gas Field and four miles northwest of Stockton, California (**Figure 2.1-1**) within the southern Sacramento Basin. The project is comprised of six injectors (three into the Mokelumne and three into the Starkey Formation), surface facilities, and monitoring wells. This supporting documentation applies to the six injection wells.

CTV will actively communicate project details and submitted regulatory documents to County and State agencies:

- California Geologic Energy Management Division (CalGEM)
  Senior Oil and Gas Engineer – Erwin Sison
  715 P Street, MS 1804
  Sacramento, CA 95814
  (916) 203-7734

- CA Assembly District 13
  Assemblyman Carlos Villapudua
  31 East Channel Street, Suite 306
  Stockton, CA 95202
  (209) 948-7479
- San Joaquin County
  District 3 Supervisor –Tom Patti
  (209) 468-3113
  tpatti@sjgov.org
- San Joaquin County Community Development
  Director – David Kwong
  1810 East Hazelton Avenue
  Stockton, CA 95205
  (209) 468-3121
- San Joaquin Council of Governments
  Executive Director – Diane Nguyen
  555 East Weber Avenue
  Stockton, CA 95202
  (209) 235-0600
- Region 9 Environmental Protection Agency
  75 Hawthorne Street
  San Francisco, CA 94105
  (415) 947-8000

2. Site Characterization

2.1 Regional Geology, Hydrogeology, and Local Structural Geology [40 CFR 146.82(a)(3)(vi)]

2.1.1 Field History

The CTV V storage site is located nine miles east of major gas field Rio Vista in the depleted King Island gas field ("the Field"). Two smaller gas fields lie closer to the project area: East Islands Gas to the north and Rindge Tract Gas to the south (**Figure 2.1-1**). The Field produced 10.8 billion cubic feet (Bcf) of natural gas. Estimated ultimate recovery (EUR) for the field was envisioned to be 11.3 Bcf. The Field produced 95.6% of reserves and is currently shut-in and pressure-depleted. There are three operators of record at the Field: Princeton Natural Gas, LLC, Diversified Resources, LLC, and Pacific Gas and Electric (PG&E). The Field has three idle dry-gas wells.

East Islands is due north of the Field and produced from the Meganos Canyon and Mokelumne River Formation. There are two operators of record at East Islands: Gold Coast Holdings LLC and Princeton Natural Gas, LLC. Gold Coast has one idle dry-gas well at East Islands. Rindge Tract Gas produced from the Mokelumne River Formation. Princeton Natural Gas is the

operator of record and has one plugged well on the field. Since 2021, there has been no production from the Field, East Islands, or Rindge Tract Gas Fields.

In 2014, PG&E was issued a Class V Experimental Compressed Air Energy Storage (CAES) Test Injection/Withdrawal Well Permit (No. R9UIC-CA5-FY13-1). The project consisted of the injection of oxygen-depleted air into the depleted natural gas reservoir in the Mokelumne River Formation for the purpose of building an air bubble as part of a "Compression Test." During and after the building of the air bubble, a series of injection, shut-in, and flow tests were conducted to investigate the reservoir's performance for a CAES application. Performance of the reservoir was monitored by measuring specific parameters and observing formation behavior in two existing nearby wells that served as observation wells, in addition to the Test Well.

2.1.2 Geology Overview

The CTV V storage site lies within the Sacramento Basin in northern California (**Figure 2.1-2**). The Sacramento Basin is the northern, asymmetric sub-basin of the larger, Great Valley Forearc. This portion of the basin, which contains a steep western flank and a broad, shallow eastern flank, spans approximately 240 miles in length and is 60 miles wide (Magoon, 1995).

Basin Structure

The Great Valley was developed during mid- to late-Mesozoic time. The advent of this development occurred under convergent-margin conditions via eastward, Farallon Plate subduction of oceanic crust beneath the western edge of North America (Beyer, 1988). The convergent, continental margin that characterized central California during the Late Jurassic through Oligocene time was later replaced by a transform-margin tectonic system. This occurred as a result of the northward migration of the Mendocino Triple Junction (from Baja California to its present location off the coast of Oregon), located along California's coast (**Figure 2.1-3**). Following this migration, the progressive cessation of both subduction and arc volcanism occurred as the progradation of a transform fault system moved in as the primary tectonic environment (Graham, 1984). The major current-day fault, the San Andreas, intersects most of the Franciscan subduction complex, which consists of the exterior region of the extinct convergent-margin system (Graham, 1984).

Basin Stratigraphy

The structural trough that developed subsequent to these tectonic events was named the Great Valley, which became a depocenter for eroded sediment and thereby currently contains a thick infilled sequence of sedimentary rocks. These sedimentary formations range in age from Jurassic to Holocene. The first deposits occurred as an ancient seaway, and through time were built up by the erosion of the surrounding structures. The basin is constrained on the west by the Coast Range Thrust, on the north by the Klamath Mountains, on the east by the Cascade Range and Sierra Nevada, and on the south by the Stockton Arch Fault (**Figure 2.1-2**). To the west, the Coastal Range boundary was created by uplifted rocks of the Franciscan Assemblage (**Figure 2.1-4**). The Sierra Nevada Mountains that make up the eastern boundary are a result of a chain of ancient volcanoes fed by pre-transform fault subduction.

Basin development is broken out into evolutionary stages at the end of each time period of the arc-trench system, from Jurassic to Neogene, in **Figure 2.1-5**. As previously stated, sediment infill began as an ancient seaway and was later sourced from the erosion of the surrounding structures. Sedimentary infill consists of Cretaceous-Paleogene fluvial, deltaic, shelf, and slope sediments. Due to the southward tilt of the basin, sedimentation thickens towards the southern end near the Stockton Arch Fault, creating sequestration-quality sandstones.

In the southern Sacramento Basin, the Mokelumne River and Starkey formations are comprised of thick-bedded sandstones that create the principal reservoir facies in the project area. Structure in this area is characterized as a homocline that dips about 2 degrees to the southwest.

Submarine Canyons

Falling sea level and tectonics caused the Paleogene Markley, Martinez, and Meganos submarine canyons (Meganos Gorge) to form throughout the Sacramento Basin (**Figure 2.1-2**). The erosional events associated with these canyons played a large part in the current distribution and continuity of Upper Cretaceous and early Tertiary formations within the basin (Downey, 2010). The Late Paleocene/Early Eocene Meganos canyon reaches the AoR. Trending in a northeast-southwest direction and cutting deeply into sediments of the Mokelumne River Formation, this erosional event spans approximately 25-30 miles from southern Sacramento County through northwestern San Joaquin County, and then westward into Contra Costa County. This event caused erosional troughs that were later filled in with fine-grained submarine fan deposits and transgressive deep-water shale due to renewed rising sea levels. This infilled sequence can be seen outcropping on the flanks of Mount Diablo, where it has a minimum thickness of 2,200 feet and serves as the primary trapping mechanism for the Brentwood Oil Field (Downey, 2010). The Field is an erosional remnant surrounded by Meganos canyon fill.

2.1.3 Geological Sequence

Figure 2.1-6 is a schematic cross-section depicting the stratigraphy and major structural features in the region east of the Midland Fault, where the project area is located. The six injection wells for the project will inject CO_2 into the Cretaceous-aged Mokelumne River and Starkey formations, shown in light red fill. The average injection depth for the Mokelumne River Formation within the project area is approximately -6,074 feet true vertical depth (TVD). The average injection depth for the Starkey Formation within the project area is -7,185 feet TVD. The upper Starkey Formation is characterized by interbedded shale and sand. The main sandstone in the Starkey is the Peterson Sandstone Member.

Following its deposition, the Starkey Formation was buried by the H&T Shale which is found throughout the southern Sacramento Basin and serves as an internal barrier between the Upper and Lower Injection Zones (**Figure 2.1-6 and Figure 2.1-7a**). Next, the Mokelumne River Formation was deposited and subsequently overlain by the Capay Shale. The Capay Shale serves as the upper confining zone for the project due to its low permeability, thickness, and regional continuity that spans beyond the AoR (**Figure 2.1-7b**). Above the Capay Shale lies the Domengine Formation (monitoring zone) and the Nortonville Shale (an additional barrier between the upper injection zone and the lowermost underground source of drinking water [USDW]).

2.2 Maps and Cross-Sections of the AoR [40 CFR 146.82(a)(2), 146.82(a)(3)(i)]

2.2.1 Data

To date, six wells have been drilled to various depths within the project AoR (separate from shallow water wells discussed in Section 2.7 below). **Figure 2.2-1** shows the location of the proposed injector wells and the existing, production, abandoned or plugged wells. **Figure 2.2-2** shows the location of wells with well log data. In addition to well-log data, this project utilizes seismic coverage, core, and reservoir performance data such as production and pressure to give an adequate description of the reservoir. The storage site was the site of EPA-approved Class V injection of compressed air by PG&E into the Mokelumne River Formation. Information from that activity is available for the current Class VI permit application.

Well data are used in conjunction with two -dimensional (2D) and three -dimensional (3D) seismic to define the structure and stratigraphy of the injection zones and confining layers (**Figure 2.2-3**). **Figure 2.2-4** shows outlines of the seismic data used to build a structural framework for the area. The 3D surveys were mapped in their entirety, and an additional 2D seismic line was incorporated to the east to constrain the structural model in conjunction with well control. The 3D surveys were pre-stack merged as part of a larger regional effort in 2013 to incorporate advances in seismic processing and allow for a seamless interpretation. Also shown are the seismic well ties made to the 2D and 3D data. Available seismic data were mapped for the following surfaces:

- A shallow marker to aid in controlling the structure of the velocity field
- Domengine
- Mokelumne River
- H&T Shale
- Winters
- Forbes

The Forbes Formation was chosen to be the base of the model due to its reliability as a seismic marker and its depth beneath the injection zones. A basement reflector could not be picked across the entirety of the mapped area due to the depth to basement increasing to the west. Interpretation of these layers began with a series of well ties at well locations shown in **Figure 2.2-4**. These well ties create an accurate relationship between wells, which are in depth, and the seismic, which is in time. The layers listed above were then mapped in time and gridded across the 3D surveys and 2D seismic line. Alongside this mapping was the interpretation of any faulting in the area, which is discussed further in Section 2.3 (Faults and Fractures) of this document.

The gridded time maps and a sub-set of the highest quality well ties and associated velocity data were then used to create a 3D velocity model. This model is guided between well control by the time horizons and is iterated to create an accurate and smooth function. The velocity model is used to convert both the gridded time horizons and any interpreted faults into the depth domain.

The result is a series of depth grids of the layers listed above, which are then used in the next step of this process.

The depth horizons are the basis of a framework which uses conformance relationships to create a series of depth grids that are controlled by formation well tops picked on well logs. The grids are used as structural control between these well tops to incorporate the detailed mapping of the seismic data. These grids incorporate the thickness of zones from well control and the formation strike, dip, and any fault offset from the seismic interpretation. The framework is set up to aid in building the following depth grids for input into the geologic and plume growth models:

- Upper Injection Zone Model:
  - Nortonville Shale
  - Domengine
  - Capay Shale Top
  - Mokelumne River Formation Top and Base
- Lower Injection Zone Model:
  - Mokelumne River Formation Base / H&T Shale Top
  - Base H&T Shale (Top Starkey)
  - Base Starkey (Top Winters)

2.2.2 Stratigraphy

Major stratigraphic intervals within the project area, from oldest to youngest, include the Sacramento Shale (L. Cretaceous), Winters Shale (L. Cretaceous), Starkey Formation (L. Cretaceous), H&T Shale (L. Cretaceous), Mokelumne River Formation (L. Cretaceous-E. Paleocene), Capay Shale (E. Eocene), Domengine Sandstone (L. Eocene), and Nortonville Shale (L. Eocene) (**Figure 2.2-5**). As shown in **Figure 2.2-5**, the Capay Shale is the sealing rock that separates the injection zones from the overlying formations and underground sources of drinking water (USDWs). An additional barrier is provided by the regionally extensive Nortonville Shale.

During Paleogene time, marine and deltaic sequences were deposited in the basin until the activity of the Stockton Arch began to separate Sacramento Basin from the San Joaquin Basin in late Paleogene time (Downey, 2010).

Sacramento Shale-Winters Shale (Below Lower Injection Zone)

Sacramento Shale

The Sacramento Shale is a regionally extensive marine shale that was deposited above the Forbes Formation and is the oldest in a series of transgressive Late Cretaceous shales in southern Sacramento Basin (Downey, 2006).

Winters Shale

The Winters Formation is an upward-fining sequence of Late Cretaceous sandstones and shale deposited as part of a deep-sea fan system sourced from the Sierra Nevada and fed into the

system via submarine canyons and feeder channels (Williamson, 1981). Sandstones are present in the central portion of the Sacramento Basin but pinch out along the eastern side where the entire section is dominated by the Winters Shale.

Starkey Formation (Lower Injection Zone)

The Starkey Formation is comprised of several reservoir-quality sands deposited as multiple progradational deltaic complexes along the eastern margin of the basin (Downey, 2006). The formation occurs in northern San Joaquin Basin and throughout the southern Sacramento Basin where its limits are defined by truncation by a post-Cretaceous angular unconformity. Downcutting by the mud-filled Markley Submarine Canyon has locally eroded all or part of the Starkey in northwest Sacramento and southeast Yolo counties (Downey, 2010). Deposition of Starkey sands over the Sacramento Shale and Winters Shale in the southern Sacramento Basin was oriented in a northwest-southeast trend. The sands range from a few feet to a few hundred feet in thickness and thin towards the west. Within the project AoR, the thickness ranges from 843 to 1,835 feet and varies in depth from 6,221 to 6,750 feet TVD (**Figure 2.2-6).**

Three injectors will inject into the Starkey Formation sands as shown above in **Figure 2.2-6**. A total of six injectors are planned for the combined Starkey and Mokelumne River Formations (**Figure 2.2-7**).

H&T Shale (Internal Barrier)

The H&T Shale is a regional seal that conformably overlies the Starkey Formation. West of the project area, the H&T Shale progressively thickens and is eventually offset by the Midland fault (10 miles to the west). Due to its low permeability, this formation acts as an internal barrier between the Upper and Lower Injection Zones, thus preventing the upward migration of CO_2 from the Starkey Formation. Within the project AoR, the thickness ranges from 75 to 179 feet and varies in depth from 6,086 to 6,634 feet TVD (**Figure 2.4-6).**

Mokelumne River Formation (Upper Injection Zone)

The Mokelumne River Formation contains reservoir-quality sands whose trap types include fault truncations, stratigraphic traps, and unconformity traps sealed by intervening shales as well as overlying Meganos submarine canyon mudstone infill (Downey, 2006). Deposited as a fluvial-deltaic sequence, this sandstone was sourced by the Sierra Nevada terrain to the east and prograded west-southwestward into the forearc basin. This formation truncates to the north by the post-Cretaceous angular unconformity until it pinches out in southern Yolo and Sutter Counties (Downey, 2006). These thick sands can be locally eroded or completely absent due to the downcutting by the Meganos submarine canyons. In the northwestern portion of Sacramento County, the sandstone is as shallow as 2,000 feet and deepens to over 10,500 feet moving to south-central Solano County. Thickness in this area ranges from hundreds of feet thick, separated by thin shales, to 2,500 feet thick (Downey, 2010). Within the project AoR, the thickness ranges from 100 to 1,490 feet and varies in depth from 4,713 to 6,523 feet TVD (**Figure 2.2-8**).

Three injectors will inject into the Mokelumne River Formation sands as shown above in **Figure 2.2-8**. A total of six injectors are planned for the combined Starkey and Mokelumne River formations (**Figure 2.2-7**).

Capay Shale (Upper Confining Zone)

The Capay Shale is a regionally continuous sealing facies present throughout Sacramento Basin that acts as the upper confining zone for the storage project. This Eocene-aged formation was deposited as a transgressive surface blanketing the shelf with shales. East of the Midland fault zone, the Martinez Shale has been stripped away by erosion, and the Mokelumne River Formation is unconformable overlain by the Capay Shale. At the storage site, the lower Capay Shale was deposited in an outer neritic environment, and the upper Capay was deposited in an inner neritic to brackish-water environment, implying a partial shoaling of the basin during the Eocene. Due to its low permeability, the Capay Shale serves as the sealing facies above the Upper and Lower Injection Zones; it will prevent the upward migration of CO_2 from the storage reservoirs, thus protecting USDWs. Within the project AoR, the thickness ranges from 73 to 1,353 feet and varies in depth from 4,483 to 5,228 feet TVD (**Figure 2.4-5**).

Domengine Sandstone (Monitoring Zone)

The Domengine Formation is approximately 800 to 1,200 feet thick on the north flank of Mt. Diablo (Nilsen, 1975). Prograding across the Capay Shelf in early-middle Eocene, this formation is characterized by interbedded sandstones, shales, and coals. This sand ranges from medium- to coarse-grained silty mudstone and fine sandstone and onlaps the Capay Shale. It is separated from the Capay by a regional unconformity which progressively truncates older units until the Domengine rests on Cretaceous rocks, moving west. The Domengine consists of an upper and lower portion. The lower member is made up of fluvial and estuarine sandstones. Regionally, the lower member is separated from the upper member by an extensive surface of transgression and change in depositional style. This formation serves as a monitoring zone above the Upper and Lower Injection Zones. At the storage site, the Domengine Sand consists of alternating layers of marine sand and shale with sand being the dominant lithology.

Nortonville Shale (Additional Barrier)

Above the Domengine Sandstone is the Nortonville Shale, which is separated by a widespread surface of transgression and acts as an additional barrier between the lowermost USDW and the Upper and Lower Injection Zones. The Nortonville Shale is a mudstone member of the Kreyenhagen Formation. It is approximately 500 feet thick on the north flank of Mt. Diablo and is considered the upper portion of the Domengine Sandstone (Nilsen 1975). Overlying the Domengine Sandstone, this shale acts as a seal throughout most of the southern Sacramento and northern San Joaquin Basins. At the storage site, the Markley Sand at the top of the Nortonville is a poorly consolidated deltaic deposit containing interbedded sand and shale.

Undifferentiated Sediments (Marine and Non-Marine)

The upper Paleogene and Neogene sequence begins with the Valley Springs Formation, which represents fluvial deposits that blanket the entire southern Sacramento Basin. The unconformity at the base of the Valley Springs marks a widespread Oligocene regression and separates the more-deformed Mesozoic and lower Paleogene strata below from the less-deformed uppermost

Paleogene and Neogene strata above. Base USDWs within the undifferentiated sediments are discussed in Section 2.7 of this document.

2.2.3 Maps of the Area of Review

As required by 40 CFR 146.82(a)(2), **Figure 2.2-9** shows surface bodies of water, surface features, transportation infrastructure, political boundaries, and cities and the project AoR. AoR delineation is presented in **Attachment B** (AoR and Corrective Action Plan). Major surface water bodies located in the area include the San Joaquin River, Bear Creek River, and Calaveras River run through the AoR. More details concerning these and other surface water bodies are included in Section 2.7.1.

The project AoR is in San Joaquin County. **Figure 2.2-9** does not show the surface trace of known and suspected faults because there are no known surface faults in the AoR. Based on publicly available data from Conservation Division of Mine Reclamation (DMR) and the U.S. Geological Survey (USGS) there are also no known mines or quarries in the AoR.

Figure 2.2-10 indicates the locations of State- or EPA-approved subsurface cleanup sites. This cleanup site information was obtained from the State Water Resources Control Board's GeoTracker database, which contains records for sites that impact, or have the potential to impact, groundwater quality. Water wells within and adjacent to the AoR are discussed in Section 2.7.7 of this document.

40 CFR 146.82(a)(2) requires that the application includes a map showing the injection wells, the AoR, and the below list of items and these are shown on the indicated maps where present:

- Existing injection wells, producing wells, abandoned wells, plugged wells or dry holes, deep stratigraphic boreholes (**Figure 2.2-1**).
- Surface bodies of water, springs, mines (surface and subsurface), quarries, State, Tribal, and Territory boundaries, roads and other pertinent surface features (**Figure 2.2-9**).
- State- or EPA-approved subsurface cleanup sites (**Figure 2.2-10**).
- Water wells (Figure 2.7-7; see Section 2.7)
- **Figure 2.2-11** is a compilation of the above data including index numbers to well names. Referenced index number are listed in **Table 2.2-1** and **Table 2.2-2**.

2.3 Faults and Fractures [40 CFR 146.82(a)(3)(ii)]

2.3.1 Overview

A combination of 2D and 3D seismic and well control were used to define the structure and any faulting within the area (**Figure 2.2-4**). **Figure 2.3-1** shows the locations of faulting identified within proximity of the AoR. The green lines show the fault traces at the Mokelumne River level. None of the faulting identified intersects the plume boundaries. Faulting in the area is characterized as normal in nature, with relatively small offset and bound within the sedimentary section. Dip directions of these faults vary, leading to down-thrown blocks on opposite sides in

similarly striking features. **Figure 2.3-2** and **Figure 2.3-3** show generalized sections across the faults that are nearest the AoR and intersect the pressure front (**Appendix 9, Figure 1**).

In addition to the reviewed sub-surface data, public data from the California Geologic Survey (CGS) support a general absence of major faulting within the project AoR. **Figure 2.3-4** shows the Fault Activity Map generated by the Geologic Survey over a regional surrounding area. The CGS does not document a fault of any classification within the AoR.

2.3.2 Fault Sealing

An Allan diagram, shale gouge ratio (SGR), and shale smear factor (SSF) analysis were completed for the two faults that fall within the pressure front (**Appendix 9, Figure 1)** to demonstrate the sealing nature of the faults. Allan diagrams display across fault juxtaposition along a mapped fault plane, SGR is a fault seal algorithm used to estimate the sealing potential of a fault-zone, and SSF calculates the likelihood of intact shale smears within the fault plane (Yielding et al, 2010).

The SGR calculation takes stratigraphic thickness, throw, and clay volume into consideration using the following equation:

$$SGR = \frac{\sum(Vcl \times \Delta z)}{throw} \times 100\% \qquad \text{(Eq-1)}$$

where Vcl is the clay volume content, Δz is the stratigraphic layer thickness, and $throw$ is the offset of the layer of interest. SGR values can vary vertically and laterally along a fault as stratigraphic changes occur (Freeman et al., 1998). SGR values greater than 20 percent imply there is a high chance of fault zone seal (Yielding et al, 2010).

The SSF calculation takes shale layer throw and thickness into consideration using the following equation:

$$SSF = \frac{throw}{thickness} \qquad \text{(Eq-2)}$$

Where $throw$ is the offset of a single shale bed and $thickness$ is the thickness of the shale bed. SSF values can vary laterally along a fault as stratigraphic thickness or changes in offset occur. Small values of SSF, generally less than 4-5, imply a high probability of continuous smear. (Yielding et al, 2010).

West Normal Fault

The West Normal Fault (**Figure 2.3-2**) is located to the west of the AoR. The West Normal Fault is a west-side-down normal fault that strikes towards the south and dips to the west. An Allan diagram, SGR, and SSF analysis were completed to demonstrate the sealing nature of the West Normal Fault. The Allan diagram is shown in **Figure 2.3-5**. The top of Mokelumne Formation on the footwall side of the fault is partially juxtaposed against the Capay Shale on the hanging wall side of the fault. The bottom of the Mokelumne Formation on the hanging wall side of the fault is juxtaposed against the H&T Shale on the footwall side of the fault. Since the fault does

not have a large enough offset to completely offset the Mokelumne Formation against another formation, the SGR values only vary vertically. **Figure 2.3-6** displays the SGR calculation for the top and bottom of the Mokelumne Formation (Upper Injection Zone) and **Figure 2.3-7** displays the SGR calculation for the top and bottom of the Starkey Formation (Lower Injection Zone). These SGR calculations use the Δz of the layer that moved past a given point, and the Vcl of the layer to which it is juxtaposed. $throw$ was calculated using the offset for both the top and bottom of the Mokelumne and Starkey Formations. The stratigraphic thickness and throw values were calculated using the Allan diagram. The Vcl values were averaged from 4 wells; BOULDIN_DEVELOPMENT_CO_1 (04077202170000), EAST_BOULDIN_ISLAND_1 (04077202730000), BOULDIN_1-14 (04077204900000), and TRANSAMERICA_1-19 (04077203360000). The well locations and Vcl values are displayed in **Figure 2.3-6** and **Figure 2.3-7**. **Figure 2.3-8** displays the SSF calculations for the Capay and H&T Shale offsets which demonstrates the vertical sealing nature of the West Normal Fault above the Mokelumne and Starkey Injection Zones.

The SGR analysis for the Mokelumne Formation results in values of 46 percent for the top and 45 percent for the bottom of the Upper Injection Zone. The Analysis for the Starkey Formation results in values of 45 percent for the top and 26 percent for the bottom of the Lower Injection Zone. All of these values are larger than the 20 percent threshold which shows a high likelihood of fault sealing capability. The SSF analysis for both the Capay and H&T Shale layers results in a value of 1, which supports a continuous shale smear along the fault. Both SGR and SSF values support that the West Normal Fault is sealing at the top and base of both the Upper and Lower Injection Zones (Yielding et al., 2010).

East Normal Fault

The East Normal Fault (**Figure 2.3-3**) is located to the east of the AoR. The East Normal Fault is a south-side-down normal fault that strikes towards the east and dips to the south. An Allan diagram, SGR, and SSF analysis were completed to demonstrate the sealing nature of the East Normal Fault. The Allan diagram is shown in **Figure 2.3-9**. The top of Mokelumne Formation on the footwall side of the fault is partially juxtaposed against the Capay Shale on the hanging wall side of the fault. The East Normal Fault does not extend to the H&T Shale, therefore the bottom of the Mokelumne Formation is not offset. Since the fault does not have a large enough offset to completely offset the Mokelumne Formation against another formation, the SGR values for the top of the Mokelumne Formation only vary vertically. **Figure 2.3-10** displays the SGR calculation for the top of the Mokelumne Formation (Upper Injection Zone). The SGR calculation uses the Δz of the layer that moved past a given point, and the Vcl of the layer to which it is juxtaposed. $throw$ was calculated using the offset for the top of the Mokelumne Formation. The stratigraphic thickness and throw values were calculated using the Allan diagram. The Vcl values were averaged from 4 wells; CPC_HATCH_31-1 (04077204560000), WOODBRIDGE_UNIT_ONE_1 (04077201830000), PIACENTINE_1 (04077005150000), and KCY_RESERVE_MOBIL_FINKBOHNER_UNIT_1 (04077004790000). The well locations and Vcl values are displayed in **Figure 2.3-10**. **Figure 2.3-11** displays the SSF calculation for the Capay Shale offset which demonstrates the vertical sealing nature of the East Normal Fault above the Mokelumne Formation (Upper Injection Zone).

The SGR analysis for the top of the Mokelumne Formation results in a value of 46 percent for the Upper Injection Zone. This value is larger than the 20 percent threshold which shows a high likelihood of fault sealing capability. The SSF analysis for the Capay Shale layer results in a value of 1, which supports a continuous shale smear along the fault. Both SGR and SSF values support that the East Normal Fault is sealing at the top of the Upper Injection Zone (Yielding et al., 2010).

2.4 Injection and Confining Zone Details [40 CFR 146.82(a)(3)(iii)]

2.4.1 Mineralogy

Some quantitative mineralogy information exists within the AoR boundary from the Citizen_Green_1 well. In addition, several wells outside the AoR have mineralogy over the formations of interest, and that data is presented below. The locations of wells used for mineralogy are shown in **Figure 2.2-2**, and the mineralogy data is posted in **Table 2.4-1**. Mineralogy data will be acquired across all the zones of interest as part of pre-operational testing.

Upper Confining Zone

Mineralogy data are available for the upper confining zone from three wells in the Rio Vista Gas Field (RVGU_209, RVGU_248, and Wilcox_20). RVGU_209 has Fourier-transform infrared spectroscopy (FTIR) data, while the other two wells have x-ray diffraction (XRD) data. Nine samples show an average of 29% total clay, with mixed-layer illite/smectite being the dominant species, and kaolinite and chlorite still prevalent. They also contain 32% quartz, 39% plagioclase and potassium feldspar, minimal pyrite, and less than 1% calcite and dolomite.

Upper Injection Zone

Mineralogy data are available for the Upper Injection Zone in the form of XRD data from the Citizen_Green_1 well within the AoR. Reservoir sand from six samples within this well average 32% quartz, 50% plagioclase and potassium feldspar, and 18% total clay. The primary clay minerals are kaolinite, chlorite and illite/mica. Calcite and dolomite were not detected in any of the samples.

Internal Barrier

Mineralogy data are available for the internal barrier zone from the Speckman_Decarli_1 well. A mix of XRD and FTIR data on nine samples show an average of 46% total clay, with mixed layer illite/smectite being the dominant species, and kaolinite and chlorite still prevalent. They also contain 23% quartz, 29% plagioclase and potassium feldspar, 2% pyrite, and 1% calcite and dolomite.

Lower Injection Zone

Mineralogy data are available for the Lower Injection Zone in the form of XRD data from the Citizen_Green_1 well within the AoR. Reservoir sand from three samples within this well average 40% quartz, 43% plagioclase and potassium feldspar, and 14% total clay. The primary clay minerals are chlorite, illite/mica, and mixed-layer illite/smectite.

Winters Formation

Mineralogy data are available for the Winters Shale in the form of XRD data from the Lopes_Transamerica_1 well in the Thornton Gas Field. Twenty-two samples show an average of 41% total clay, with chlorite being the dominant species, with illite/mica and smectite common. They also contain 25% quartz, 26% plagioclase and potassium feldspar, 2% pyrite, and less than 1% calcite and dolomite. Two samples show calcite cementation.

Sacramento Shale

Mineralogy data are available for the Sacramento Shale in the form of XRD data from the Lopes_Transamerica_1 well in the Thornton Gas Field. Ten samples show an average of 47% total clay, with chlorite and smectite being the dominant species, and illite/mica common. They also contain 22% quartz, 27% plagioclase and potassium feldspar, 1% pyrite, and less than 1% calcite and dolomite.

2.4.2 Porosity and Permeability

Wireline log data were acquired with measurements that include but are not limited to spontaneous potential (SP), natural gamma ray, borehole caliper, compressional sonic, resistivity, as well as neutron porosity and bulk density. Whole core was also cut in the Upper Injection Zone and overlying Capay/Meganos canyon fill during the PG&E King Island CAES program.

Formation porosity is determined one of two ways: from bulk density using 2.65 grams per cubic centimeter (g/cc) matrix density as calibrated from core grain density and core porosity data, or from compressional sonic using 55.5 microseconds per foot (µsec/ft) matrix slowness and the Wyllie time-average equation. See **Table 2.4-2** for explanation of which equations were used in each zone.

Clay volume is determined by SP and is calibrated to core data. Log-derived permeability is determined by applying a core-based transform that utilizes capillary pressure porosity and permeability along with clay values from XRD or FTIR. Core data from two wells (RVGU 209 and RVGU 215) with 13 data points was used to develop a permeability transform. Well locations are displayed in **Attachment B** (AoR and Corrective Action Plan), Figure 3.6. An example of the transform from core data is illustrated in **Figure 2.4-1**.

Comparison of the permeability transform to log-generated permeability (Timur-Coates method) from a nuclear magnetic resonance (NMR) log in the Citizen_Green_1 well in the storage area is almost 1:1 and matches rotary sidewall core permeability (**Figure 2.4-2**).

Upper Confining Zone

The average porosity of the upper confining zone is 28%, based on 10 wells with porosity logs and 3,155 individual logging data points. See **Figure 2.4-3** for location of wells used for porosity and permeability averaging. The geometric average permeability of the upper confining zone is 0.36 millidarcy (mD) based on the Citizen_Green_1 well NMR permeability from the Timur-Coates method.

Core data are available for the upper confining zone from the DOE report DOE-PGE-00194-4 (Medeiros, et al., 2018). The cited report states that the vertical permeability for the upper confining zone is between 0.04-0.06 mD based on two different analysis methods for samples from the Piacentine_2-27 well. This is lower than the permeability from the NMR log in Citizen_Green_1, and confirms that the upper confining zone has good sealing potential

Upper Injection Zone

The average porosity for the Upper Injection Zone is 32.2%, based on 38 wells with porosity logs and 33,891 individual logging data points. The geometric average permeability for the Upper Injection Zone is 216 mD, based on 38 wells with porosity logs and 33,768 individual logging data points. This is in agreement with the NMR permeability in the Citizen_Green-1 well, which had a geometric mean of 225 mD for the upper injection zone. Twenty-one core data points from Citizen_Green_1 and Wiskey_Slough_1A-E wells (see **Figure 2.2-2** for well location) are from the upper injection zone (see **Table 2.4-3**). Permeability was measured and is in agreement with the log averages.

Core data are available for the upper injection zone from the DOE Report DOE-PGE-00194-4 in the PG&E Piacentine 2-27 well (Medeiros, et al., 2018). The cited report states that the upper injection zone has an average porosity of 25% and a horizontal permeability arithmetic average of 807 mD based on 162 samples in the Piacentine_2-27 well. The horizontal permeability is very similar to the average of the core data in **Table 2.4-3**, which has an arithmetic average of 780 mD. Vertical permeability measurements from that well showed an average Kv/Kh ratio of 0.8, which is similar to data from Whiskey_Slough_1A-E (**Table 2.4-3**), which shows an average Kv/Kh ratio of 0.74.

Internal Barrier

The average porosity of the internal barrier zone is 25%, based on 23 wells with porosity logs and 9,854 individual logging data points. The geometric average permeability of the internal barrier zone is 1.3 mD, based on the Citizen_Green_1 well NMR permeability from the Timur-Coates method.

Lower Injection Zone

The average porosity of the Lower Injection Zone is 25.5%, based on 21 wells with porosity logs and 12,798 individual logging data points. The geometric average permeability of the Lower Injection Zone is 52 mD, based on 20 wells with porosity logs and 11,602 individual logging data points. This is in agreement with the NMR permeability in the Citizen_Green-1 well, which had a geometric mean of 53 mD for the lower injection zone. Five core data points from Citizen_Green_1 well are from the lower injection zone. Permeability was measured and is in agreement with the log averages (see **Table 2.4-4**).

Winters Formation

The average porosity of the Winters Formation is 16.8%, based on 11 wells with porosity logs and 3,529 individual logging data points. The geometric average permeability of the Winters Formation is 0.20 mD, based on 11 wells with porosity logs and 3,296 individual logging data points. Thirty-seven core data points from the Lopes_Transamerica_1 and

GP_Dohrman_1_RD1 wells are from the Winters Formation. Permeability was measured and is in agreement with the log averages (see **Table 2.4-5**).

Sacramento Shale

The average porosity of the Sacramento Shale is 20%, based on 10 wells with porosity logs and 19,549 individual logging data points. The geometric average permeability of the Sacramento Shale is 0.47 mD, based on 10 wells with porosity logs and 19,265 individual logging data points.. Eleven core data points from the Lopes_Transamerica_1 wells are from the Sacramento Shale. Permeability was measured and is in agreement with the log averages (see **Table 2.4-5**).

2.4.3 Injection and Confining Zone Capillary Pressure

Capillary pressure is the difference across the interface of two immiscible fluids. Capillary entry pressure is the minimum pressure required for an injected phase to overcome capillary and interfacial forces and enter the pore space containing the wetting phase.

Capillary pressure data within the project area are available from four sidewall core samples taken from well Citizen_Green_1. Two samples were collected from the Upper Injection Zone and two samples were collected from the Lower Injection Zone using mercury-injection capillary pressure (MICP). The raw data was downloaded from the NETL EDX server, and required a closure correction (Shafer & Neasham, 2000). Using the XRD data (**Table 2.4-1**), the mercury injection pressures and saturations were then corrected for clay bound water using the methodology prescribed in Juhasz, 1979. The corrected air-mercury capillary pressure was then converted to reservoir conditions of CO_2-brine using the equation below (Lohr & Hackley, 2018).

$$P_{CO_2-Brine} = P_{Hg-Air} \frac{\sigma_{CO_2-Brine} \cos\theta_{CO_2-Brine}}{\sigma_{Hg-Air} \cos\theta_{Hg-Air}} \quad (1)$$

An interfacial tension (IFT) of 480 dynes per centimeter (dynes/cm) was used for air-mercury and 30 dynes/cm was used for CO_2-brine. The cosine of contact angles of 0.766 and 0.875 degrees were also used for air-mercury and CO_2-brine, respectively. The values of IFT and contact angles for CO_2-brine were based on published studies (Chiquet et al., 2009; Haeri et al., 2020). See **Figure 2.4-4** for final CO_2-brine corrected curves for the four samples.

The report DOE-PGE-00194-4 cites caprock threshold pressure tests that were performed on samples from the upper confining zone. A delta pressure was held across three separate core samples, none of which showed any brine production at the highest delta pressure of 2,000 psi. As stated in the report, “These results support a conclusion that the upper confining zone is an impermeable seal at reservoir conditions” (Medeiros, et al., 2018).

2.4.4 Depth and Thickness

Depth and thickness of the Upper Confining Zone, Upper Injection Zone, barrier, and Lower Injection Zone (**Table 2.4-6**) are determined by structural and isopach maps (**Figure 2.4-5** and

Figure 2.4-6) based on well data (wireline logs). Variability of thickness and depth measurements within the project AoR is caused by the following factors:

- Structural variability within the Capay Shale is caused by the Meganos submarine canyon erosional event.
- Structural and thickness variability within the Mokelumne River Formation is due to erosion associated with the Meganos submarine canyon.
- Structural and thickness variability across the Starkey Formation is due to deposition on the east flank of the Sacramento Basin, where structure dips west-southwest and thickness increases towards the basin axis.

2.4.5 Structure Maps

Structure maps (**Figure 2.4-5** and **Figure 2.4-6**) are provided to indicate a depth to formation adequate for supercritical-state injection.

Isopach Maps

SP logs from surrounding gas wells were used to identify sandstones. Negative millivolt (mV) deflections on these logs, relative to a baseline response in the enclosing shales, define the sandstones. These logs were baseline-shifted to 0 mV. Due to the log vintage variability, there is an effect on quality which creates a degree of subjectivity within the gross sand; however, this will not have a material impact on the maps.

In addition to well log data, site specific depth and thickness information for the Capay Shale, Mokelumne River Formation sandstones and Starkey Formation sandstones are also available from seismic data (**Figure 2.2-4**). The coverage of the 3D and 2D seismic data and the well control in the structural model area provide confidence in the thickness and continuity of the injection and confining zones. Based on the computational modeling results discussed in **Attachment B** (AoR and Corrective Action Plan), the structural variability in the thickness and depth of either the Capay Shale or the Mokelumne River Formation sandstone resulting from the Meganos submarine canyon erosional event, do not impact confinement. CTV will use thickness and depth shown when determining operating parameters and assessing project geomechanics. In addition, the Meganos canyon was infilled by deep water shales and fine-grained submarine fan deposits. The canyon fill provides additional vertical and lateral confinement for the injected CO_2.

2.5 Geomechanical and Petrophysical Information [40 CFR 146.82(a)(3)(iv)]

2.5.1 Caprock Ductility

Ductility and the unconfined compressive strength (*UCS*) of shale are two properties used to describe geomechanical behavior. Ductility refers to how much a rock can be distorted before it fractures, while the *UCS* is a reference to the resistance of a rock to distortion or fracture. Ductility generally decreases as compressive strength increases.

Ductility and rock strength calculations were performed based on the methodology and equations from Ingram & Urai (1999) and Ingram, et al. (1997). Brittleness is determined by comparing the log-derived *UCS* to an empirically derived *UCS* for a normally consolidated rock (UCS_{NC}).

$$\log UCS = -6.36 + 2.45 \log\left(0.86V_p - 1172\right) \quad (2)$$

$$\sigma' = OB_{pres} - P_p \quad (3)$$

$$UCS_{NC} = 0.5\sigma' \quad (4)$$

$$BRI = \frac{UCS}{UCS_{NC}} \quad (5)$$

Units for the *UCS* equation are *UCS* in megapascals (MPa) and V_p (compressional velocity) in meters per second (m/s). OB_{pres} is overburden pressure, P_p is pore pressure, σ' is effective overburden stress, and *BRI* is brittleness index.

If the value of *BRI* is less than 2, empirical observation shows that the risk of embrittlement is lessened, and the confining zone is sufficiently ductile to accommodate large amounts of strain without undergoing brittle failure. However, if *BRI* is greater than 2, the "risk of development of an open fracture network cutting the whole seal depends on more factors than local seal strength, and therefore the *BRI* criterion is likely to be conservative, so that a seal classified as brittle may still retain hydrocarbons" (Ingram & Urai, 1999).

Upper Confining Zone

Within the project area, 16 wells had compressional sonic data over the upper confining zone to calculate ductility, comprising 8,863 individual logging data points (pink circles in **Figure 2.2-2)**. The same 16 wells were used to calculate *UCS*, comprising 8,863 individual logging data points. The average ductility of the upper confining zone based on the mean value is 1.34. The average rock strength of the confining zone, as determined by the log-derived *UCS* equation above, is 1,589 psi.

PG&E performed an EPA-approved Class V compressed air injection test within the Upper Injection Zone. The test was successful in pressurizing and depressurizing the reservoir without impacting the Upper Confining Zone or bounding Meganos canyon fill.

Additional Barrier between Upper Injection Zone and Lowermost USDW

Additionally, ductility and rock strength were calculated over the additional barrier between the Upper Injection Zone and the lowermost USDW (see Section 2.2.2.7) and the internal barrier zone. A total of 15 wells had sufficient data for the additional barrier, comprising 6,288 individual logging data points. The average ductility of the additional barrier based on the mean value is 1.43. The average rock strength of the additional barrier, as determined by the log-derived *UCS* equation above, is 1,125 psi.

Internal Barrier

Nine wells had sufficient data to calculate ductility and rock strength over the internal barrier zone, comprising 3,974 individual logging data points. The average ductility of the internal barrier zone based on the mean value is 2.0. The average rock strength of the internal barrier zone, as determined by the log-derived *UCS* equation above, is 3,088 psi.

An example calculation for the well "1_Chevron" is shown in **Figure 2.5-1**. *UCS_CCS_VP* is the *UCS* based on the compressional velocity, *UCS_NC* is the *UCS* for a normally consolidated rock, and *BRI* is the calculated brittleness using this method. Brittleness less than 2 (representing ductile rock) is shaded red.

Within the upper confining layer, the brittleness calculation drops to a value less than 2. Additionally, the additional barrier has a brittleness value less than 2. The internal barrier zone also has a brittleness value less than 2. As a result of the confining layer ductility, there are no fractures that will act as conduits for fluid migration from the injection zones. This conclusion is supported by the fact that prior to discovery, the upper confining zone provided a seal to the underlying gas reservoirs of the Mokelumne River Formation for millions of years in several gas fields surrounding and within the project AoR.

2.5.2 Stress Field

The stress of a rock can be expressed as three principal stresses. Formation fracturing will occur when the pore pressure exceeds the least of the stresses. In this circumstance, fractures will propagate in the direction perpendicular to the least principal stress (**Figure 2.5-2**).

Stress orientations in the Sacramento Basin have been studied using both earthquake focal mechanisms and borehole breakouts (Snee and Zoback, 2020; Mount and Suppe, 1992). The azimuth of maximum principal horizontal stress (S_{Hmax}) was estimated at N40ºE ± 10º by Mount and Suppe (1992). Data from the World Stress Map 2016 release (Heidbach et al., 2016) shows an average S_{Hmax} azimuth of N37.4ºE once several far-field earthquakes with radically different S_{Hmax} orientations are removed (**Figure 2.5-3**), which is consistent with Mount and Suppe (1992). The earthquakes in the area indicate a strike-slip/reverse-faulting regime.

Within the project AoR, there is a site-specific fracture gradient for the Upper Injection Zone, but not for the Lower Injection Zone or any of the confining zones. A step-rate test will be conducted as per the pre-operational testing plan (**Attachment I**) in the injection zones. A step-rate test (SRT) was performed in the PG&E TEST_INJECTION_WITHDRAWAL_WELL_1 with a resultant fracture gradient of 0.822 psi/ft in the Upper Injection Zone. Several additional wells in the Sacramento Basin have formation integrity tests (FIT) or leak-off tests (LOT) performed at similar depth ranges to the project injection and confining zones. Tests from seven wells average 0.82 psi/ft from tests in the depth range of 4,800 to 11,050 feet TVD. See **Figure 2.5-4** for the location of the wells. For the computational simulation modeling and well-performance modeling, a frac gradient of 0.76 psi/ft was assumed for now as a safety factor.

The overburden stress gradient in the injection and confining zones is 0.87 to 0.94 psi/ft. No data currently exist for the pore pressure of the confining zone. This will be determined as part of the preoperational testing.

2.5.3 Fault Reactivation

The stability of the faults adjacent to the CTV V project area were analyzed using Mohr coulomb criteria. Four faults were studied, numbered one through four (**Figures 2.5-5**). Each injection zone was modeled independently, and the input parameters for the Mohr Circle calculations are shown in **Table 2.5-1** and can be referenced in Sections 2.3 and 2.5.2. The maximum horizontal stress gradient was determined using Aφ data from Lund-Snee and Zoback (2020). The maximum horizontal stress direction is 37.4º as stated in Section 2.5.2. Fault strike and dip were averaged over each fault's length. The coefficient of friction was assumed to be 0.6 and the faults were prescribed a cohesive strength of 0 psi. Based on Mohr circle analysis, all of the faults are currently far from failure and will continue to be stable even after CO_2 injection has ceased for both injection zones (**Figures 2.5-5 through 2.5-8**). Analysis by Mohr circle shows that the required pore pressure increase to reactivate any of the faults is over 1,500 psi above present day conditions (**Tables 2.5-2 and 2.5-3**). This equates to a reservoir pressure gradient in both injection zones of over 0.68 psi/ft, far above the expected final pressure gradients after CO_2 injection has ceased. Pressures in the CTV V project area along the four modeled faults are only expected to increase by approximately 140 psi at most, which equates to a pressure gradient of 0.446 psi/ft (**Tables 2.5-2 and 2.5-3**). This final pressure gradient is very similar to the discovery pressure of the Mokelumne River Formation in Rio Vista Gas Field, where the Midland Sand (a subzone of the Mokelumne River gas reservoir) is trapped against the Midland Fault. In deeper reservoirs in direct contact with both the Midland and Stockton Arch faults in the project vicinity, discovery pressures approached 0.49 to 0.53 psi/ft. The fact that these faults held natural gas reservoirs with these pressure gradients for long periods of geologic time helps to reinforce the Mohr circle explanation of these faults being stable at higher reservoir pressures.

2.6 Seismic History [40 CFR 146.82(a)(3)(v)]

2.6.1 Recent Seismicity

As discussed in prior sections, 2D and 3D seismic along with well data were used to create depth surfaces within the AoR. Faults identified are classified as typical normal faults as seen in the extended area beyond the AoR. These faults are interpreted to be bound within the sedimentary section of the Sacramento Basin. The California Geologic Survey (CGS) has produced a Fault Activity Map, which captures a compilation of mapped faults within the state. This map is shown for the project area in **Figure 2.3-4** and indicates there are no mapped faults within the greater proximity of the project area.

USGS provides an earthquake catalog tool (https://earthquake.usgs.gov/earthquakes/search/) which can be used to search for recent seismicity that could be associated with faults for movement. A search was made for earthquakes in the greater vicinity of the project area from 1900 to modern day with events of a magnitude greater than 2.5. **Figure 2.6-1** shows the results of this search. **Table 2.6-1** summarizes data taken from these events. The events were confirmed

to be the same as those in the Northern California Earthquake Data Center catalog (NCEDC, 2014).

There are seventeen events within a 15-mile radius of the project area. The events occur between 1909 and 2021, at 4 to 15 kilometers (km) depth. The injection zones are between 1.25 and 2.5 km deep. There are no earthquakes within the AoR or in the injection/containment layers. Given the typical nature of the faults identified on the seismic data, the lack of major faults mapped by the CGS, and the absence of historical earthquakes within or close to the AoR, the faults identified are not considered to be active or high-risk sources of seismicity.

Lund-Snee and Zoback (2020) published updated maps for crustal-stress estimates across North America. **Figure 2.6-2** shows a modified image from that work highlighting the project area. This work agrees with previous estimates of maximum horizontal stress in the region of approximately N40°E in a strike-slip to reverse-stress regime (Mount and Suppe, 1992) and is consistent with World Stress map data for the area (Heidbach et al., 2016). **Attachment C** of this application (Testing and Monitoring Plan) discusses the seismicity monitoring plan for this injection site.

2.6.2 Seismic Hazard Mitigation

CTV V is in an area of little historical seismicity, and no active faults have been documented by the CGS for the area. This document defines the confining zones that separate the injection intervals from USDWs.

The following is a summary of CTVs seismic hazard mitigation for CTV V:

The project has a geologic system capable of receiving and containing the volumes of CO_2 proposed to be injected.

- Extensive historical operations in the Sacramento Basin across multiple geologic formations, such as those at Rio Vista and Union Island in the southern portion of the Basin, provide valuable experience to understand operating conditions such as injection volumes and reservoir containment.
- There are no faults or fractures identified in the AoR that will impact the confinement of CO_2 injectate.

Will be operated and monitored in a manner that will limit risk of endangerment to USDWs, including risks associated with induced seismic events.

- Injection pressure will be lower than the fracture gradient of the sequestration reservoir with a safety factor (90% of the fracture gradient).
- Injection and monitoring well pressure monitoring will ensure that pressures are beneath the fracture pressure of the sequestration reservoir and confining zone.
- A seismic monitoring program will be designed to detect events lower than seismic events that can be felt. This will ensure that operations can be modified with early warning events, before a felt seismic event.

Will be operated and monitored in a way that in the unlikely event of an induced event, risks will be quickly addressed and mitigated.

- Via monitoring and surveillance practices (pressure and seismic monitoring program), CTV personnel will be notified of events that are considered an early warning sign. Early warning signs will be addressed to ensure that more significant events do not occur.
- CTV will establish a central control center to ensure that personnel have access to the continuous data being acquired during operations.

Minimizing potential for induced seismicity and separating any events from natural to induced.

- Pressure will be monitored in each injector and sequestration-monitoring well to ensure that pressure does not exceed the fracture pressure of the reservoir or confining zone.
- Seismic monitoring program will be installed pre-injection for a period to monitor for any baseline seismicity that is not being resolved by current monitoring programs.
- Average depth of prior seismic hazard in the region based on reviewed historical seismicity has been approximately 5.0 km, which is significantly deeper than the proposed injection zones.

2.7 Hydrologic and Hydrogeologic Information [40 CFR 146.82(a)(3)(vi), 146.82(a)(5)]

The California Department of Water Resources (DWR) has defined 515 groundwater basins and subbasins within the state. The project AoR is within the San Joaquin Valley Groundwater Basin. The majority of the AoR is in the Eastern San Joaquin Subbasin (ESJS; DWR Basin No. 5-022.01). A small southwest portion (approximately 1%) of the AoR is in the Tracy Subbasin (DWR Basin No. 5-022.15) (DWR, 2020). **Figure 2.7-1** illustrates the project AoR, subbasins, and the surrounding areas.

The ESJS is generally bounded on the north and northwest by the Mokelumne River, on the west by the San Joaquin River, on the south by the Stanislaus River, and on the east by consolidated bedrock (DWR, 2006a). The Tracy Subbasin is bounded by the Diablo Range on the west, the Mokelumne and San Joaquin Rivers on the north, the San Joaquin River to the east, and the San Joaquin-Stanislaus County line on the south (DWR, 2006b).

Portions of the text below regarding hydrologic features of the area are adopted from ESJGA (2019).

2.7.1 Hydrologic Information

The major surface water bodies located in the ESJS include San Joaquin River, Bear Creek River, and Calaveras River, and sloughs and the perennial stream tributaries (**Figure 2.7-1**). The surface water bodies are shown in more detail on **Figure 2.2-9.** The San Joaquin River, Bear Creek, sloughs, and cuts connecting sloughs run in the vicinity of the project AoR.

With a watershed of approximately 1,195 square miles, the San Joaquin River begins at Thousand Island Lake high in the south-central Sierra Nevada at an elevation of nearly 10,000 feet above sea level (Strelzoff, 2022). The San Joaquin River travels over 300 miles, making it the longest river in central California. The mainstem of the San Joaquin River is divided into three sections: the upper, middle, and lower sections. The upper San Joaquin River is defined as the mainstem upstream (south) of Friant Dam (Millerton Reservoir) and includes the north, middle, and south forks. The upper watershed includes approximately 1,675 square miles (sq. mi.) (approximately 1.1 million acres), and the river flows 66 miles from the south fork to Friant Dam. The lower San Joaquin River is defined as the mainstem north (downstream) of the confluence with the Merced River to Vernalis. The watershed comprises 12,250 square miles (approximately 7.8 million acres), and the lower portion of the river is approximately 115 miles long (NOAA, 2022). The San Joaquin river provides irrigation water and drinking water to the San Joaquin Valley.

The Calaveras River, also with headwaters in the Sierra Nevada, drains a watershed of about 530 sq. mi. and flows into and across the Subbasin to its confluence with the San Joaquin River on the northwest side of Stockton. Flow in the Calaveras River below the New Hogan Reservoir varies seasonally from 608 acre-feet per day (AF/day) to 19,800 AF/day and is dependent on discharges from the on-stream reservoir. These flows correlate to discharges from 223 to over 10,000 cubic feet per second (cfs) reported by the USGS below the New Hogan Reservoir (ESJGA, 2019).

The Mokelumne River drains a watershed of about 2,140 sq. mi. and flows through the dissected uplands between Jackson and San Andreas into Pardee Reservoir, where it is released to flow downstream into Camanche Reservoir and out along the alluvial plains and fans toward its confluence with the San Joaquin River near Isleton. On the north boundary of the ESJS is Dry Creek and the Lower Dry Creek Watershed, the majority of which is within Cosumnes Subbasin. Dry Creek is mapped as an ephemeral drainage and is tributary to the Mokelumne River with its confluence near Thornton. Flow in the Mokelumne River below the Camanche Reservoir varies seasonally and is dependent on discharges from the on-stream reservoir, from less than 200 AF/day during the dry season to 9,900 AF/day during the wet season. These flows correlate to discharges from as low as 100 to no more than 5,000 cfs reported by the USGS below the Camanche Dam. Major watersheds of the river are the Upper Mokelumne River (most of which is outside of the Subbasin to the east with a small portion overlapping with Cosumnes Subbasin) and the Lower Mokelumne River (mostly contained in the Subbasin with a small portion intersecting the South American and Solano Subbasins) (ESJGA, 2019).

2.7.2 Base of Fresh Water and Base of USDWs

The owner or operator of a proposed Class VI injection must define the general vertical and lateral limits of all USDWs and their positions relative to the injection zone and confining zones. The intent of this information is to demonstrate the relationship between the proposed injection formation and any USDWs, and it will support an understanding of the water resources near the proposed injection well. A USDW is defined as an aquifer or its portion which supplies any public water system; or which contains a sufficient quantity of ground water to supply a public water system and currently supplies drinking water for human consumption; or contains fewer than 10,000 mg/L TDS; and which is not an exempted aquifer. The freshwater aquifer zone is

defined by California State Water Resources Control Board Resolution 88-63 as containing less than 3,000 mg/L TDS. For the California Sustainable Groundwater Management Act (SGMA), the bottom of the groundwater basin is defined as the approximated bottom of the Mehrten Formation (ESJGA, 2019).

Base of Fresh Water

The base of fresh water helps define the aquifers that are used for public water supply. Local water agencies in the subbasins have participated in various studies to comply with SGMA. There is a significant thickness of sedimentary strata overlying basement bedrock. Therefore, it is appropriate to consider water quality when delineating the basin bottom (DWR, 2016a).

USGS mapped the base of fresh groundwater based on measured specific conductance of less than 3,000 micromhos per centimeter, which is approximately 2,000 mg/L TDS (Kang et al., 2020). The base of fresh groundwater is deepest in the southwestern portion of the AoR (**Figure 2.7-2**). The base of fresh water within the AoR as estimated by the Eastern San Joaquin Groundwater Authority (ESJGA) groundwater sustainability plan shown in **Figure 2.7-3** (ESJGA, 2019). The base of freshwater for the southernmost portion of the AoR is also shown in cross-section in **Figure 2.7-4** (ESJGA, 2019)

Calculation of Base of Fresh Water and USDW

CTV has used geophysical logs to investigate the USDWs and the base of the USDWs. The calculation of salinity from logs used by CTV is a four-step process:

1. Convert measured density or sonic to formation porosity, using the following equation:

$$POR = \frac{(Rhom - RHOB)}{(Rhom - Rhof)} \quad (6)$$

where POR = formation porosity
Rhom = formation matrix density, g/cc; 2.65 g/cc is used for sandstones
RHOB = calibrated bulk density taken from well log measurements (g/cc)
Rhof = fluid density (g/cc); 1.00 g/cc is used for water-filled porosity

The equation to convert measured sonic slowness to porosity is:

$$POR = -1\left(\frac{\Delta tma}{2\Delta tf} - 1\right) - \sqrt{\left(\frac{\Delta tma}{2\Delta tf} - 1\right)^2 + \frac{\Delta tma}{\Delta tlog} - 1} \quad (7)$$

where POR = formation porosity
Δtma = formation matrix slowness (μs/ft); 55.5 μs/ft is used for sandstones
Δtf = fluid slowness (μs/ft); 189 μs/ft is used for water-filled porosity
Δtlog = formation compressional slowness from well log measurements (μs/ft)

2. Calculate apparent water resistivity using the Archie equation:

$$Rwah = \frac{POR^m R_t}{a} \quad (8)$$

where Rwah = apparent water resistivity (ohm-m)
POR = formation porosity
m = the cementation factor; 2 is the standard value
R_t = deep reading resistivity taken from well log measurements (ohm-m)
a = the archie constant; 1 is the standard value

3. Correct apparent water resistivity to a standard temperature of 75°F:

$$Rwahc = Rwah \frac{TEMP+6.77}{75+6.77} \quad (9)$$

where Rwahc = apparent water resistivity (ohm-m), corrected to surface temperature
TEMP = downhole temperature based on temperature gradient (°F)

4. Convert temperature-corrected apparent water resistivity to salinity (Davis 1988):

$$SAL\_a\_EPA = \frac{5500}{Rwahc} \quad (10)$$

where SALa_EPA = salinity from corrected Rwahc (parts per million [ppm])

The evaluation of electrical logs from gas exploration and production wells located in and near the King Island Gas Field indicates that the base of freshwater occurs at about 750 feet below the ground surface and is separated from the target injection reservoir by about 2,600 feet of sedimentary rocks, including two competent shale formations (the Nortonville Shale and the Capay Shale). The base of freshwater (TDS <3,000 mg/L) is shown on the geologic cross section displayed in **Figure 2.2-5.** The base of the lowermost USDW (between 3,000 and 10,000 mg/L TDS) occurs at approximately 2,287 feet below ground surface within the project AoR. The base of the lowermost USDW is shown on the geologic cross section displayed in **Figure 2.2-5** and in map view on **Figure 2.7-5.**

2.7.3 Formations with USDWs

The groundwater basin is composed of six hydraulically connected formations that store and transmit water: (1) Younger Alluvium and Modesto/Riverbank Fms., (2) Turlock Lake Fm., (3) Laguna Fm., (4) Mehrten Fm., (5) Valley Springs Fm., (6) Ione Fm, and (7) Marine and Non-Marine Strata. These formations comprise the principal aquifer. **Table 2.7-1** provides the relationships between formation name and geologic age.

Younger Alluvium and Modesto/Riverbank

The Younger Alluvium includes recent sediments that have been deposited by streams including the Cosumnes River and Mokelumne River. The maximum thickness of Younger Alluvium, where it exists, is 50 feet and is comprised of continental unconsolidated gravel and coarse to medium sand deposited along present stream channels (ESJGA, 2019). The sand and gravel

deposits are highly permeable and comprise a significant avenue for percolation to underlying formations (ESJGA, 2019).

The maximum thickness of the Modesto Formation is 65 to 130 feet and is composed of mainstream arkosic sediments and associated deposits of local derivation laid down during the last major series of aggradation events in the eastern San Joaquin Valley (Marchand & Allwardt, 1981). Gravel, sand, and silt were deposited as a series of coalescing alluvial fans extending continuously from the Kern River drainage on the south to the Sacramento River tributaries in the north (ESJGA, 2019).

Riverbank Formations materials are similar in character to the Modesto Formation. The Riverbank Formation shows a variable thickness that tends to increase toward the major river channels, with a maximum thickness ranging from 150 to 250 feet (ESJGA, 2019). Together the Modesto and Riverbank formations make up an unconfined aquifer with moderate permeability (ESJGA, 2019).

Turlock Lake

The Turlock Lake Formation consists primarily of arkosic alluvium, mostly fine sand, silt, and in places clay, at the base grading upward into coarse sand and occasional coarse pebbly sand or gravel (Marchand & Allwardt, 1981). The Turlock Lake commonly stands topographically above the younger fans and terraces throughout the northeastern San Joaquin Valley in a broad band between the Merhten, Laguna, and the younger Riverbank and Modesto alluvial fans to the west. A buried soil separates the Turlock Lake Formation into two units (Upper and Lower) in the northeastern San Joaquin Valley. The thickness of the Turlock Lake is variable and appears to increase toward the east. The maximum thickness is 1,000 feet, and the formation has generally low permeability and is a confined to an unconfined aquifer (ESJGA, 2019).

Laguna Formation

The Pliocene to Pleistocene Laguna Formation is composed of discontinuous lenses of unconsolidated to semiconsolidated alluvial sands, gravels, and silts and is typically light brown. These poorly exposed stream-laid alluvial deposits form high terraces and are associated with the last major uplift in the Sierra Nevada. A transition zone occurs between the Laguna Formation and underlying Mehrten Formation, where non-volcanic sediments of the Laguna Formation are interbedded with the volcanic sediments of the Mehrten Formation (DWR, 1974). The Laguna Formation outcrops in the northeastern part of San Joaquin County and dips at 90 feet per mile (ft/mi) and reaches a maximum thickness of 1,000 feet, with the thickest areas (400 to 1,000 feet) observed near the Mokelumne River in the Stockton Area (DWR, 1967). The Laguna Formation is moderately permeable with some reportedly highly permeable coarse-grained fresh water-bearing zones (ESJGA, 2019).

Mehrten Formation

Overlying the Valley Springs Formation is the Miocene Age Mehrten Formation, described as being stream channel, alluvial, and mudflow deposits derived mainly from andesitic volcanic rocks. The Mehrten Formation consists of two elements: (1) black volcanic sand, silt, and clay layers called “Black Sands”; and (2) dense tuff breccia (DWR, 1974). The Black Sands range

between five to 20 feet thick and are highly permeable, which yield moderate to high quantities of groundwater to wells. The tuff breccia beds act as local confining layers (DWR, 1974). The base of the Mehrten Formation is a thick bed of hard gray sandstone (DWR, 1974).

The Mehrten thickens in the northeastern part of the San Joaquin Valley can be more than 700 to 1,200 feet thick at depths ranging from more than 300 feet below ground on the east side of the valley to depths exceeding 1,400 feet along the central portion of the valley. The contact between the Mehrten Formation and underlying Valley Springs Formation is a non-distinct unconformity (ESJGA, 2019).

Valley Springs Formation

The Oligocene-age Valley Springs Formation is a stream channel and alluvial deposits derived mainly from rhyolitic volcanic rocks including some white, welded tuffs, and ash flows. The basal contact of the Valley Springs Formation is characterized, locally, by the presence of rhyolitic conglomerate. These tuffs may display alteration to clays, and, in extreme cases, only a claystone bed with relict tuffaceous texture remains. Pure deposits of rhyolitic ash exist in areas, while many sand and ash beds are present. In general, the clay beds of the Valley Springs Formation are greenish in color, may contain silt, sand, and large pumice fragments. The sandstones range in grainsize from fine to coarse and are typically well-cemented. Predominantly composed of quartz and pre-Cretaceous material, the relatively sparse conglomerate lenses within the tuff, clay, and sandstone may also contain pumice fragments. The Valley Springs Formation has a maximum thickness of approximately 500 feet and is predominantly fine-grained, containing less coarse-grained deposits. In the Central Valley, the Valley Springs Formation is considered to be largely non-water-bearing due to its low permeability (ESJGA, 2019).

Ione Formation

The Eocene-age Ione Formation has been mapped along the eastern margin of the ESJS and, as described by Loyd (1983), contains interbedded kaolinitic clay, quartz sand, sandy clay, and lignite. The Ione Formation is characteristically light in color, with color influenced by iron oxide, lignite, and carbonaceous mud rocks and shale (Creely & Force, 2007). The Ione Formation contains saline waters except where flushed in outcrop areas (ESJGA, 2019). Ione sand has a white color with a pearly luster and appears massive; however, closer examination usually reveals cross-stratification, heavy mineral laminae, and burrows (Creely & Force, 2007). Quartz is abundant with varying feldspar content in both members.

Undifferentiated Sediments (Marine and Non-Marine)

Undifferentiated sediments below the Ione Formation and above the Nortonville Shale contain approximately 3,000 to 10,000 mg/L TDS water and represent the lowermost USDW in the project area.

2.7.4 Geologic Cross-Sections Illustrating Formations with Base of Fresh Water

Hydrogeologic cross-section B-B’ along the southern edge of the AoR (**Figures 2.7-3 and 2.7-4**) illustrates the vertical distribution of geologic formations and aquifer material that comprise the

sediments that could reasonably be tapped for groundwater supply (ESJGA, 2019). Cross-Section B-B' extends for approximately 28 miles. The cross-section was reproduced from ESJGA (2019) based on the 330 well logs in the Subbasin. From this data, well depths for municipal and irrigation wells range from 75 to over 800 feet bgs, with an average depth of 350 feet bgs. Well logs were reviewed for the following information used in putting together the cross-section:

- Depth of water table
- Depth and thickness of saturated fine to coarse-grained sand and gravel layers
- Depth and thickness of discrete layers of sands
- Depth and thickness of discrete clay or silt layers that locally confine groundwater
- Depth of water-bearing aquifer materials (e.g., sands and gravels) down to the base of fresh water and deeper, where available

Analysis identified significant permeable zones with high production rates and good water quality at relatively shallow depths (less than 700 feet bgs) due to the following conditions:

- The relatively shallow depths of production wells had high specific capacity that met the water supply demand and reduced the cost associated with drilling deeper.
- The base of fresh groundwater throughout the ESJB ranges from depths of 700 to 1,900 feet bgs.
- Deeper water is saline and not considered suitable for potable or agricultural use.

2.7.5 Principal Aquifer

In the SGMA regulations, principal aquifers are defined as aquifers or aquifer systems that store, transmit, and yield significant or economic quantities of groundwater to wells, springs, or surface water systems. There is one principal aquifer in the project area, which is primarily composed of post-Eocene sedimentary deposits. The principal aquifer is divided into the shallow zone, intermediate zone, and the deep zone. The zones have favorable aquifer characteristics that deliver a reliable water resource because of their basin location and sand thickness (ESJGA, 2019).

The zones are as follows:

- Shallow Aquifer Zone that consists of the alluvial sands and gravels of the Modesto, Riverbank, and Upper Turlock Lake Formations
- Intermediate Aquifer Zone that consists of the Lower Turlock Lake and Laguna Formations
- Deep Aquifer Zone that consists of the consolidated sands and gravels of the Mehrten Formation

Details on the formations are provided in Section 2.7-3

Shallow Aquifer Zone

The shallow, water-bearing zone is composed of permeable sediments from recent alluvium, Modesto/Riverbank Formations, and the upper unit of the Turlock Lake Formation that are present west of the older geologic formations and extend across the majority of the ESJS. This zone is generally unconfined above the aquitards (clays/silts, including Corcoran clay, and old soil horizons/hardpan layers; ESJGA, 2019).

The depositional structure on the eastern side of the valley trough is depicted on the hydrogeologic cross-sections A-A' and B-B' (**Figure 2.7-4**). This structure results in the groundwater flow that follows both the dip of the beds and hydraulic head differentials. Erosional and depositional features dominate aquifer characteristics. The cross-sections also depict the aquifer thickness from 30 feet to greater than 300 feet (ESJGA, 2019).

Intermediate Aquifer Zone

As depicted on the hydrogeologic cross-sections A-A' and B-B' (**Figure 2.7-4**), sands, typically from 10 to over 60 feet thick, are found below the low permeability clay layers. The sands and gravels are developed with one relatively continuous sand unit at 350 feet bgs, within the top of the lower unit of the Turlock Lake Formation and Laguna Formation, thinning out at topographic highs to the east. Eastern basin depositional structure shows pinching, wedging, and combination water-bearing zones with the surficial alluvium (ESJGA, 2019).

The aquifer characteristics are supported by the sand thickness information detailed herein for the principal aquifer. The eastern distribution of this water-bearing zone near the surface suggests unconfined groundwater conditions. Typically, this zone is found semi-confined with high-yielding wells and is considered the current primary production zone (ESJGA, 2019).

Deep Aquifer Zone

The water-bearing black sands of the semi-consolidated Mehrten Formation are considered a significant source of water for ESJS production wells. The formation is thick in the west, with a limited number of deep wells that penetrate the entire depth of this unit. This water-bearing zone is confined due to the thick overlying clay units, consolidation, and basin location. Semi-confined conditions are more likely to the east because of the dipping of beds and stratigraphic layer thinning and erosion of clay/silt beds. Consolidated sediments of the Mehrten and Valley Springs Formations are at valley bottom depth and exposed on the eastern foothills. Recharge to these aquifer formations occurs because of the high topographic setting with increased rainfall and exposure of weathered surface and runoff from the adjacent fractured Sierran bedrock (ESJGA, 2019).

2.7.6 Groundwater Levels and Flow

Figure 2.7-6 shows a groundwater contour map reproduced from the ESJS Groundwater Sustainability Plan for the fourth quarter 2017 (ESJGA, 2019). The horizontal groundwater flow direction for the ESJS is typically towards areas of lower groundwater near the center of the Subbasin. The flow generally mirrors topography and is relatively consistent over time. The flow direction follows the overall east dipping gradient of the geologic formations in the eastern

portions of the Subbasin. Higher groundwater elevations are in the foothills on the east side of the Subbasin, and the elevations decrease following the topography. In the western portion of the Subbasin, groundwater flows east toward areas with relatively lower groundwater elevation. Groundwater elevation is typically lower in monitoring wells with deeper screen placement, suggesting downward flow of groundwater (ESJGA, 2019).

2.7.7 Water Supply and Groundwater Monitoring Wells

The California State Water Resources Control Board Groundwater Ambient Monitoring Assessment Program (GAMA), the DWR, California Statewide Groundwater Elevation Monitoring (CASGEM), and other public databases were searched to identify any water supply and groundwater monitoring wells within a one-mile radius of the AoR. DWR's Water Data Library reports groundwater data collected from a variety of well types including irrigation, stock, domestic, and public supply wells. The State Water Board's GAMA Program was established in 2000 to create a comprehensive groundwater monitoring program throughout California and to increase public availability and access to groundwater quality and contamination information (State Water Board, 2018).

Over 125 water wells were identified within one mile of the AoR, 74 of which are production wells. Data provided from public databases indicate that the wells identified are completed much shallower than the proposed injection zone. A map of well locations and table of information are found in **Figure 2.7-7** (Water Well Map) and **Table 2.7-2** (Water Well Information), respectively.

The primary uses for groundwater obtained from the principal aquifer are irrigated agriculture, public supply, and rural domestic. Well-screen depth is provided for 18 of the 74 production wells from **Table 2.7-2**. Depths of the bottom perforated interval range from 34 to 238 feet, with an average depth of 112 feet.

2.8 Geochemistry [40 CFR 146.82(a)(6)]

2.8.1 Formation Geochemistry

All formation geochemistry information is presented in the mineralogy section (Section 2.4.1).

2.8.2 Fluid Geochemistry

Three water samples from the storage zones exist within the AoR and from surrounding gas fields in close proximity to the AoR(see **Figure 2.8-1** for well locations).

Upper Injection Zone

For the Upper Injection Zone, the well Piacentine_2-27 was sampled in 2013 from within the AoR. The measurement of TDS for the sample is 14,000 mg/L. The complete water chemistry is shown in **Figure 2.8-2**.

The well Midland_Fee_Water_Injection_1 was sampled in 1980 in the Rio Vista Gas Field. The measurement of TDS for the sample is 13,889.4 mg/L. The complete water chemistry is shown in **Figure 2.8-3**.

Salinity calculations were also performed on logs from wells within the AoR, and these showed TDS in the Upper Injection Zone being approximately 13,000 to 18,000 ppm. A conservative TDS of 14,000 ppm was used for the computational model.

Historically, King Island was a gas producing field from the Mokelumne River Formation. Analytical results from natural gas sample collected within the Upper Injection Zone within the boundaries of the AoR from Piacentine 1-27 indicates that the gas comprises nearly 92 percent methane and 8 percent nitrogen with trace amounts of ethane, propane and carbon dioxide (Medeiros, M., et al., 2018).

Lower Injection Zone

For the Lower Injection Zone, the well Trigueiro_4 was sampled in 1990 in the Rio Vista Gas Field. The measurement of TDS for the sample is 14,415 mg/L. The complete water chemistry is shown in **Figure 2.8-4**.

Salinity calculations were also performed on logs from wells within the AoR, and these showed TDS in the Lower Injection Zone being approximately 13,000 to 18,000 ppm. A conservative TDS of 14,000 ppm was used for the computational model.

No gas production is present within the Lower Injection Zone within the boundaries of the AoR, so no hydrocarbon analysis is available.

2.8.3 Fluid-Rock Reactions

Upper Confining Zone

There is no fluid geochemistry analysis for the upper confining zone. The shale will only provide fluid for analysis if stimulated. However, given the low permeability of the rock and the low carbonate content, the upper confining zone is not expected to be impacted by the CO_2 injectate.

Upper Injection Zone

Mineralogy and formation fluid interactions have been assessed for the Upper Injection Zone. The following applies to potential reactions associated with the CO_2 injectate:

- The Upper Injection Zone has a negligible quantity of carbonate minerals and is instead dominated by quartz and feldspar. These minerals are stable in the presence of CO_2 and carbonic acid, and any dissolution or changes that occur will be on grain surfaces.
- The water within the Upper Injection Zone contains minimal calcium and magnesium cations, which would be expected to react with the CO_2 to form calcium-bearing minerals in the pore space. Also, the salinity being less than 30,000 ppm will reduce the “salting out” effect seen in higher salinity brine under the presence of CO_2.

Internal Barrier

There is no fluid geochemistry analysis for the internal barrier zone. The shale will only provide fluid for analysis if stimulated. However, given the low permeability of the rock and the low carbonate content, the internal barrier is not expected to be impacted by the CO_2 injectate.

Lower Injection Zone

Mineralogy and formation fluid interactions have been assessed for the Lower Injection Zone. The following applies to potential reactions associated with the CO_2 injectate:

- The Lower Injection Zone generally has a negligible quantity of carbonate minerals and is instead dominated by quartz and feldspar. These minerals are stable in the presence of CO_2 and carbonic acid, and any dissolution or changes that occur will be on grain surfaces. The few intervals that do have higher concentrations of carbonate minerals are very thin, tight streaks caused by calcite cementing of sands. Dissolution of these will only result in the reduction of vertical permeability barriers within the formation.
- The water within the Lower Injection Zone contains minimal calcium and magnesium cations, which would be expected to react with the CO_2 to form calcium-bearing minerals in the pore space. Also, the salinity being less than 30,000 ppm will reduce the "salting out" effect seen in higher salinity brine under the presence of CO_2.

Geochemical Modeling

Using fluid geochemistry data for the injection zones, and the available mineralogy data for the injection zones and confining zones, geochemical modeling was conducted using PHREEQC (ph-REdox- Equilibrium), the USGS geochemical modeling software, to evaluate the compatibility of the injectates being considered for the project with formation rocks and fluid.

The PHREEQC software was used to evaluate the behavior of minerals and changes in aqueous chemistry and mineralogy over the life of the project, and to identify major potential reactions that may affect injection or containment.

Based on the geochemical modeling, the injection of CO_2 at the CTV V site does not cause significant reactions that will affect injection or containment. Detailed methodology and results can be found in **Appendix 3** submitted with this application.

2.9 Other Information (Including Surface Air and/or Soil Gas Data, if Applicable)

No additional information necessary.

2.10 Site Suitability [40 CFR 146.83]

Sufficient data from both wells and seismic demonstrate the integrity through lateral continuity of the storage reservoirs as well as the confining zone. Regional mapping completed by West Coast Regional Carbon Sequestration Partnership (WESTCARB), CGS, and the National Energy and Technology Lab (NETL) support the local stratigraphy, both indicating lateral continuity and regional thickness across the project AoR (Downey, 2010). This study covers formations with

sequestration and seal potential from southern Sutter County down to the Stockton Arch Fault-San Joaquin County, encompassing an area far beyond the project AoR. WESTCARB (Burton et al., 2016) evaluated CO_2 storage potential in the California Central Valley at four sites including King Island and determined that King Island met scientific criteria objectives best among all the sites.

The vertical confinement and laterally continuous geologic formations described in this report will make the site ideal for CO_2 sequestration. The Capay Shale (upper confining zone) is a regionally continuous shale that will guide the lateral dispersion of CO_2 across the AoR (**Figure 2.10-1**). The average Capay Shale thickness across the AoR is 723 feet and is sufficient to contain the total volume of injected CO_2. The Capay Shale thickness at each injection well is presented in **Table 2.10-1.** Additionally, oil and gas fields adjacent to the project AoR demonstrate adequate seal capacity in the upper confining zone. Corrosion-resistant alloy (CRA) will be used for completion of the injection and monitoring wells, inhibiting any reaction between CO_2 and wellbores.

Due to the regional continuity, thickness, and low permeability of the upper confining zone, no secondary confinement is necessary; however, another shale barrier, the Nortonville Shale, exists above the Domengine Formation monitoring sand. This additional shale unit creates another impermeable barrier that separates the injection zones from the lowermost USDW.

CTV's estimated storage for the project is 16.7 MMT of CO_2. This was arrived at through computational modeling as described below.

As discussed in **Attachment B** (Area of Review and Corrective Action Plan), a dynamic model was generated for each target injection zone with data from the static model (structure, porosity, absolute permeability, net to gross ratio, facies), special core analysis (relative permeability and capillary pressure), pressure, volume, temperature (PVT) analysis (fluid PVT), geochemical analysis (water salinity). Injector locations are based on geologic interpretation, petrophysical properties, and economic optimization. Injection rates were analyzed with flexibility to handle offset well failure during the project period. Injectors were also designed with a maximum allowable injection pressure limit. To assure storage site safety during the injection period, reservoir pressure was also controlled by critical pressure. Dynamic model results predicted a storage volume of 16.7 MMT at 25 years, using six CO_2 injection wells.

3. AoR and Corrective Action

CTV's AoR and Corrective Action Plan (**Attachment B**) pursuant to 40 CFR 146.82(a)(4), 40 CFR 146.82(a)(13) and 146.84(b), and 40 CFR 146.84(c) describes the process, software, and results to establish the AoR, and the wells that require corrective action.

AoR and Corrective Action GSDT Submissions
GSDT Module: AoR and Corrective Action

Tab(s): All applicable tabs

Please use the checkbox(es) to verify the following information was submitted to the GSDT:

☒ Tabulation of all wells within AoR that penetrate confining zone ***[40 CFR 146.82(a)(4)]***

☒ AoR and Corrective Action Plan *[40 CFR 146.82(a)(13) and 146.84(b)]*

☒ Computational modeling details ***[40 CFR 146.84(c)]***

4. Financial Responsibility

CTV's Financial Responsibility demonstration pursuant to 140 CFR 146.82(a)(14) and 40 CFR 146.85 (**Attachment H**) is met with a line of credit for Injection Well Plugging and Post-Injection Site Care and Site Closure and insurance to cover Emergency and Remedial Responses.

Financial Responsibility GSDT Submissions
GSDT Module: Financial Responsibility Demonstration ***Tab(s):*** Cost Estimate tab and all applicable financial instrument tabs Please use the checkbox(es) to verify the following information was submitted to the GSDT: ☒ Demonstration of financial responsibility ***[40 CFR 146.82(a)(14) and 146.85]***

5. Injection and Monitoring Well Construction

CTV plans to drill six new injectors for the CTV V storage project. New injection wells are planned and designed specifically for CO_2 sequestration purposes. These wells will target selective intervals within the injection zone to optimize plume development and injection conformance. Additionally, nine new monitoring wells will be constructed to support the storage project. Four injection-zone monitoring wells, one above-zone monitoring well, and four USDW monitoring wells will be constructed prior to injection (**Figure 5.0-1**).

All planned new wells will be constructed with components that are compatible with the injectate and formation fluids encountered such that corrosion rates and cumulative corrosion over the duration of the project are acceptable. The proposed well materials will be confirmed based on actual CO_2 composition such that material strength is sufficient to withstand all loads encountered throughout the life of the well with an acceptable safety factor incorporated into the

design. Casing points will be verified by trained geologists using real-time drilling data such as logging while drilling (LWD) and mud logs to ensure non-endangerment of USDW. Due to the depth of the base of the lowermost USDW, an intermediate casing string will be utilized to isolate the USDW. Cementing design, additives, and placement procedures will be sufficient to ensure isolation of the injection zone and protection of the USDW using cementing materials that are compatible with injectate, formation fluids, and subsurface pressure and temperature conditions.

The pressure within the Upper Injection Zone is approximately 2,383 psi, and the temperature is approximately 136 degrees Fahrenheit. The pressure within the Lower Injection Zone is approximately 2,994 psi, and the temperature is approximately 152 degrees Fahrenheit.

These conditions are not extreme, and CTV has extensive experience successfully constructing, operating, working over, and plugging wells in depleted reservoirs.

Appendix 5: Injection and Monitoring Well Schematics provides casing diagram figures for all injection and monitoring wells, with construction specifications and anticipated completion details in graphical and/or tabular format.

5.1 Proposed Stimulation Program [40 CFR 146.82(a)(9)]

There are no proposed stimulation programs currently.

5.2 Construction Procedures [40 CFR 146.82(a)(12)]

CTV has created Construction and Plugging documents for each project well pursuant to 40 CFR 146.82(a)(8). Each **Attachment G**: Well Construction and Plugging Plan document includes well construction information based on requirements defined within 40 CFR 146.82. The relevant attachments are:

- Attachment G1: KI-I-S1 Construction and Plugging Plan
- Attachment G2: KI-I-S2 Construction and Plugging Plan
- Attachment G3: KI-I-S3 Construction and Plugging Plan
- Attachment G4: KI-I-M1 Construction and Plugging Plan
- Attachment G5: KI-I-M2 Construction and Plugging Plan
- Attachment G6: KI-I-M3 Construction and Plugging Plan

6. Pre-Operational Logging and Testing

CTV has indicated a proposed pre-operational logging and testing plan throughout the application

documentation pursuant to 40 CFR 146.82(a)(8). Each **Attachment G**: Well Construction and Plugging Plan document (listed in Section 5.2) includes logging and testing plans for each individual project well based on requirements defined within 40 CFR 146.87.

Pre-Operational Logging and Testing GSDT Submissions
GSDT Module: Pre-Operational Testing ***Tab(s):*** Welcome tab Please use the checkbox(es) to verify the following information was submitted to the GSDT: ☒ Proposed pre-operational testing program ***[40 CFR 146.82(a)(8) and 146.87]***

7. Well Operation

7.1 Operational Procedures [40 CFR 146.82(a)(10)]

The Operational Procedures for all injectors associated with the project are detailed in **Appendix 4** (Operational Procedures) document attached with this application.

7.2 Proposed Carbon Dioxide Stream [40 CFR 146.82(a)(7)(iii) and (iv)]

CTV is planning to construct a carbon capture and sequestration "hub" project (*i.e.*, a project that collects CO_2 from multiple sources over time and injects the CO_2 stream(s) via Class VI UIC permitted injection well(s)). Therefore, CTV is currently considering multiple sources of anthropogenic CO_2 for the project. Potential sources include capture from existing and potential future industrial sources in the Sacramento Valley area, as well as Direct Air Capture (DAC). CTV would expect the CO_2 stream to be sampled at the transfer point from the source and between the final compression stage and the wellhead. Samples will be analyzed according to the analytical methods described in the "**Appendix 10**: QASP" (Table 4) document and the Testing and Monitoring Plan (**Attachment C,** see Table 1).

For the purposes of geochemical modeling, CO_2 plume modeling, AoR determination, and well design, two major types of injectate compositions were considered based on the source.

- Injectate 1: a potential injectate stream composition from DAC or a pre-combustion source (such as a blue hydrogen facility that produces hydrogen using steam methane reforming process) or a post-combustion source (such as a natural gas-fired power plant or steam generator). The primary impurity in the injectate is nitrogen.
- Injectate 2: a potential injectate stream composition from a biofuel capture source (such as a biodiesel plant that produces biodiesel from a biologic source feedstock) or from an oil and gas refinery. The primary impurity in the injectate is light end hydrocarbons (methane and ethane).

The compositions for these two injectates are shown in **Table 7.2-1**, and are based on engineering design studies and literature.

For geochemical and plume modeling scenarios, these injectate compositions were simplified to a 4-component system, shown in **Table 7.2-2** and then normalized for use in the modeling. The 4-component simplified compositions cover 99.9% by mass of Injectate 1 and 2 and cover particular impurities of concern (H_2S and SO_2). The estimated properties of the injectates at downhole conditions are specified in **Table 7.2-3**.

The anticipated injection temperature at the wellhead is 90 to 130° F.

No corrosion is expected in the absence of free-phase water provided that the entrained water is kept in solution with the CO_2. This is ensured by maintaining a <25 pounds per million cubic feet (lb/mmscf) injectate specification limit, and this specification will be a condition of custody transfer at the capture facility. For transport through pipelines, which typically use standard alloy pipeline materials, this specification is critical to the mechanical integrity of the pipeline network, and out of specification product will be immediately rejected. Therefore, all product transported through pipeline to the injection wellhead is expected to be dry-phase CO_2 with no free-phase water present.

Injectate water solubility will vary with depth and time as temperature and pressures change. The water specification is conservative to ensure water solubility across super-critical operating ranges. CRA tubing will be used in the injection wells to mitigate any potential corrosion impact should free-phase water from the reservoir become present in the wellbore, such as during shut-in events when formation liquids, if present, could backflow into the wellbore. CTV may further optimize the maximum water content specification prior to injection based on technical analysis.

8. Testing and Monitoring

CTV's Testing and Monitoring plan (**Attachment C**) pursuant to 40 CFR 146.82 (a) (15) and 40 CFR 146.90 describes the strategies for testing and monitoring to ensure protection of the USDW, injection well mechanical integrity, and plume monitoring.

Testing and Monitoring GSDT Submissions
GSDT Module: Project Plan Submissions ***Tab(s):*** Testing and Monitoring tab Please use the checkbox(es) to verify the following information was submitted to the GSDT: ☒ Testing and Monitoring Plan [40 CFR 146.82(a)(15) and 146.90]

9. Injection Well Plugging

CTV's Injection Well Plugging Plan pursuant to 40 CFR 146.92 (**Attachment G**) describes the process, materials, and methodology for injection well plugging.

Injection Well Plugging GSDT Submissions
GSDT Module: Project Plan Submissions ***Tab(s):*** Injection Well Plugging tab Please use the checkbox(es) to verify the following information was submitted to the GSDT: ☒ Injection Well Plugging Plan [40 CFR 146.82(a)(16) and 146.92(b)]

10. Post-Injection Site Care (PISC) and Site Closure

CTV has developed a Post-Injection Site Care and Site Closure Plan (**Attachment E**) pursuant to 40 CFR 146.93 (a) to define post-injection testing and monitoring.

CTV is proposing an alternative PISC timeframe as described in **Attachment E**.

PISC and Site Closure GSDT Submissions
GSDT Module: Project Plan Submissions ***Tab(s):*** PISC and Site Closure tab Please use the checkbox(es) to verify the following information was submitted to the GSDT: ☒ PISC and Site Closure Plan [40 CFR 146.82(a)(17) and 146.93(a)]
GSDT Module: Alternative PISC Timeframe Demonstration ***Tab(s):*** All tabs (only if an alternative PISC timeframe is requested) Please use the checkbox(es) to verify the following information was submitted to the GSDT: ☒ Alternative PISC timeframe demonstration ***[40 CFR 146.82(a)(18) and 146.93(c)]***

11. Emergency and Remedial Response

CTV's Emergency and Remedial Response Plan (**Attachment F**) pursuant to 40 CFR 164.94 describes the process and response to emergencies to ensure USDW protection.

Emergency and Remedial Response GSDT Submissions
GSDT Module: Project Plan Submissions ***Tab(s):*** Emergency and Remedial Response tab Please use the checkbox(es) to verify the following information was submitted to the GSDT: ☒ Emergency and Remedial Response Plan *[40 CFR 146.82(a)(19) and 146.94(a)]*

12. Injection Depth Waiver and Aquifer Exemption Expansion

No depth waiver or Aquifer Exemption expansion is being requested as part of this application.

Injection Depth Waiver and Aquifer Exemption Expansion GSDT Submissions
GSDT Module: Injection Depth Waivers and Aquifer Exemption Expansions ***Tab(s):*** All applicable tabs Please use the checkbox(es) to verify the following information was submitted to the GSDT: ☐ Injection Depth Waiver supplemental report ***[40 CFR 146.82(d) and 146.95(a)]*** ☐ Aquifer exemption expansion request and data ***[40 CFR 146.4(d) and 144.7(d)]***

13. References

Azat, J. 2019. California Central Valley Chinook Population Database Report. California Department of Fish and Wildlife. GrandTab 2019.05.07. Available at: https://www.wildlife.ca.gov/Conservation/Fishes/Chinook-Salmon/Anadromous-Assessment or http://www.calfish.org/ProgramsData/Species/CDFWAnadromousResourceAssessment.aspx.

Bartow. 1985. *Maps showing Tertiary stratigraphy and structure of the Northern San Joaquin Valley, California*. U.S. Geological Survey.

Berkstresser, C.F., Jr. 1973. *Base of fresh ground-water–Approximately 3,000 micromhos–in the Sacramento Valley and Sacramento-San Joaquin Delta, California*. U.S. Geological Survey Water-Resource Inv. 40-73. 1973

Bertoldi, G., R. Johnston, and K. Evenson. 1991. *Groundwater in the Central Valley, California –A summary report.* U.S. Geological Survey Professional Paper 1401-A. https://doi.org/10.3133/pp1401A.

Beyer, L.A. *Summary of geology and petroleum plays used to assess undiscovered recoverable petroleum resources of Sacramento Basin Province, California*. U.S. Geological Survey. 1988.

Burow, K.R., J.L. Shelton, J.A. Hevesi, and G.S. Weissmann. 2004. *Hydrologic characterization of the Modesto area, San Joaquin Valley, California*. Preliminary Draft. U.S. Geological Survey Water-Resources Investigation Report. Prepared in cooperation with Modesto Irrigation District. Sacramento, California.

Burton, E., N. Mateer, R. Myhre, and M. Stone. 2016. WESTCARB Phase III Final Report, Summary of California Activities. Prepared for California Energy Commission. Prepared by California Institute of Energy and Environment.

California Department of Water Resources (DWR). 1974a. *Bulletin 118-3, Evaluation of Groundwater Resources: Sacramento County*. Sacramento, California. July.

Chiquet, Pierre & Daridon, J.L. & Broseta, Daniel & Thibeau, S.. (2009). CO2/Water Interfacial Tensions under Pressure and Temperature and Conditions of CO2 Geological Storage. Energy Convers. Manage.. 50. 431-431.

DWR. 1974b. *Bulletin 146, San Joaquin County Investigation.* San Joaquin, California.

DWR. 1978. *Bulletin 118-6, Evaluation of Groundwater Resources: Sacramento Valley*. Sacramento, California. August.

DWR. 1995. *Delta Atlas, Sacramento-San Joaquin*. Sacramento, California. July.

DWR. 2003a. *Bulletin 118—Update 2003, California's Groundwater*. Sacramento, California. October.

DWR. 2003b. *Sacramento Valley Groundwater Basin South American Subbasin.* Accessed June 24, 2020. Available at: https://water.ca.gov/-/media/DWR-Website/Web-Pages/Programs/Groundwater-Management/Bulletin-118/Files/2003-Basin-Descriptions/5_021_65_SouthAmericanSubbasin.pdf.

DWR. 2006. *5-022.01* S*an Joaquin Valley Groundwater Basin-Eastern San Joaquin Subbasin.* Accessed May 18, 2023. Available at: https://water.ca.gov/-/media/DWR-Website/Web-Pages/Programs/Groundwater-Management/Bulletin-118/Files/2003-Basin-Descriptions/5_022_01_EasternSanJoaquinSubbasin.pdf.

DWR. 2020. *5-021.65 Sacramento Valley – South American Basin Boundaries*. May

Chapman, R.H. and C.C. Bishop. 1975. *Geophysical investigations in the Ione Area*, *Amador, Sacramento, and Calaveras Counties, California*. California Division of Mines and Geology Special Report 117: 1-27.

Creely, S. and E. Force. 2007. *Type region of the Ione Formation (Eocene), central California: Stratigraphy, paleogeography and relation to auriferous gravels*. U.S. Geological Survey.

Davis G.H., J.H. Green, S.H. Olmstead, and D.W. Brown. 1959. *Ground water conditions and storage capacity in the San Joaquin Valley, California*. U.S. Geological Survey Water Supply Paper No. 1469: 287.

Davis, K.E. 1988. *Survey of methods to determine total dissolved solids concentrations*. U.S. Environmental Protection Agency Underground Injection Control Program. Prepared by Ken E. Davis Associates under subcontract to Engineering Enterprises, INC. EPA LOE Contract No. 68-03-3416, Work Assignment No. 1-0-13, Keda Project No. 30-956.

Downey, C. and J. Clinkenbeard. 2006. *An overview of geologic carbon sequestration potential in California*. California Energy Commission, PIER Energy-Related Environmental Research Program.

Downey, C. and J. Clinkenbeard. 2010. *Preliminary geologic assessment of the carbon sequestration potential of the Upper Cretaceous Mokelumne River, Starkey, and Winters Formations – Southern Sacramento Basin, California*. California Geological Survey.

EKI Environment & Water, Inc. (EKI). 2021. *Groundwater sustainability plan for the Cosumnes Subbasin.* December 2021.

Eastern San Joaquin Groundwater Authority (ESJGA), 2019. *Eastern San Joaquin Groundwater Subbasin groundwater sustainability plan*. November 2019.

Ferriz, H. 2001. Groundwater resources of northern California: an overview. *Engineering Geology Practice in Northern California.* Bulletin 210: 19-47.

Geoconsultants, Inc. 2016. *Geological and geophysical survey for proposed basin boundary adjustment*. Sloughhouse Resource Conservation District, Sacramento County, California.

Graham, S.A., C. McCloy, M. Hitzman, R. Ward, and R. Turner. 1984. Basin evolution during change from convergent to transform continental margin in Central California. *The American Association of Petroleum Geologists* Bulletin 68, 3.

Haeri, Foad & Tapriyal, Deepak & Sanguinito, Sean & Fuchs, Samantha & Shi, Fan & Dalton, Laura & Baltrus, John & Howard, Bret & Matranga, Christopher & Crandall, Dustin & Goodman, Angela. (2020). CO2-Brine Contact Angle Measurements on Navajo, Nugget, Bentheimer, Bandera Brown, Berea, and Mt. Simon Sandstones. Energy & Fuels. XXXX. 10.1021/acs.energyfuels.0c00436.

Heidbach, O., M. Rajabi, X. Cui, K. Fuchs, B. Müller, J. Reinecker, K. Reiter, M. Tingay, F. Wenzel, F. Xie, M. O. Ziegler, M.-L. Zoback, and M. D. Zoback. 2018. The World Stress Map database release 2016: Crustal stress pattern across scales. *Tectonophysics* 744: 484-498. doi:10.1016/j.tecto.2018.07.007.

Heidbach, O., M. Rajabi Mojtaba; K. Reiter; M. Ziegler and WSM team. 2016. World Stress Map Database Release 2016*. GFZ Data Services*. doi:10.5880/WSM.2016.001.

Hotchkiss, W.R. and G.O. Balding. 1971. *Geology, hydrology, and water quality of the Tracy-Dos Palos area, San Joaquin Valley, California*. U.S. Geological Survey. Open-File Report. Hotchkiss and Balding. 1971.

Huey, W.F., 1957. Lodi Gas Field: California Division of Oil and Gas, Summary of operations – *California Oil Fields* 43, no. 1: 42-46.

Ingram G.M., J.L. Urai., M.A. Naylor. 1997. *Hydrocarbon Seals: Importance for exploration and production, sealing processes, and top seal assessment*. Norwegian Petroleum Society (NPF) Special Publication, eds. Moller-Pedersen P. and A.G. Koestler. 7: 165–175.

Ingram, G. and J. Urai. 1999. *Top-seal leakage through faults and fractures: the role of mudrock properties*. Geological Society, London, Special Publications. 158. 125-135. 10.1144/GSL.SP.1999.158.01.10.

Johnson, D.S. 1990. Depositional environment of the Upper Cretaceous Mokelumne River Formation, Sacramento Basin. California. *American Assoc. of Petroleum Geologists* Bulletin 74:5 1990: 686 p.

Jones & Stokes. 2007. *Final tribal environmental impact report for the Buena Vista Rancheria of Me-Wuk Indians of California Gaming Facility.* Prepared by Jones & Stokes. May 2007.

Juhasz, I. 1979. The Central Role Of Qv And Formation-water Salinity In The Evaluation Of Shaly Formations*. *The Log Analyst*, 20.

Kang, M., et al. 2020. *Base of fresh water, groundwater salinity, and well distribution across California.* Proceedings of the National Academy of Sciences 117.51. 32302-32307. 2020.

Larry Walker Associates/Woodard & Curran. LWA/W&C. 2021. *South American Subbasin Groundwater Sustainability Plan*. October 29, 2021.

Leong, J.K., and J.R. Tenzer. 1994. *Production optimization of a mature gas field*. Paper presented at the SPE Western Regional Meeting, Long Beach, California.

Lohr, Celeste & Hackley, Paul. (2018). [Open Access] Using mercury injection pressure analyses to estimate sealing capacity of the Tuscaloosa marine shale in Mississippi, USA: Implications for carbon dioxide sequestration. International Journal of Greenhouse Gas Control. 78. 375-387. 10.1016/j.ijggc.2018.09.006.

Loken, K.P., 1957. Thornton Gas Field: California Division of Oil and Gas, Summary of Operations. *California Oil Fields* 43, no. 1: 37-41.

Loyd, R. 1983. *Mineral Land Classification of the Sutter Creek 15-Minute Quadrangle, El Dorado and Amador Counties, California*.

Lund Snee, J-E, and M. Zoback. 2020. Multiscale variations of the crustal stress field throughout North America. *Nature Communications* 11: 1951.

Magoon, L.B. and Valin, Z.C. 1995. *Sacramento Basin Province (009).* United States Department of the Interior Geological Survey, National assessment of United States oil and gas resources-results, methodology, and supporting data.

Marchand, D.E. and Allwardt, A. 1981. Late Cenozoic Stratigraphic Units, Northeastern San Joaquin Valley, California.

Medeiros, M., et al., 2018. *Technical Feasibility of Compressed Air Storage (CAES) Utilizing a Porous Rock Reservoir*. Report Number DOE-PGE-00198-1. March 2018.

Mount, V and J. Suppe. 1992. Present-day stress orientations adjacent to active strike-slip faults –California and Sumatra. *Journal of Geophysical Research.* 971. 11995-12013. 10.1029/92JB00130.

Northern California Earthquake Data Center (NCEDC). 2014. UC Berkeley Seismological Laboratory. Dataset. doi:10.7932/NCEDC.

Nilsen, T. H., and S.H. Clarke, Jr. 1975. *Sedimentation and tectonics in the Early Tertiary Continental Borderland of Central California*. Geological Survey Professional Paper 925.

NOAA Fisheries (NOAA) 2022. *San Joaquin River Basin* August 6, 2022. www.fisheries.noaa.gov/west-coast/habitat-conservation/san-joaquin-river-basin#san-joaquin-river.

O'Geen, A, M. Saal, H. Dahlke, D. Doll, R. Elkins, A. Fulton, G. Fogg, T. Harter, J. Hopmans, c. Ingels, F. Niederholzer, S. Sandoval Solis, P. Verdegaal, and M. Walkinshaw. 2015. *Soil suitability index identifies potential areas for groundwater banking on agricultural lands.*

Page, R.W. 1974, *Base and thickness of the Post-Eocene continental deposits in the Sacramento Valley, California.* U.S. Geological Survey Water-Resources Investigations Report 73-45, 16 pp.

Page, R.W. 1986. *Geology of the fresh ground-water basin of the Central Valley, California, with texture maps and sections*. USGS Professional Paper 1401-C.

Piper A.M., H.S. Gale, H.E. Thomas, T.W. Robinson. 1939. *Geology and ground-water hydrology of the Mokelumne Area, California*. U.S. Geological Survey Water-Supply, Paper 780.

Ramboll. 2021. *TEM Geophysical Investigations Cosumnes.* tTEM & WalkTEM Surveys.

Robertson-Bryan, Inc. and WRIME. 2011. *South Basin Groundwater Management Plan.* Prepared for South Area Water Council. October 2011.

Sacramento Central Groundwater Authority (SCGA). 2012 *Groundwater Elevation Monitoring Plan*. February 2012.

Sacramento County Water Agency (SCWA). 2021. *Draft Zone 40 Water Supply Master Plan Amendment*. Prepared by Brown and Caldwell. January 13, 2021.

Shafer, John & Neasham, John & Group, Reservoir. (2000). Mercury porosimetry protocol for rapid determination of petrophysical and reservoir quality properties. Proceeding of the International Symposium of the Society of Core Analysts, SCA.

Snider, B. and B. Reavis. 2000. *Cosumnes River Chinook Salmon Spawner Escapement, Rearing and Emigration Surveys 1998-99*. California Department of Fish and Game Habitat Conservation Division Native Anadromous Fish and Watershed Branch Stream Evaluation Program. August 2000.

State Water Resources Control Board. 2018. *GAMA Program - About*. Accessed June 24, 2020.

Strelzoff, A. 2022,. Engineering water in California and the case of the San Joaquin River. *Engineering with Nature.* January 20, 2022.

https://ewn.erdc.dren.mil/engineering-water-in-california-and-the-case-of-the-san-joaquin river/#:~:text=The%20San%20Joaquin%20River%20begins,elevation%20of%20nearly%2010%2C000%20feet.

Sullivan, R. and M. Sullivan. 2012. Sequence stratigraphy and incised valley architecture of the Domengine Formation, Black Diamond Mines Regional Preserve and the Southern Sacramento Basin, California. *U.S.A. Journal of Sedimentary Research.*

Towell, T. 1992. *Public health and safety- seismic and geological hazards*. July.

U.S. Environmental Protection Agency (EPA). 1988. *Survey of methods to determine total dissolved solids concentrations*. Prepared by Ken E. Davis Associates under subcontract to Engineering Enterprises, INC. EPA LOE Contract No. 68-03-3416, Work Assignment No. 1-0-13, Keda Project No. 30-956. Underground Injection Control Program.

Unruh, J.R., and C.S. Hitchcock. 2009. *Characterization of potential seismic sources in the Sacramento-San Joaquin Delta, California*. U.S. Geological Survey National Earthquake Hazards Reduction Program.

Vista Clara Inc. 2021. *Surface NMR Survey Cosumnes River Basin.*

Wagner, D.L., E.J Bortugno, and R.D. McJunkin. 1991. *Geologic Map of the San Francisco – San Jose Quadrangle*. California Geological Survey, Regional Geologic Map No. 5A, 1:250,000 scale.

Whiteaker T.L., N. Jones, G. Strassberg, A. Lemon, D. Gallup. 2012. GIS-based data model and tools for creating and managing two-dimensional cross sections. *Computers & Geosciences* 39: 42-49.

Williamson, C.R., and D.R. Hill. 1981. *Submarine-Fan deposition of the Upper Cretaceous Winters Sandstone, Union Island Gas Field, Sacramento Valley, California.*: The Society of Economic Paleontologists and Mineralogists (SEPM) Deep-Water Clastic Sediments (CW2).

Wong, et al. .2010. *Quantifying the Earthquake Threat in the Sacramento – San Joaquin Delta, California.*

Woodard & Curran. 2021. *CoSANA: An Integrated Water Resources Model of The Cosumnes, South American, And North American Groundwater Subbasins*. November 2021.

Figures

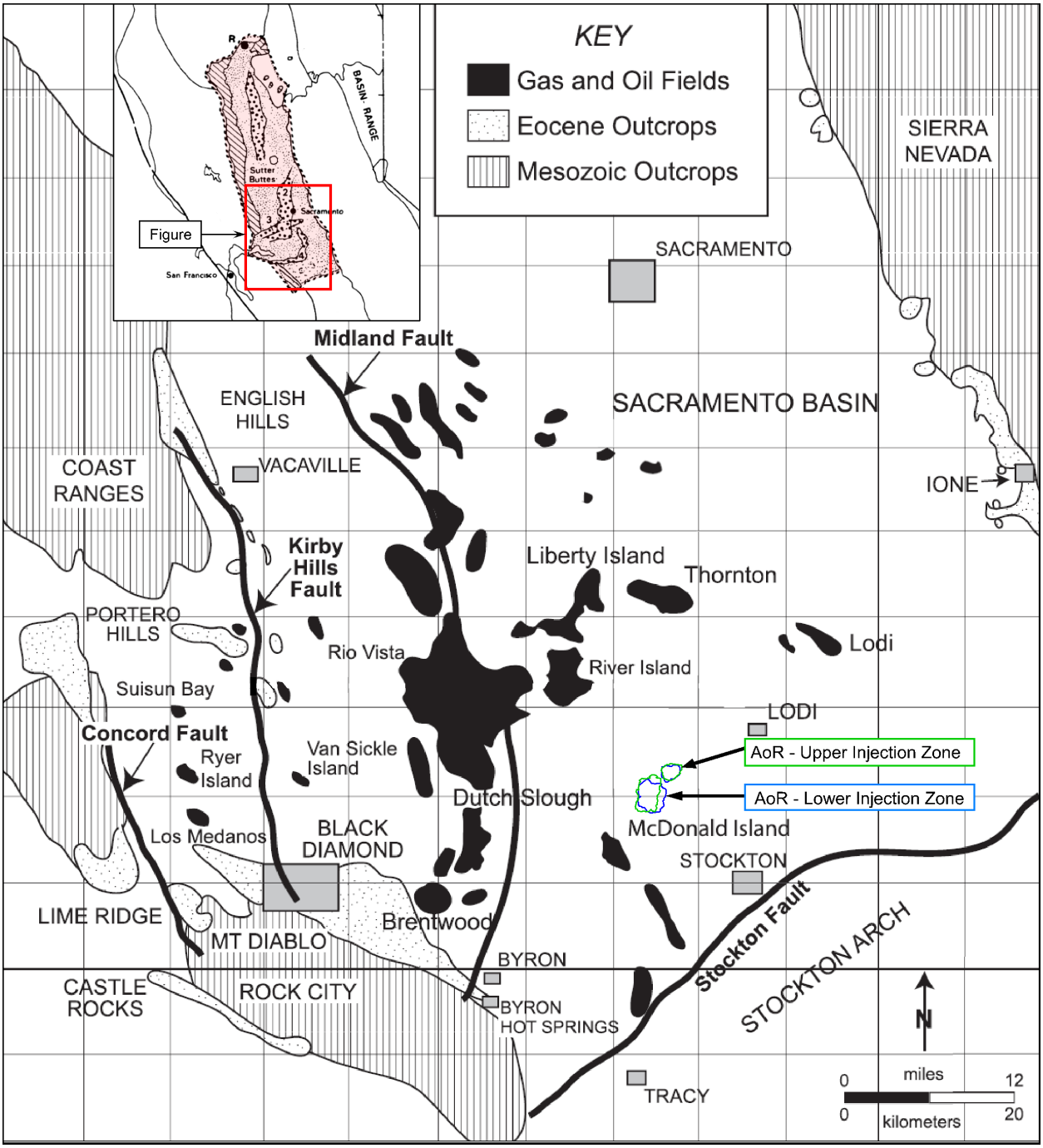

Figure 2.1-1. Location map of the project AoR for the Upper Injection Zone (green) and Lower Injection Zone (blue) in relation to the Sacramento Basin. Figure modified from Sullivan and Sullivan, 2012.

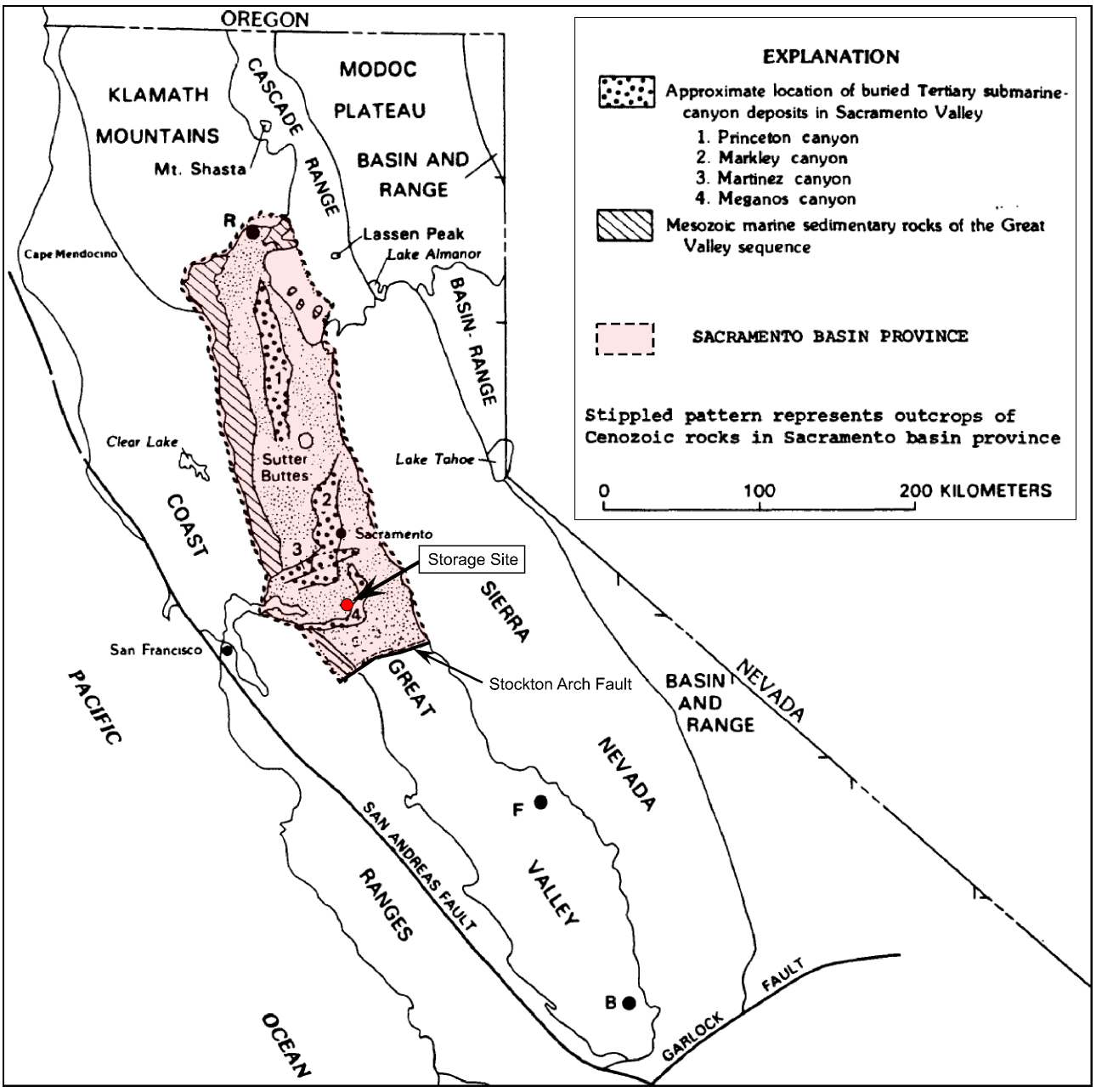

Figure 2.1-2. Location map of California modified from (Beyer, 1988) & (Sullivan, 2012). The Sacramento Basin regional study area is outlined by a dashed black line. B – Bakersfield; F – Fresno; R – Redding.

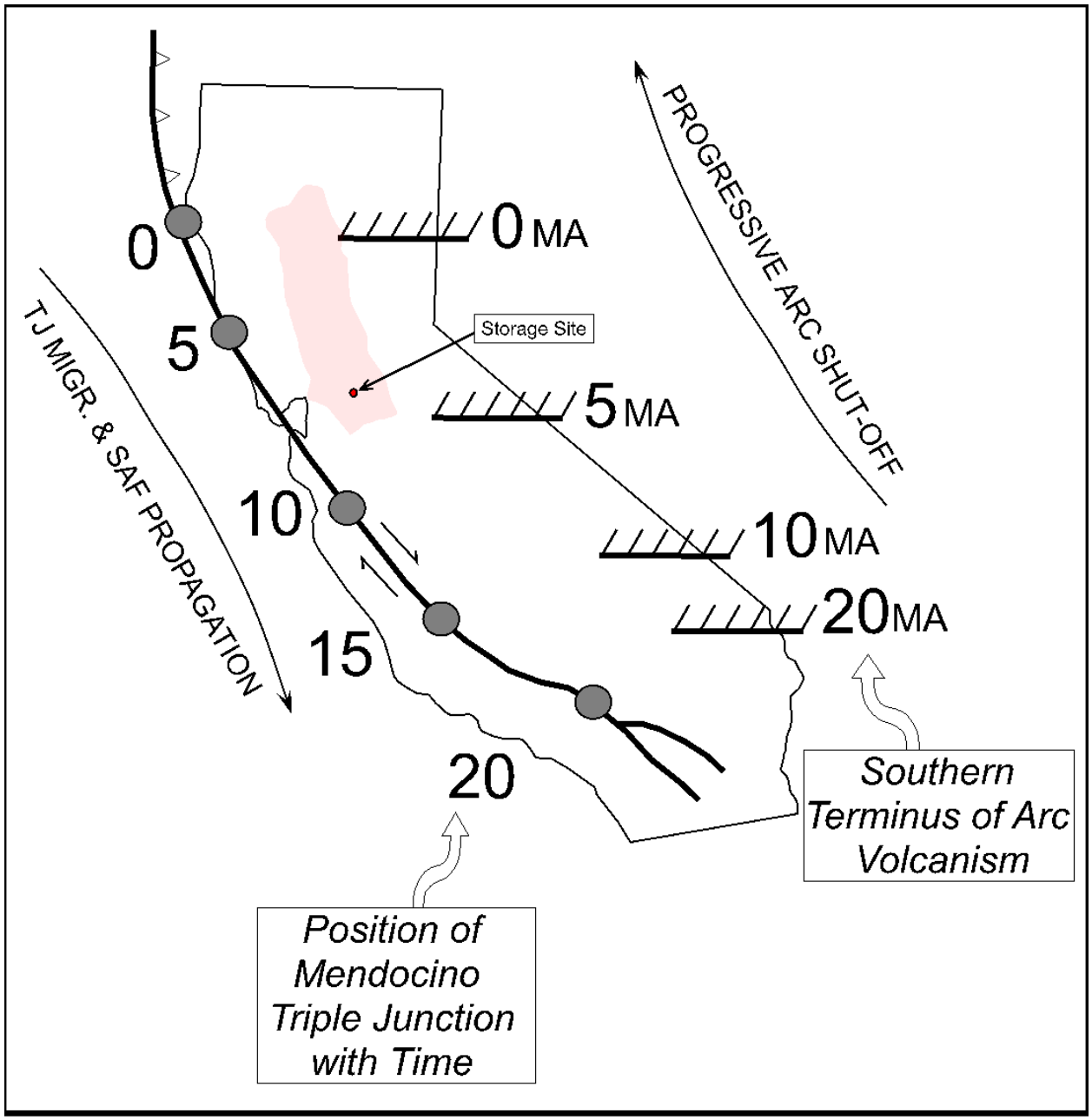

Figure 2.1-3. Migrational position of the Mendocino triple junction (Connection point of the Gorda, North American and Pacific plates) on the west and migrational position of Sierran arc volcanism in the east (Graham, 1984). The figure indicates space-time relations of major continental-margin tectonic events in California during the Miocene.

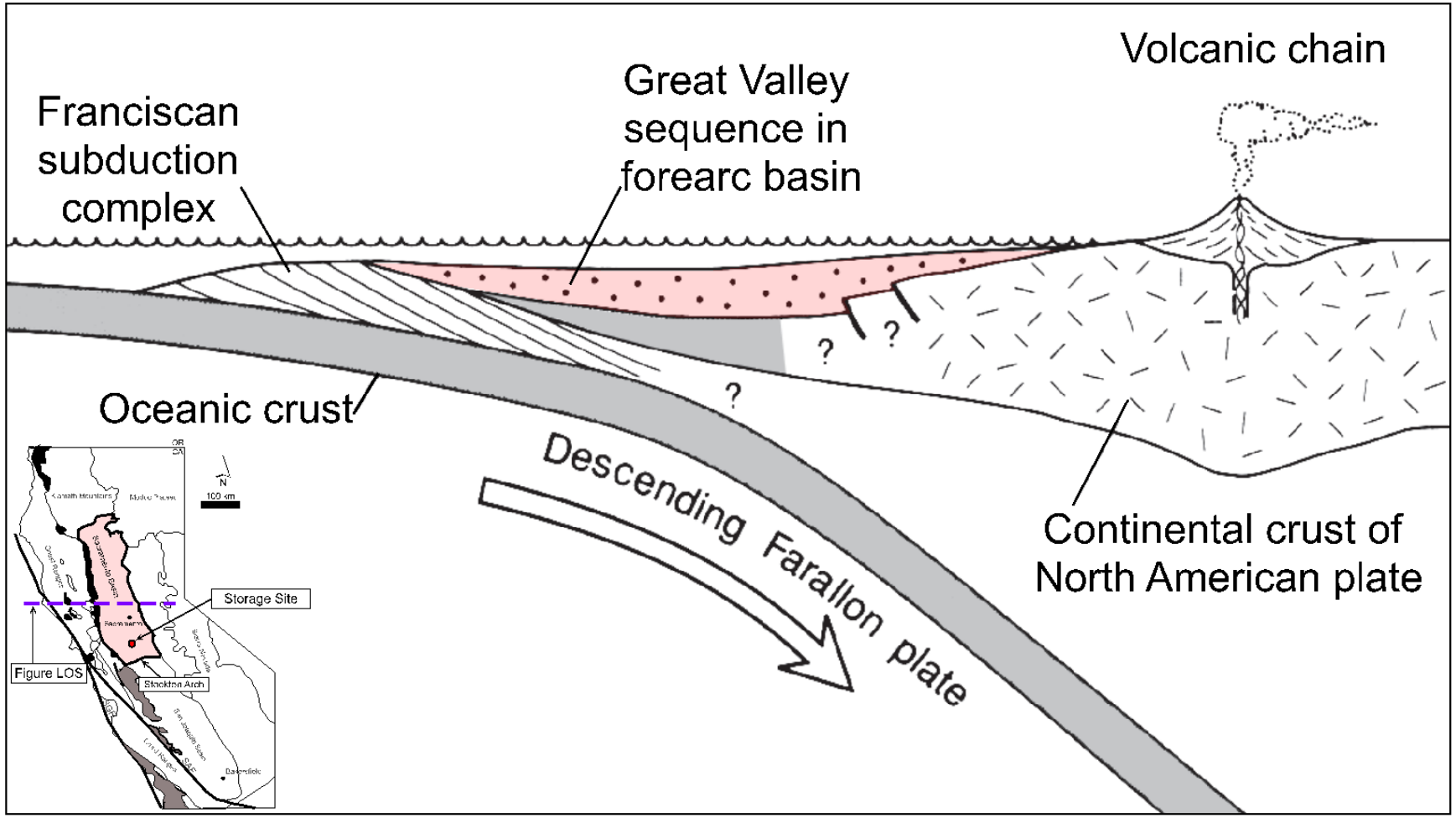

Figure 2.1-4. Schematic W-E cross-section of California, highlighting the Sacramento Basin, as a continental margin during late Mesozoic. The oceanic Farallon plate was forced below the west coast of the North American continental plate.

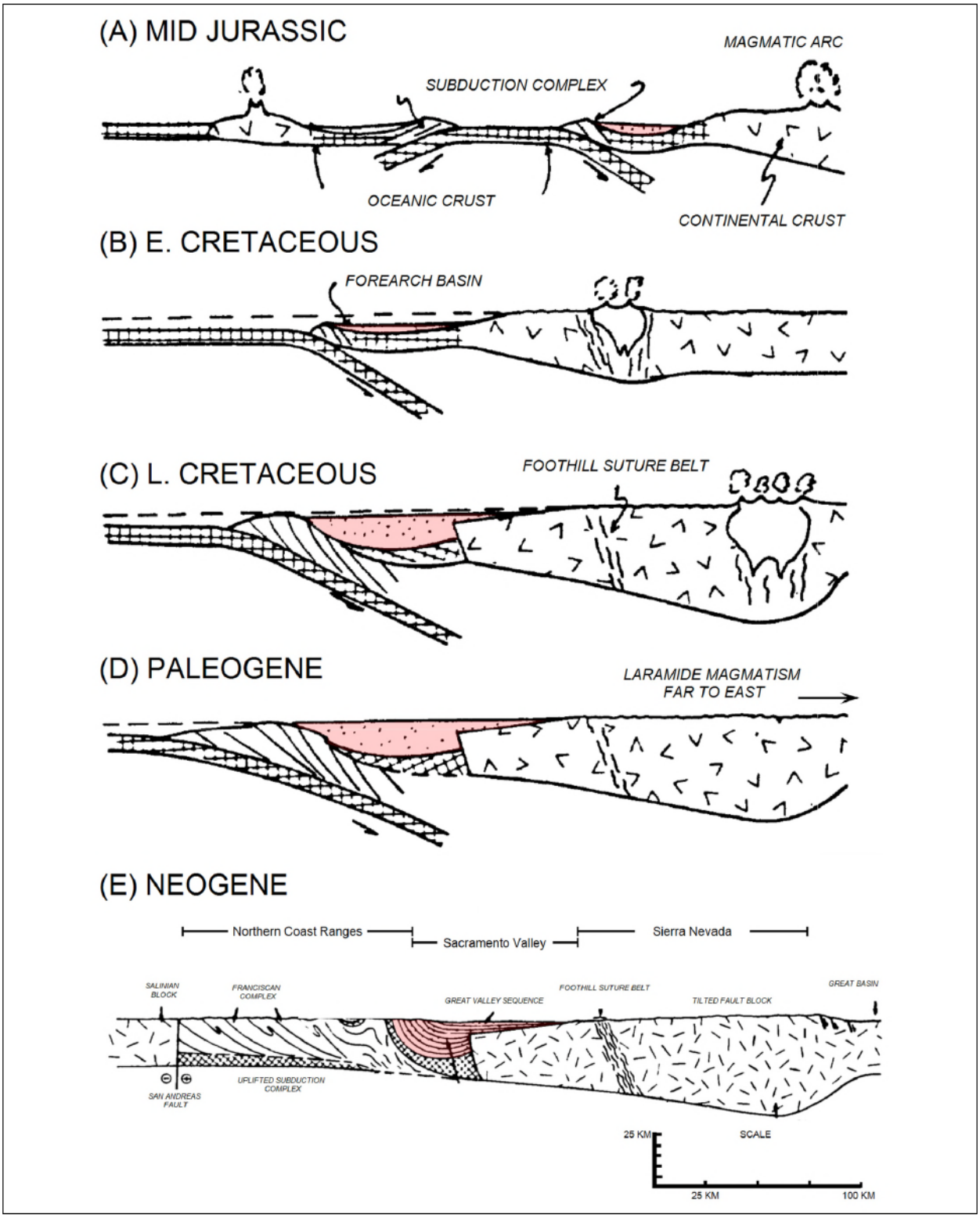

Figure 2.1-5. Evolutionary stages showing the history of the arc-trench system of California from Jurassic (A) to Neogene (E) (modified from Beyer, 1988).

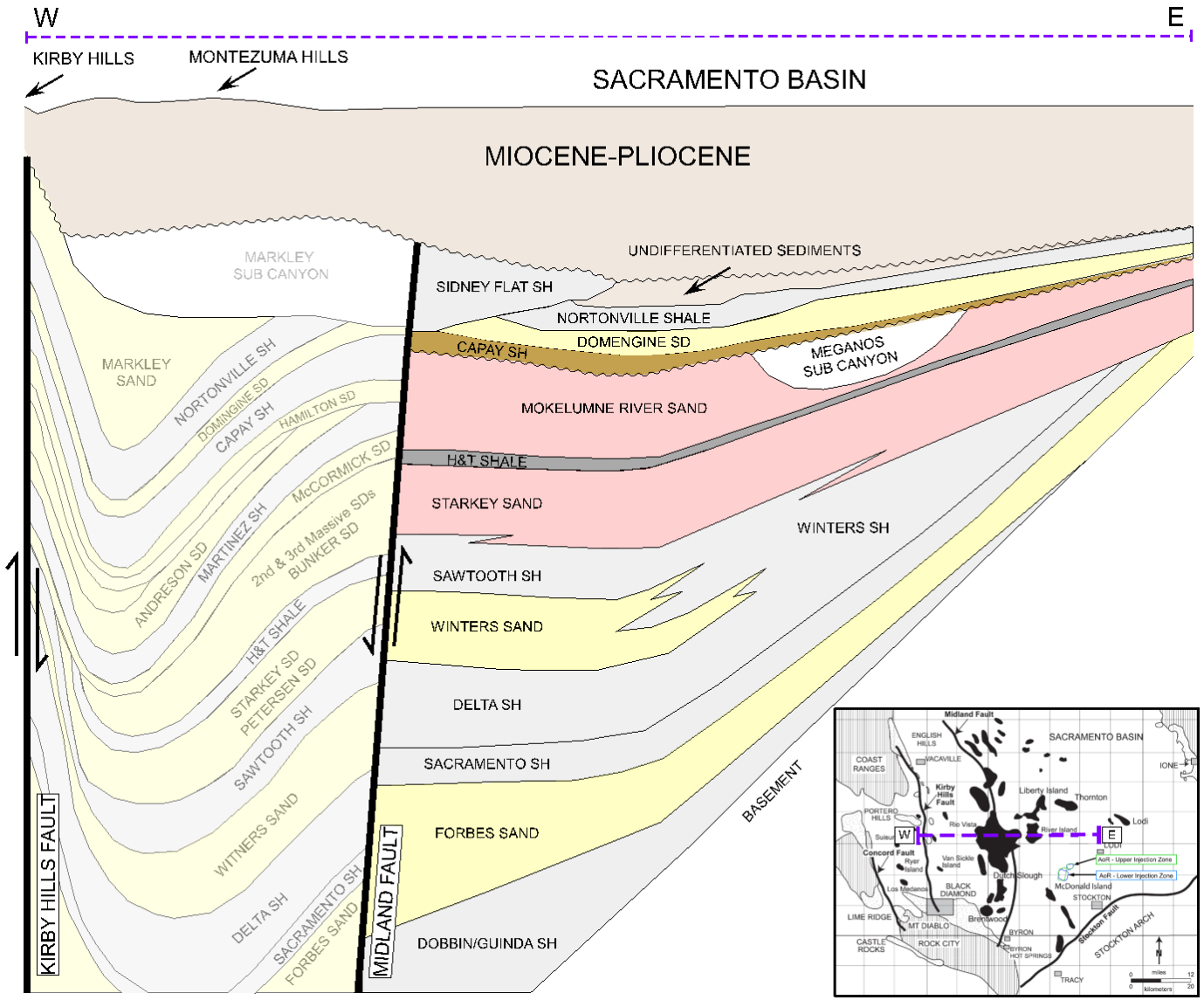

Figure 2.1-6. Schematic west to east cross section in the Sacramento basin. Figure modified from Sullivan and Sullivan, 2012.

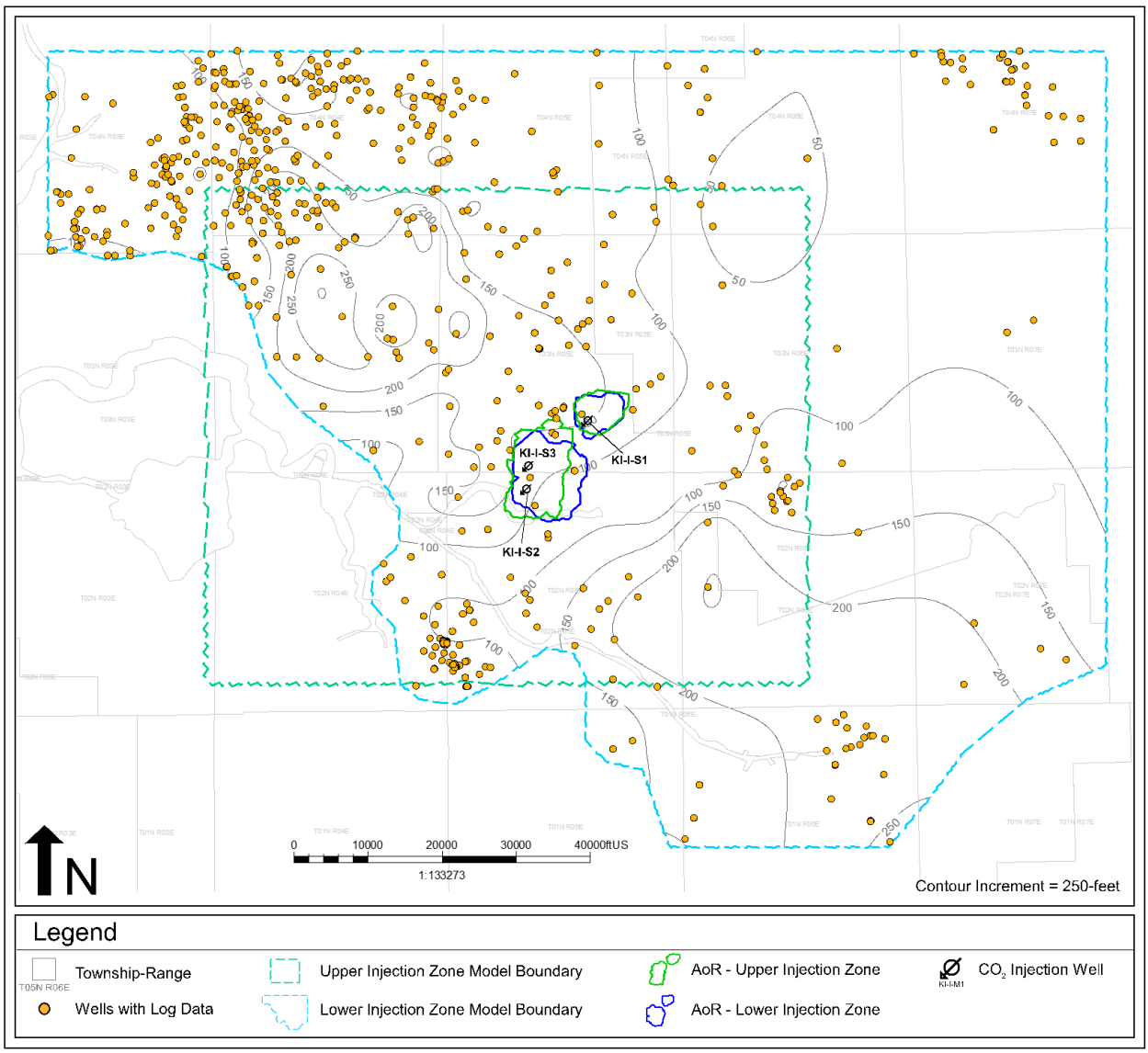

Figure 2.1-7a. H&T Shale isopach map for the greater Lower Injection Zone project area. Wells shown as orange dots on the map have open-hole logs.

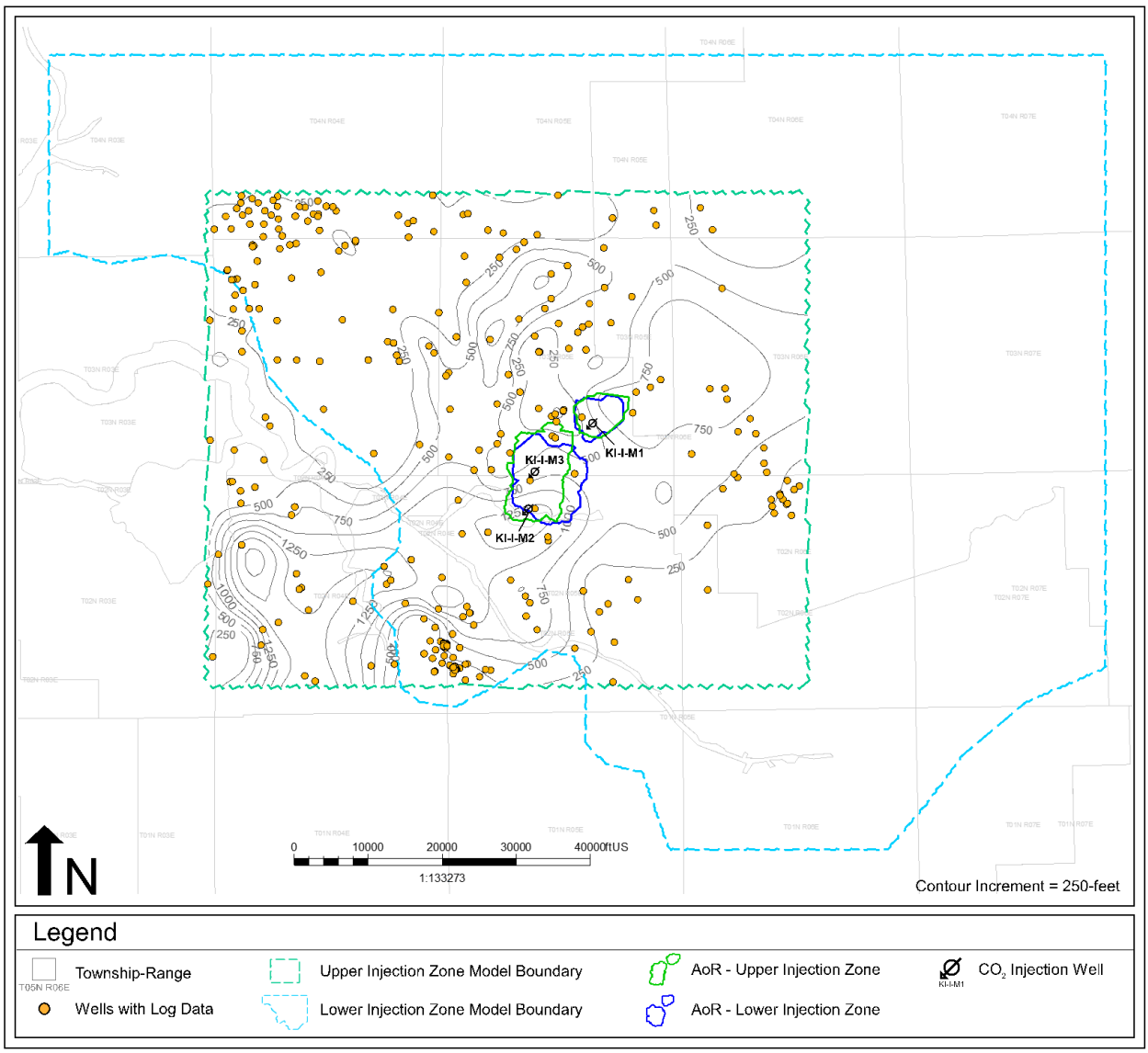

Figure 2.1-7b. Capay Shale isopach map for the greater Upper Injection Zone project area. Wells shown as orange dots on the map have open-hole logs.

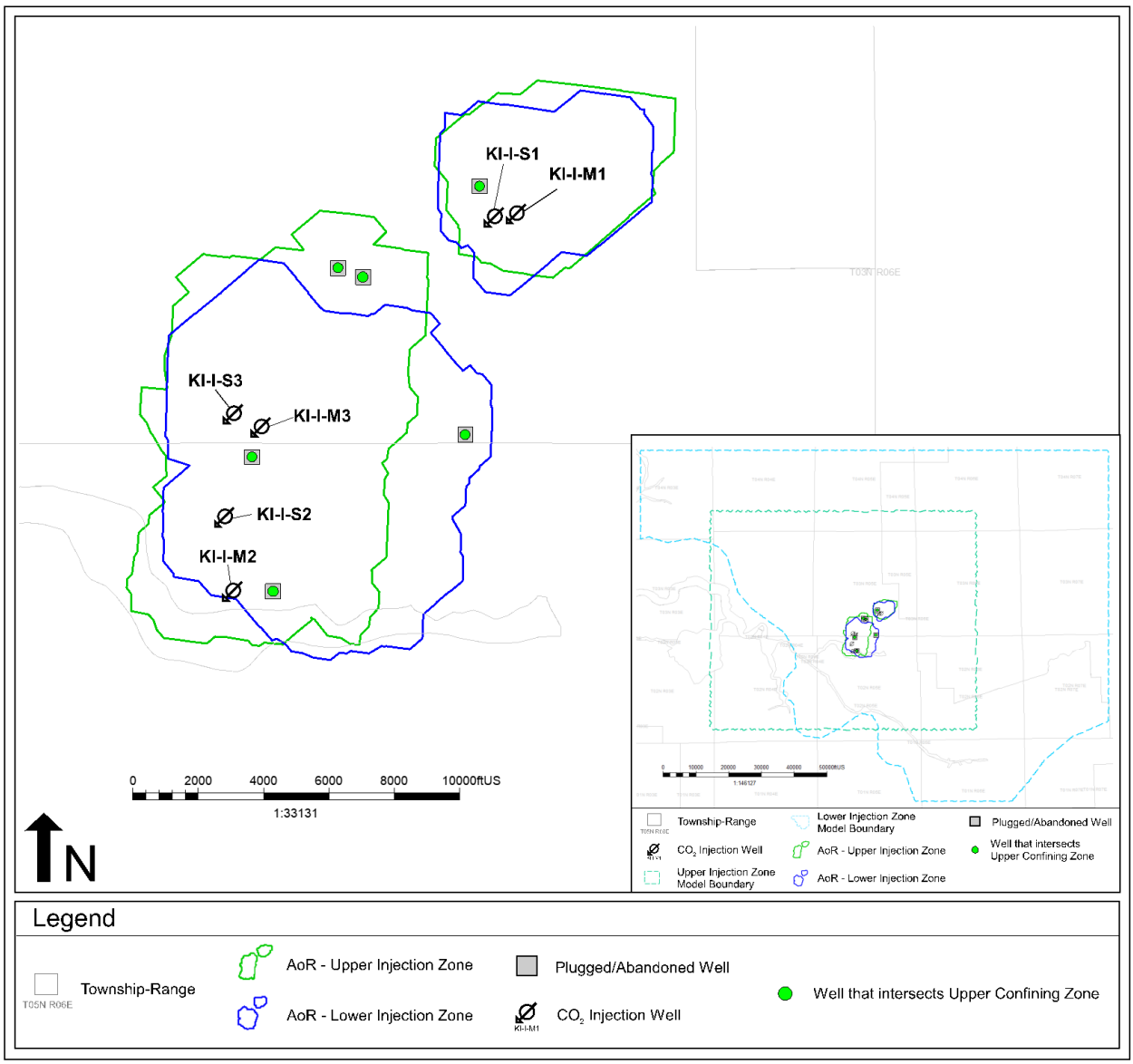

Figure 2.2-1. Existing oil/gas wells and injector well locations in the AoR.

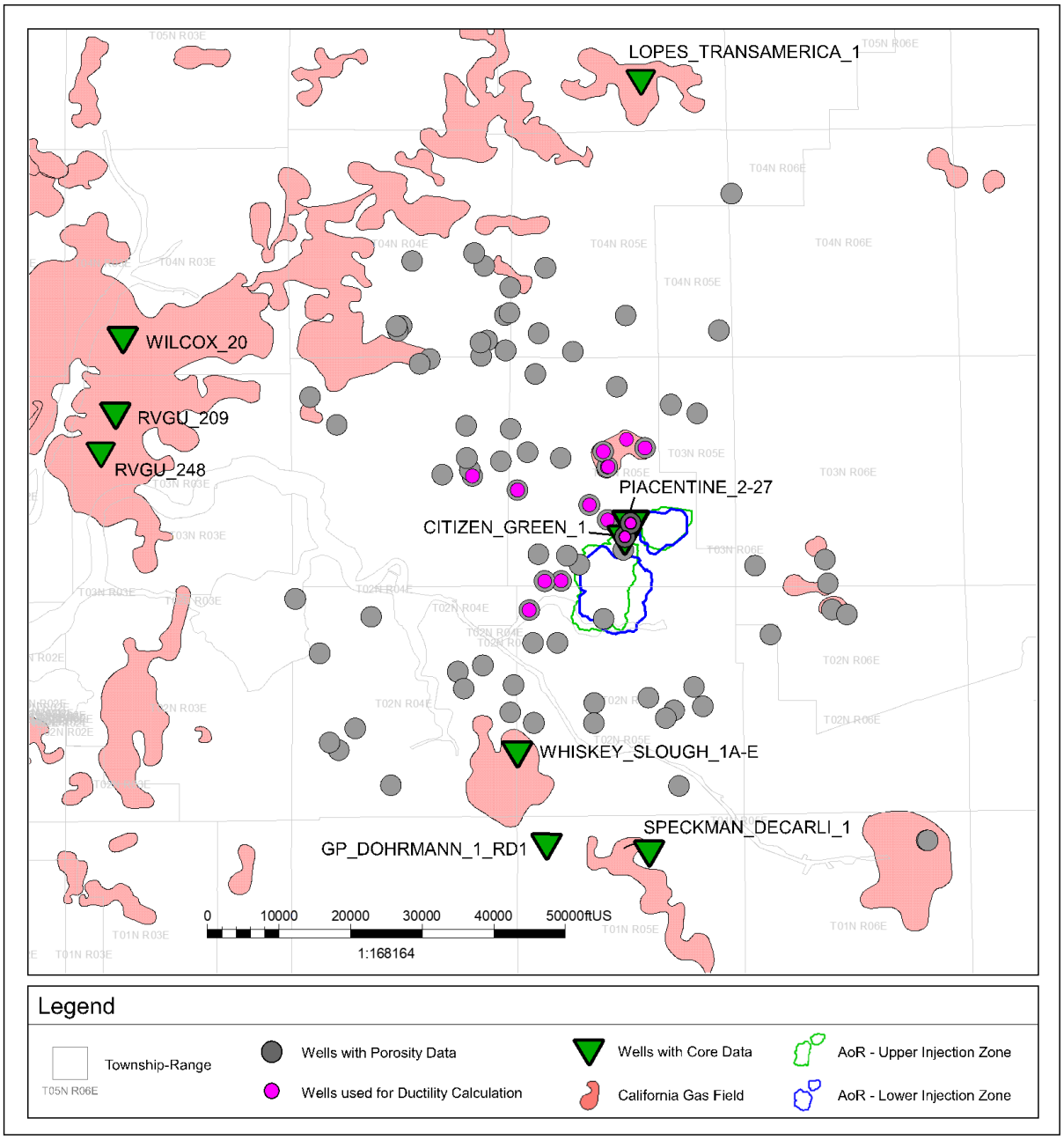

Figure 2.2-2. Wells drilled in the project area with porosity data are shown in gray, wells with core are shown in green and wells used for ductility calculation are shown in pink.

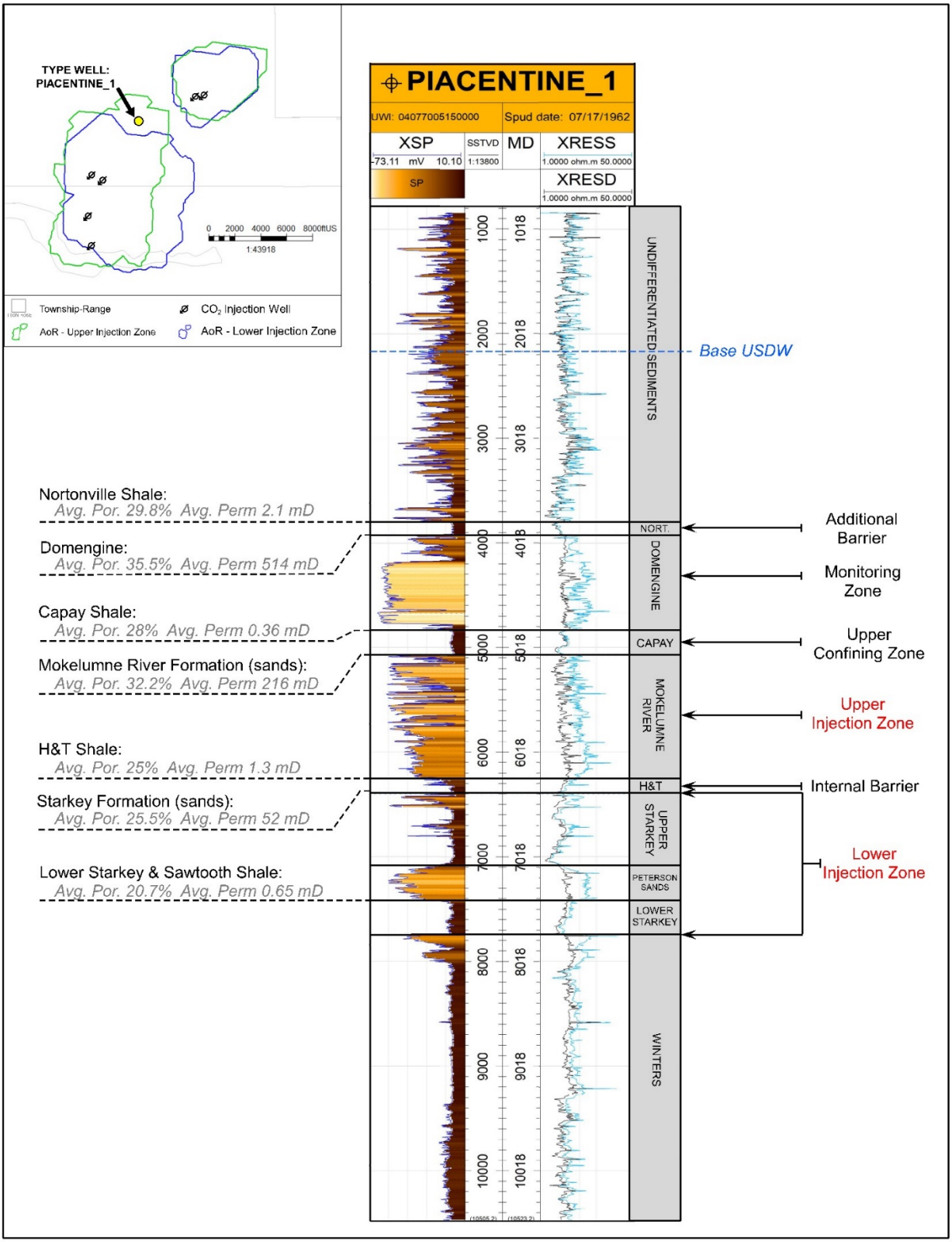

Figure 2.2-3. Type well showing average rock properties for the confining zones and injection zones within the project AoR.

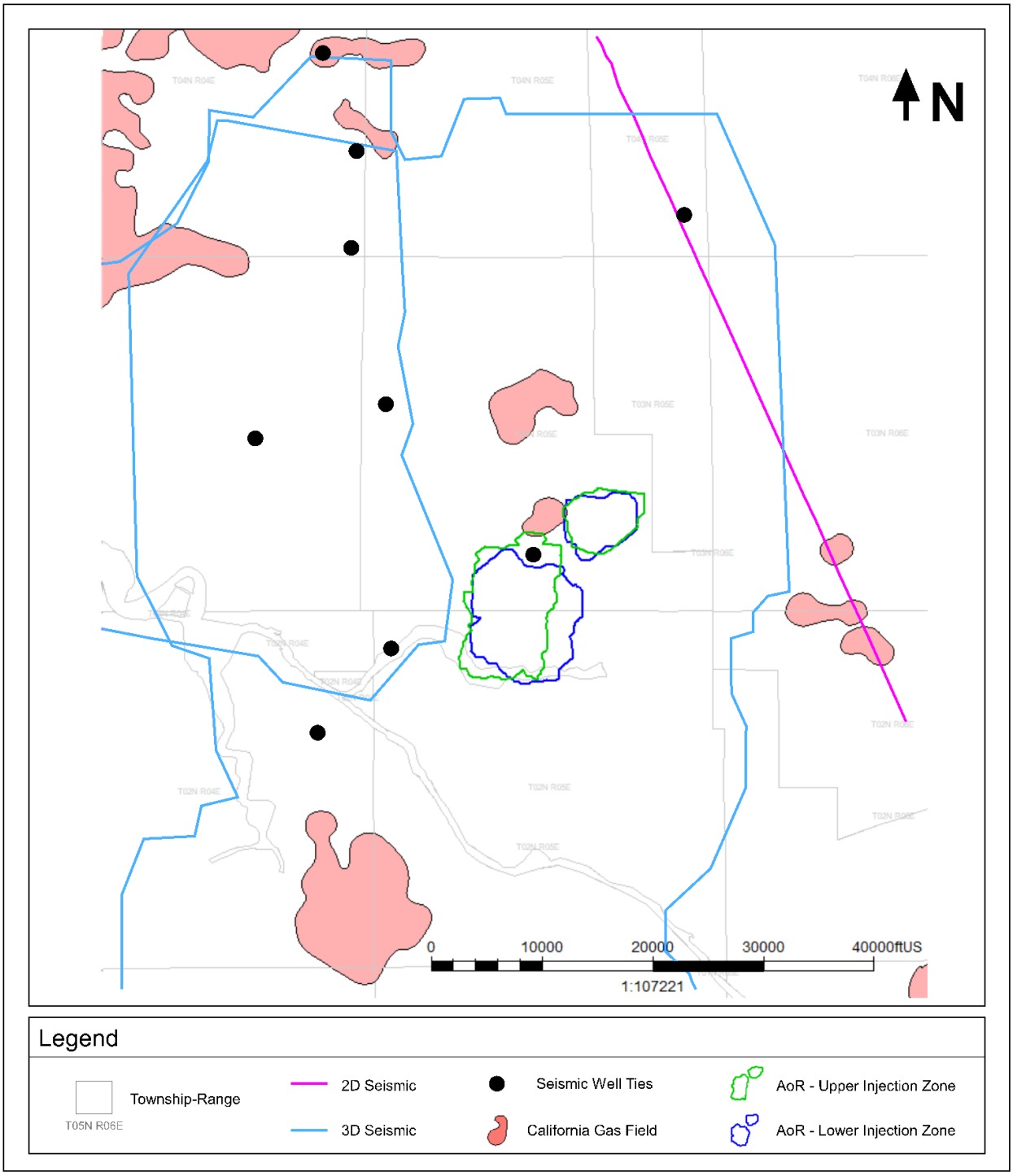

Figure 2.2-4. Summary map and area of seismic data used to build the structural model. The overlapping 3D seismic surveys used to build the structural model were acquired between 1997 and 1999. The single 2D seismic line used was acquired in 1981. California gas fields are shown in red for reference.

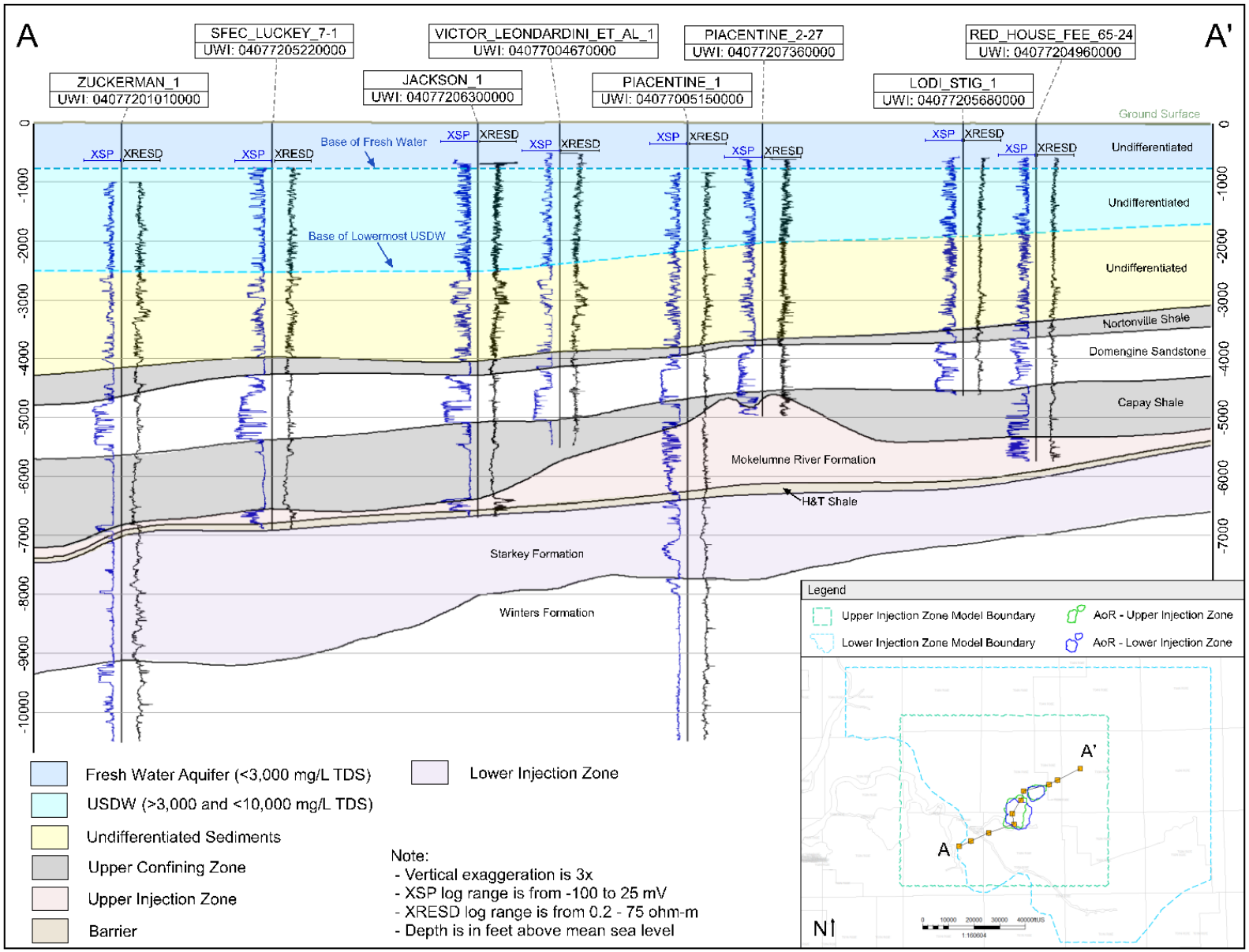

Figure 2.2-5. Cross section showing stratigraphy and lateral continuity of major formations across the AoR.

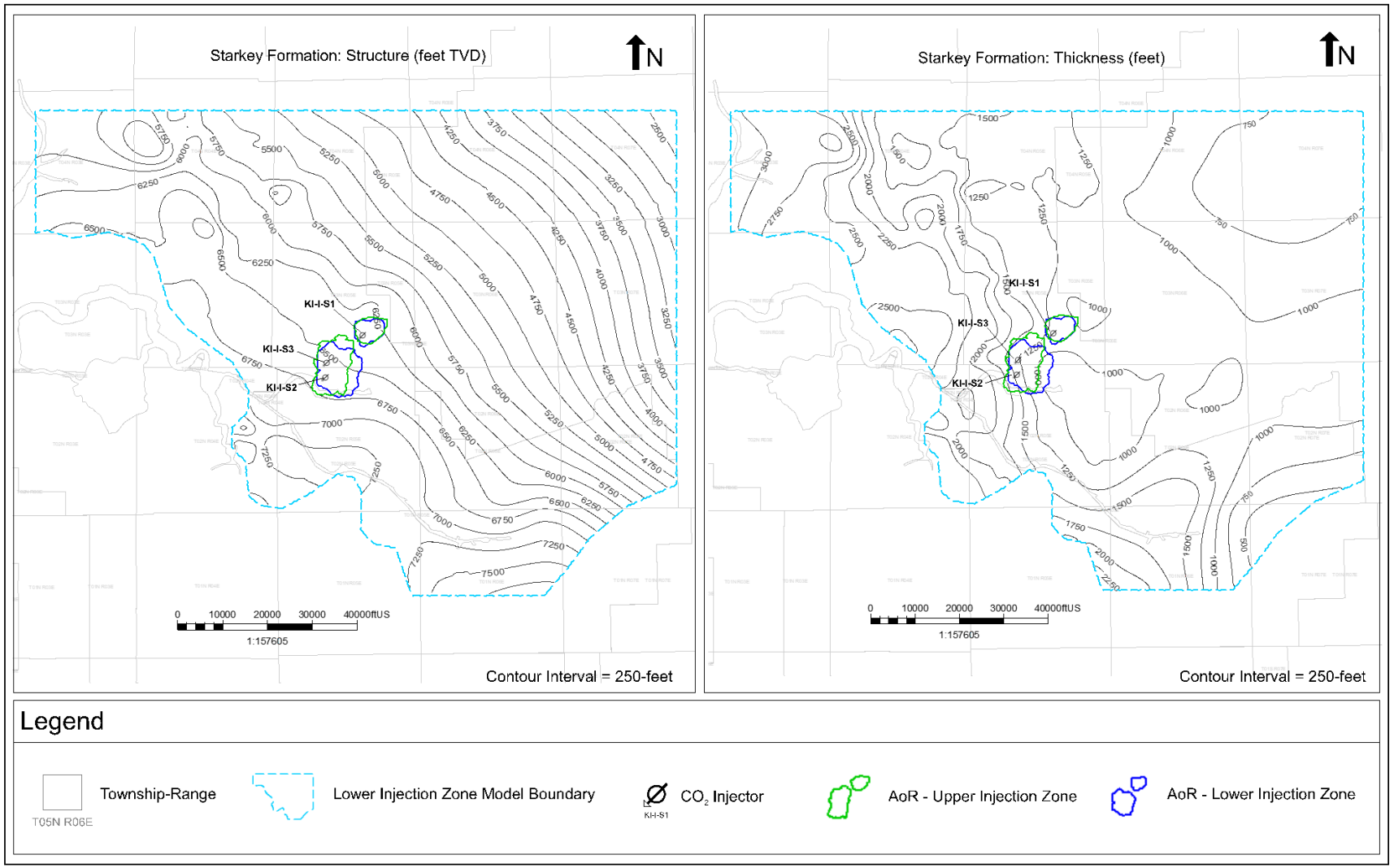

Figure 2.2-6. Lower Injection Zone structure and thickness maps.

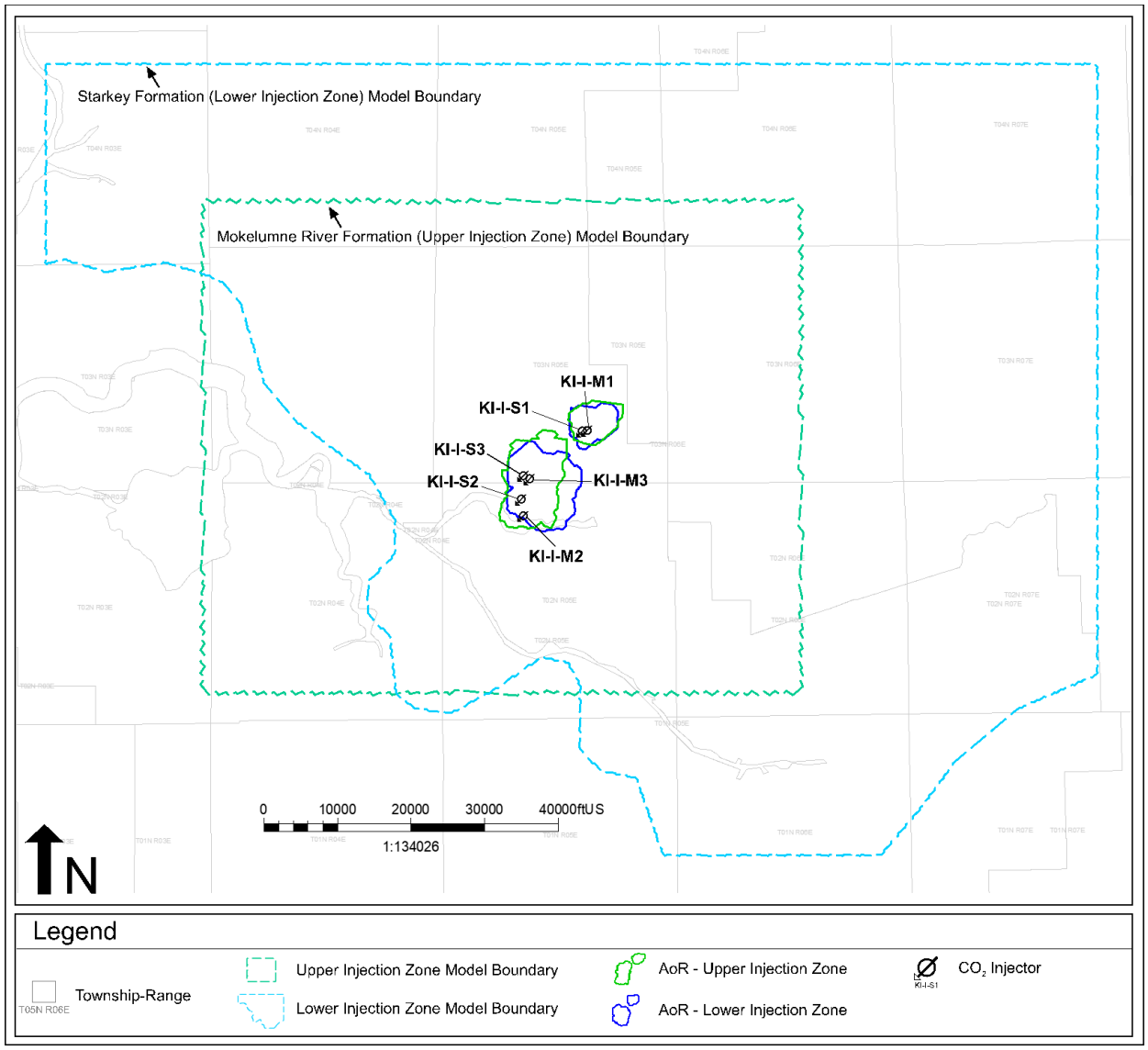

Figure 2.2-7. Injection well location map for the project area. The injection wells can be separated into two groups: Lower Injection Zone: (KI-I-S1, KI-I-S2, KI-I-S3), and Upper Injection Zone: (KI-I-M1, KI-I-M2, KI-I-M3).

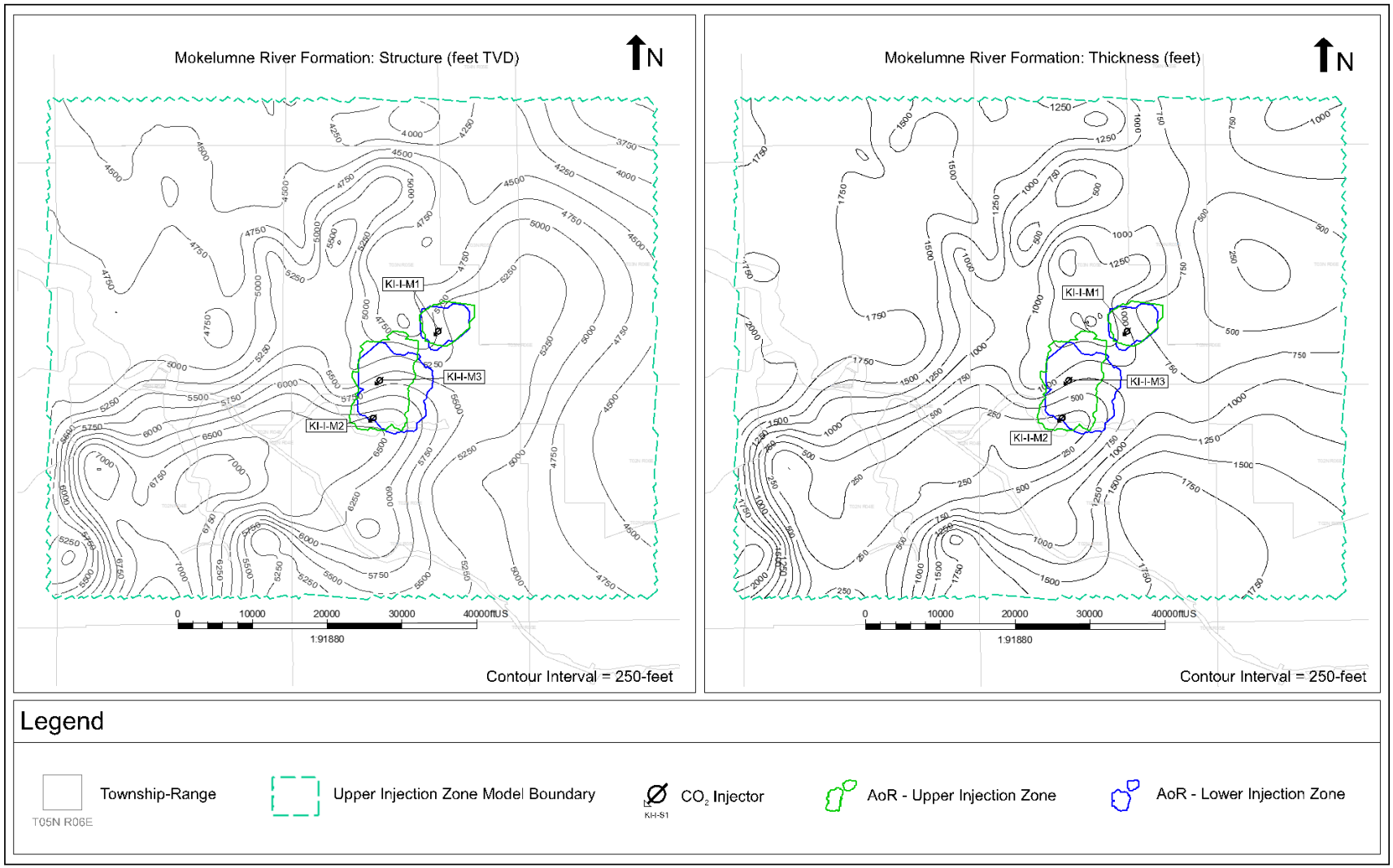

Figure 2.2-8. Upper Injection Zone structure and thickness maps.

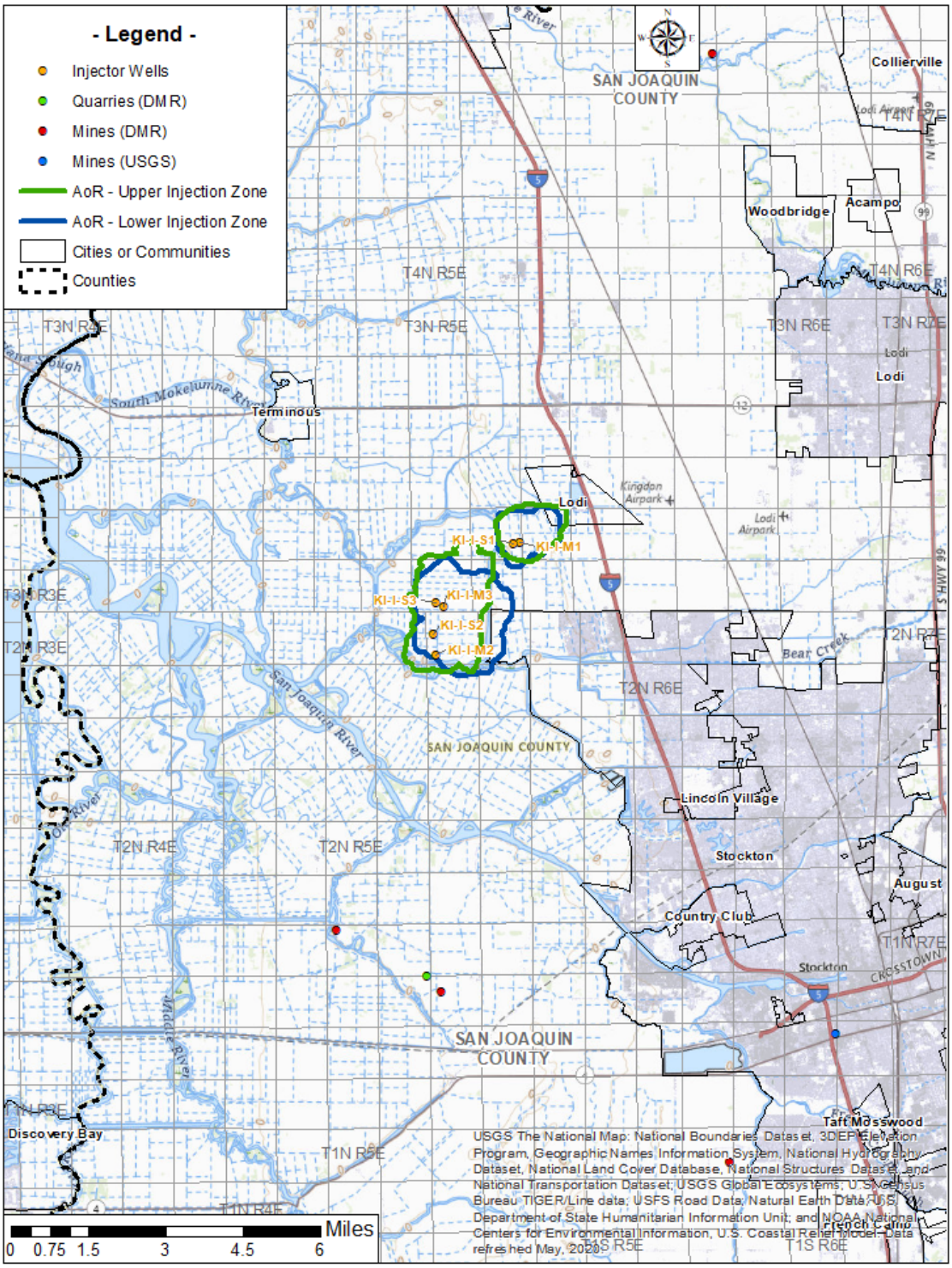

Figure 2.2-9. Map of the AoR and surface features in the project area. Mine and quarries from Conservation Division of Mine Reclamation (DMR) & U.S. Geological Survey (USGS). No springs or tribal lands are identified near AoR.

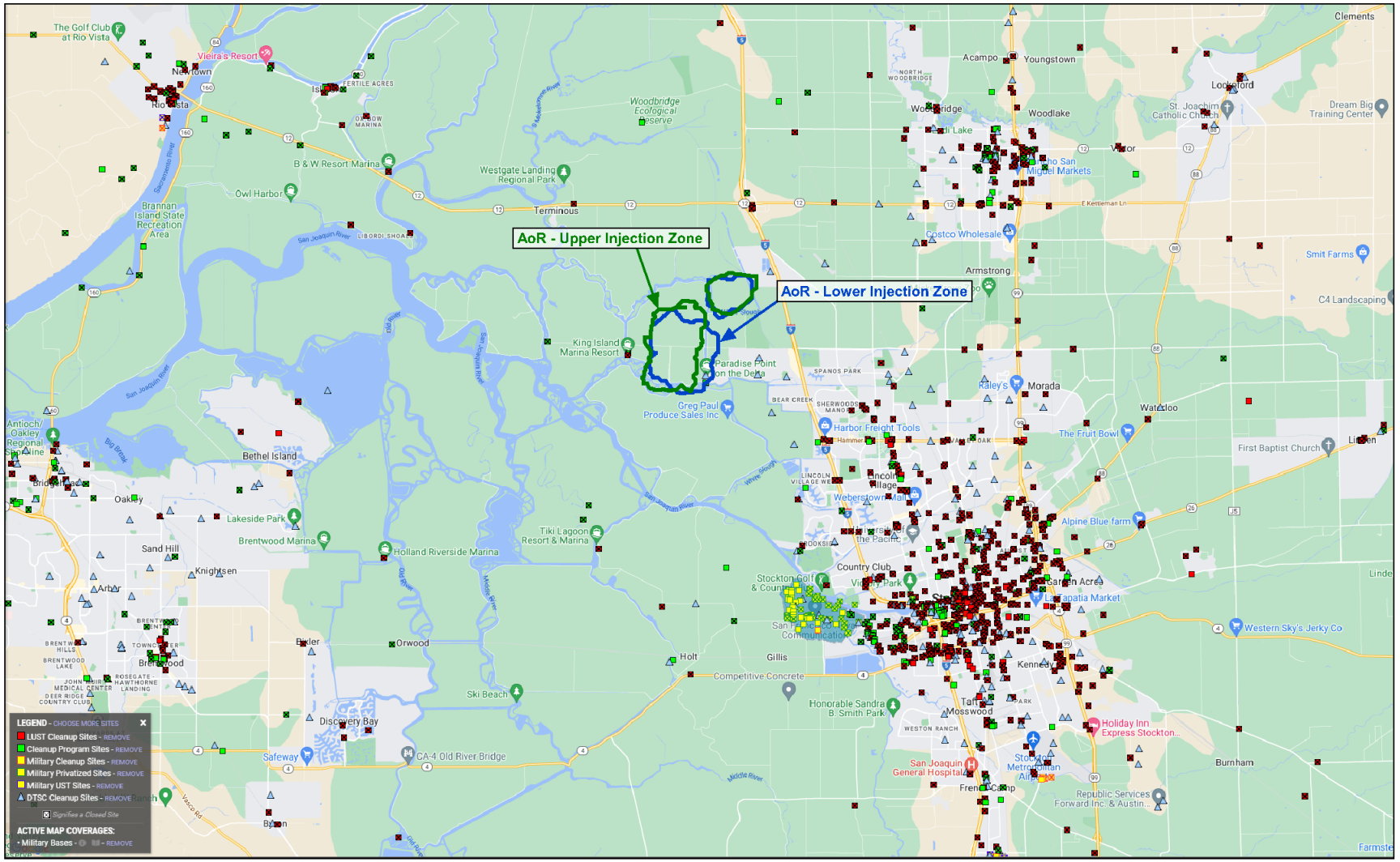

Figure 2.2-10. State- or EPA-approved subsurface cleanup sites (source: State Water Resources Control Board GeoTracker online database).

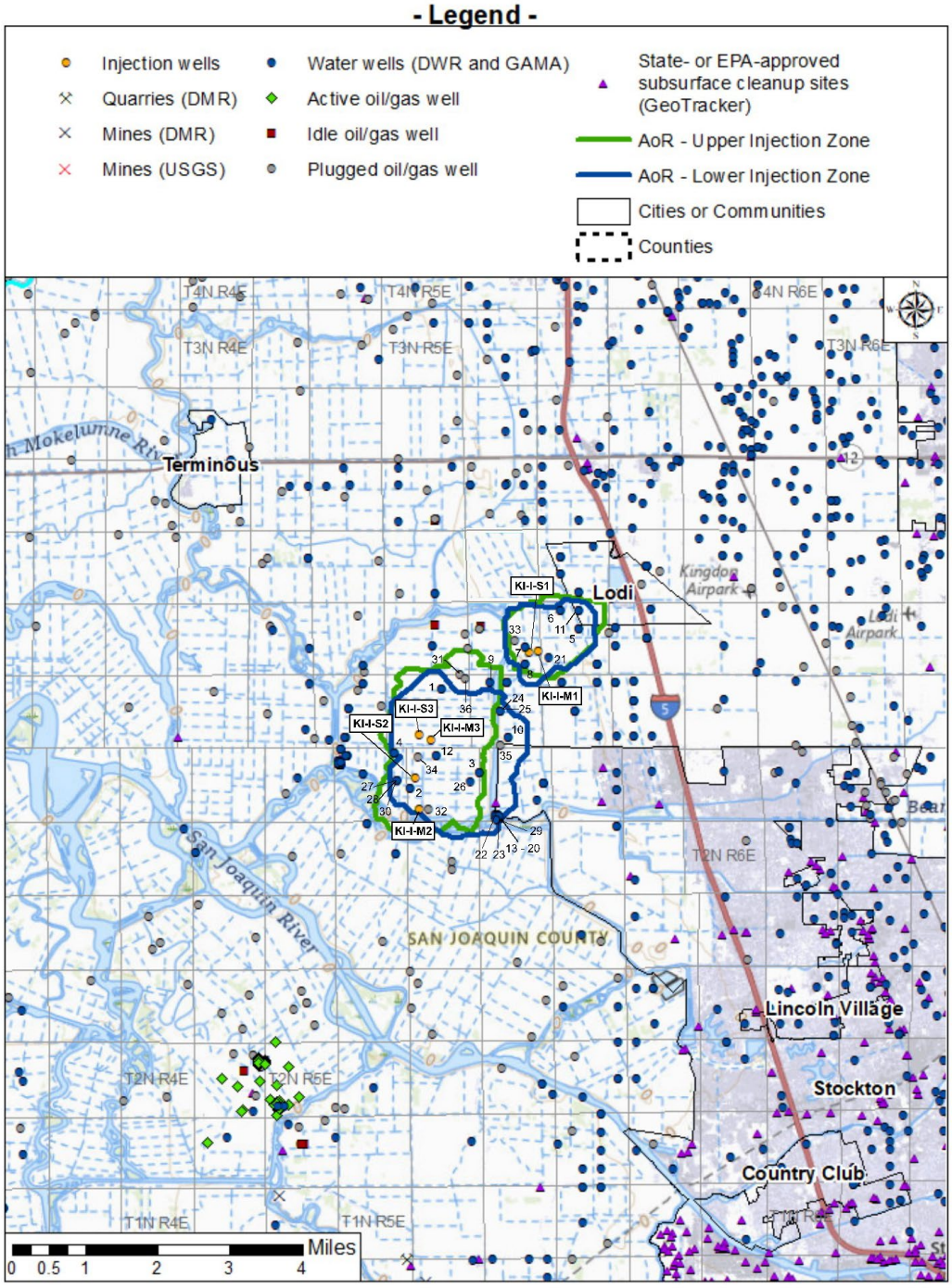

Figure 2.2-11. Summary map of the AoR, oil or gas wells, water wells, State- or EPA-approved subsurface cleanup sites, and surface features in the project area. Mine and quarries from Conservation Division of Mine Reclamation (DMR) & U.S. Geological Survey (USGS). Water wells from California Division of Drinking Water (DWR) and Groundwater Ambient Monitoring and Assessment (GAMA) program. No springs or tribal lands are identified near AoR. Active wells include: Gas Storage and Observation wells. Plugged wells include: Core holes, Dry Gas, Down Hole, Gas, and Gas Storage wells. Idle wells include: Dry Gas, Gas Storage, and Observation wells

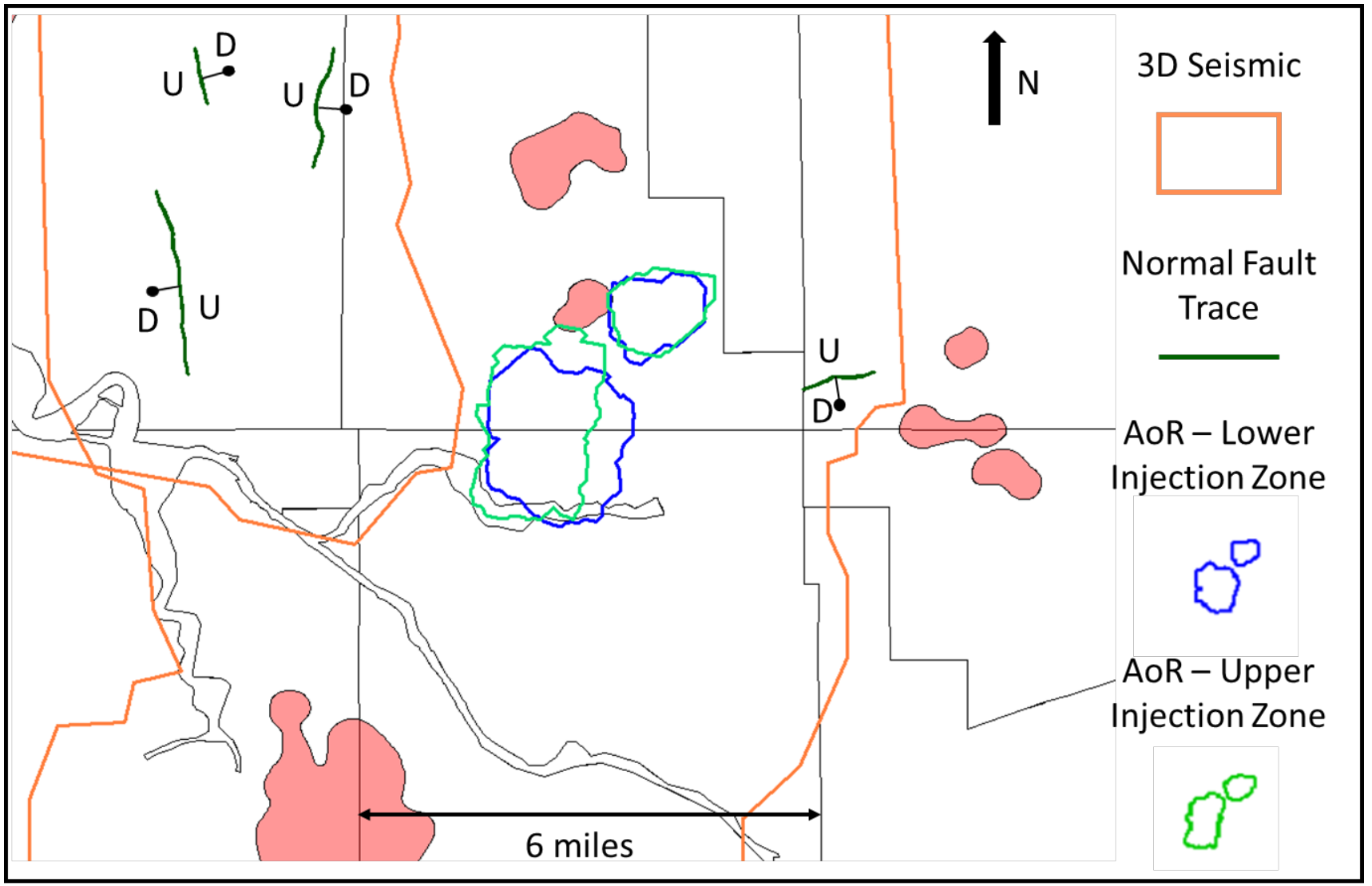

Figure 2.3-1: Reference map for normal fault traces within proximity of the AoR. The traces are shown at the Mokelumne River level and highlight the up and down thrown sides of the faults.

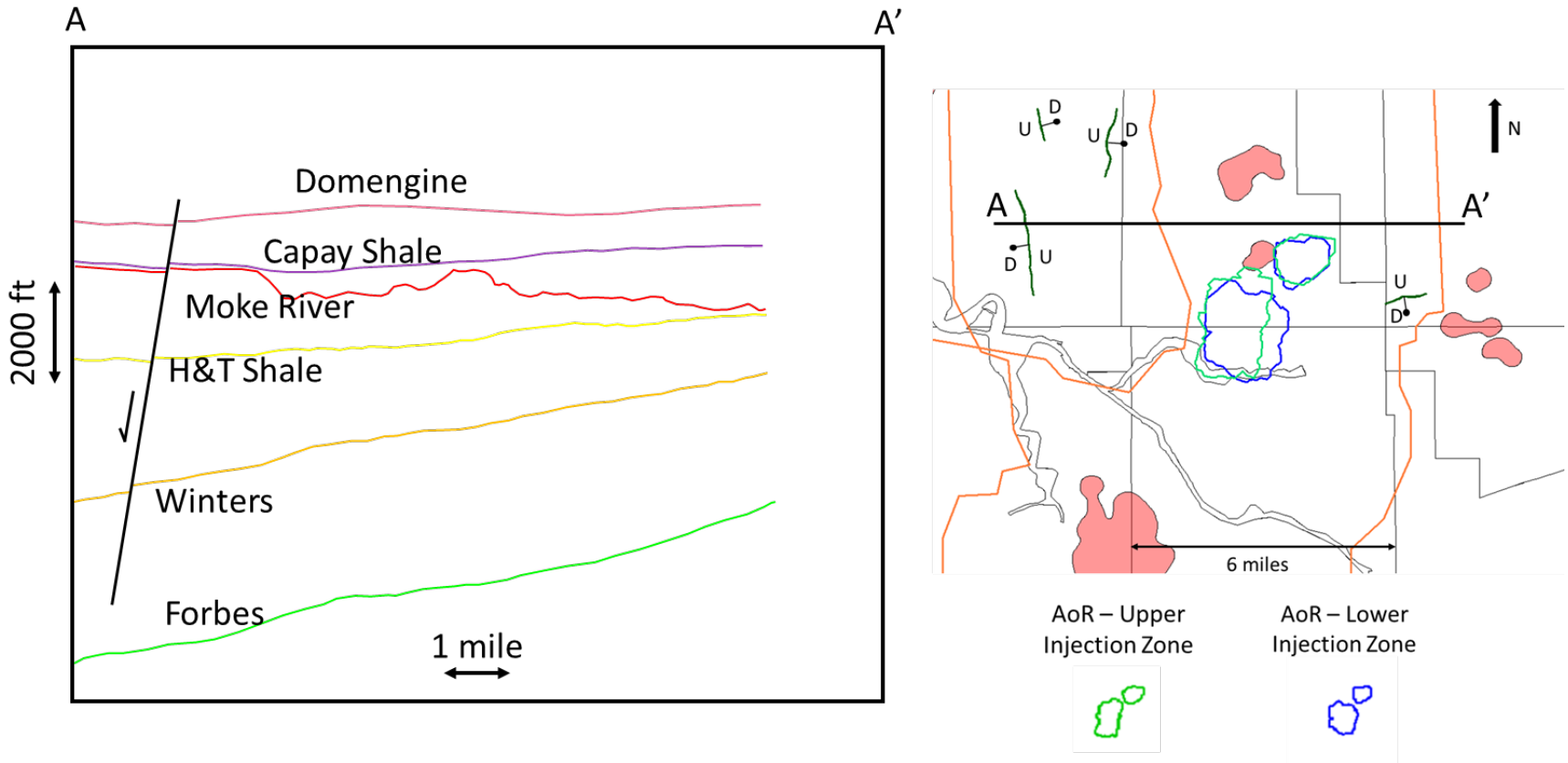

Figure 2.3-2. Generalized structural section through the interpreted normal fault identified on 3D seismic data that is to the west of the AoR. This style of faulting is typical for the area with a throw of approximately 100 feet at the H&T Shale interval.

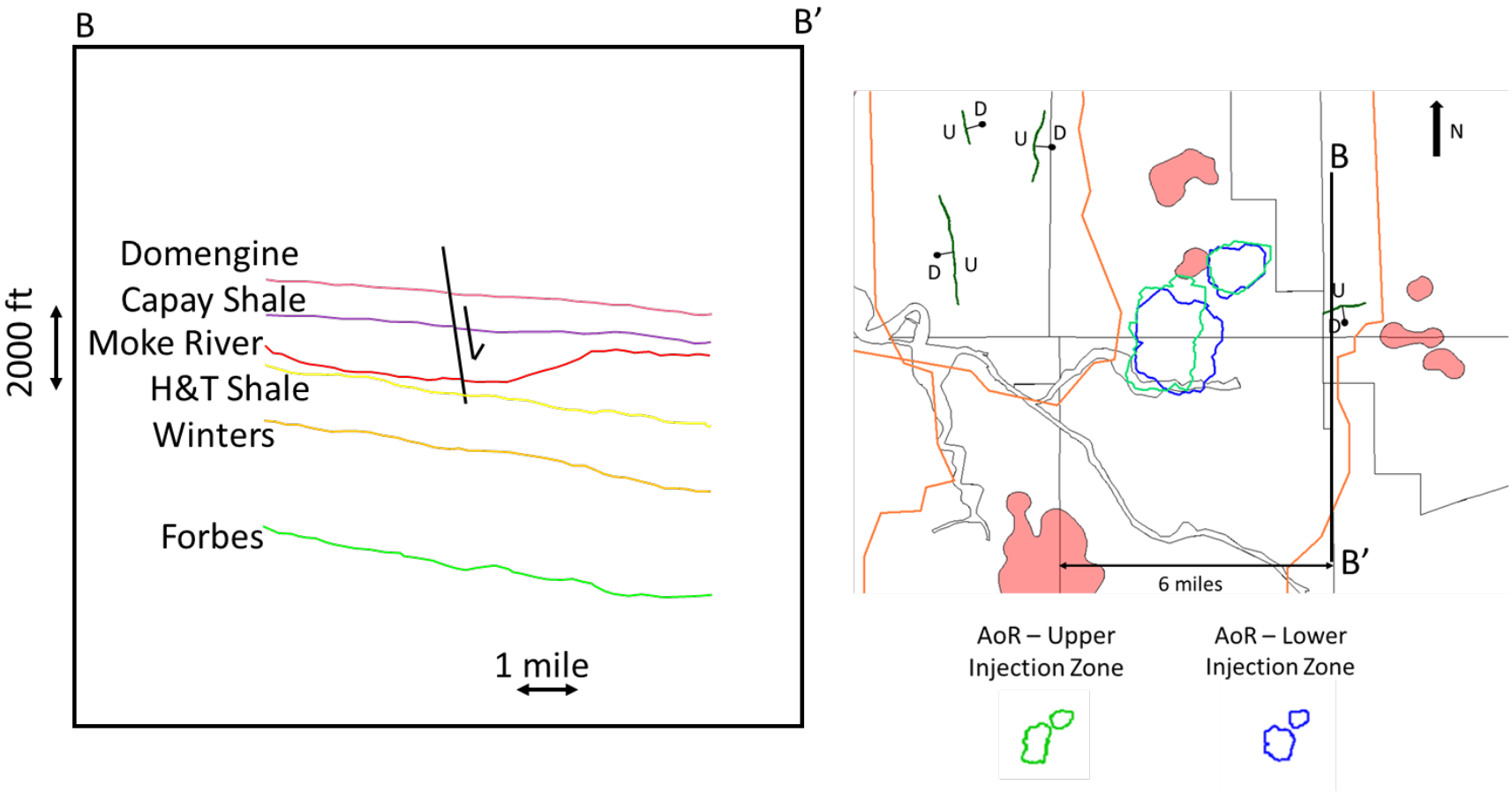

Figure 2.3-3. Generalized structural section through the interpreted normal fault identified on 3D seismic data to the east of the AoR's. This style of faulting is typical for the area with a throw of approximately 50 feet at the Capay Shale interval.

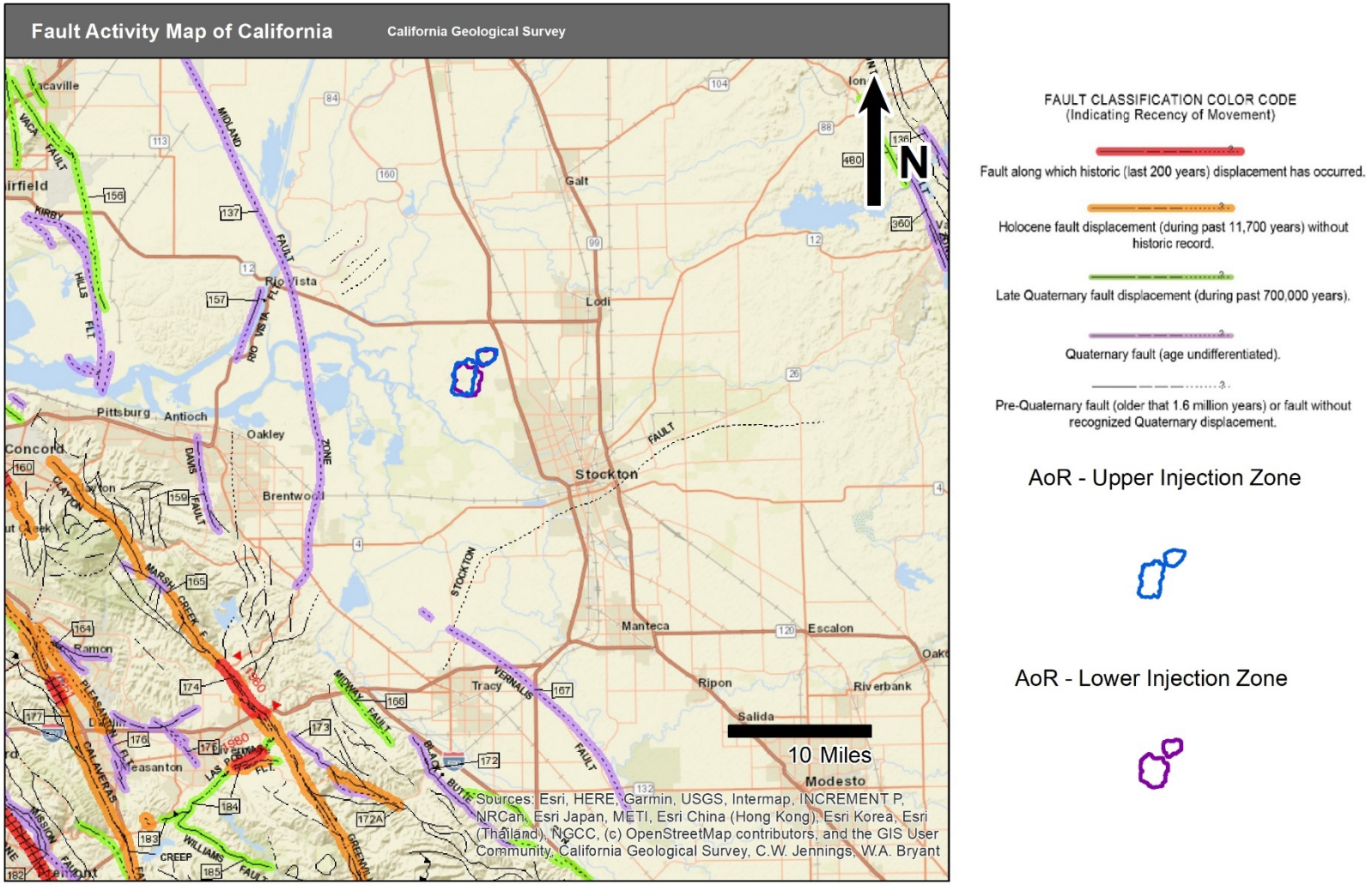

Figure 2.3-4. Fault activity map from the California Geologic Survey which shows no mapped faults within and beyond the project AoR's. (https://maps.conservation.ca.gov/cgs/fam/)

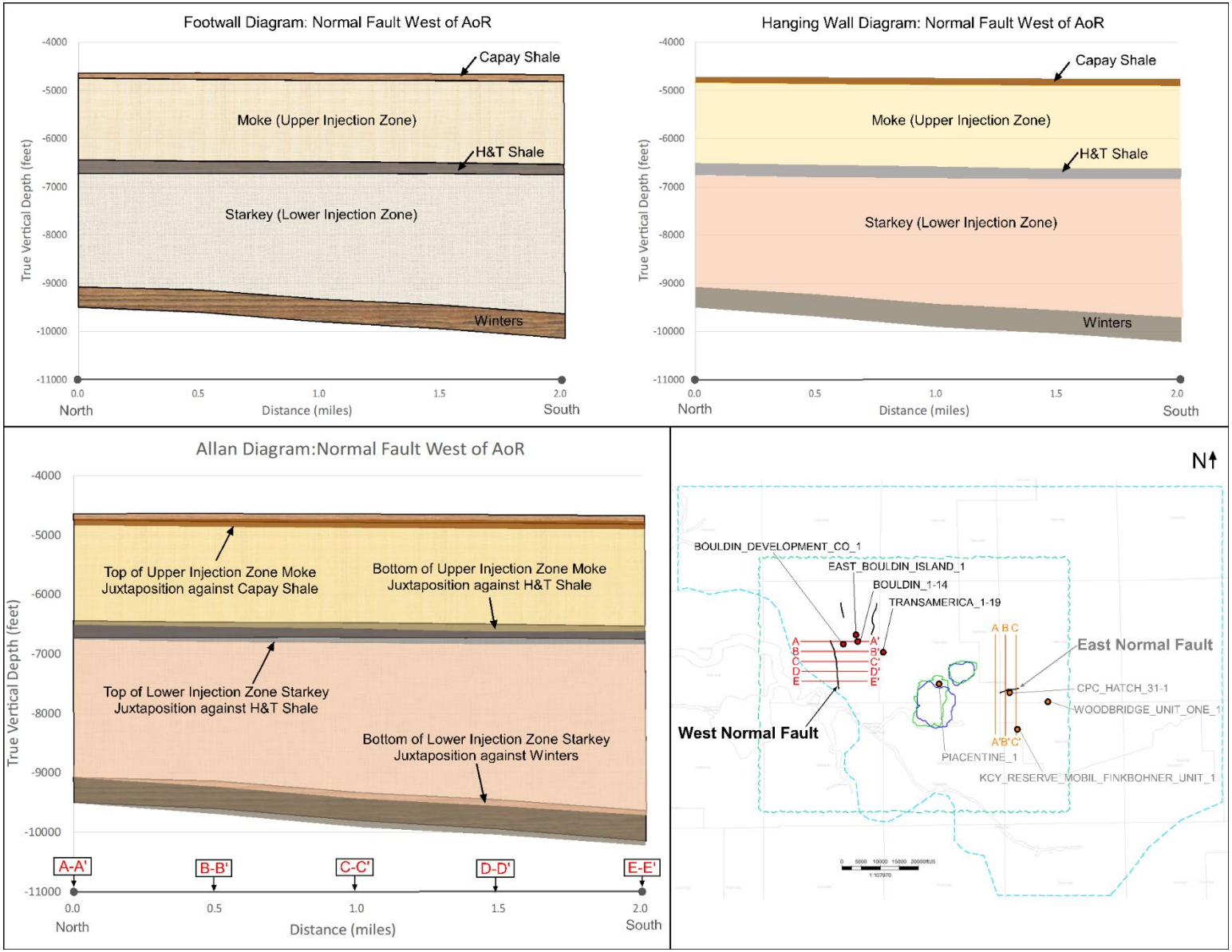

Figure 2.3-5. West Normal Fault Allan Diagram.

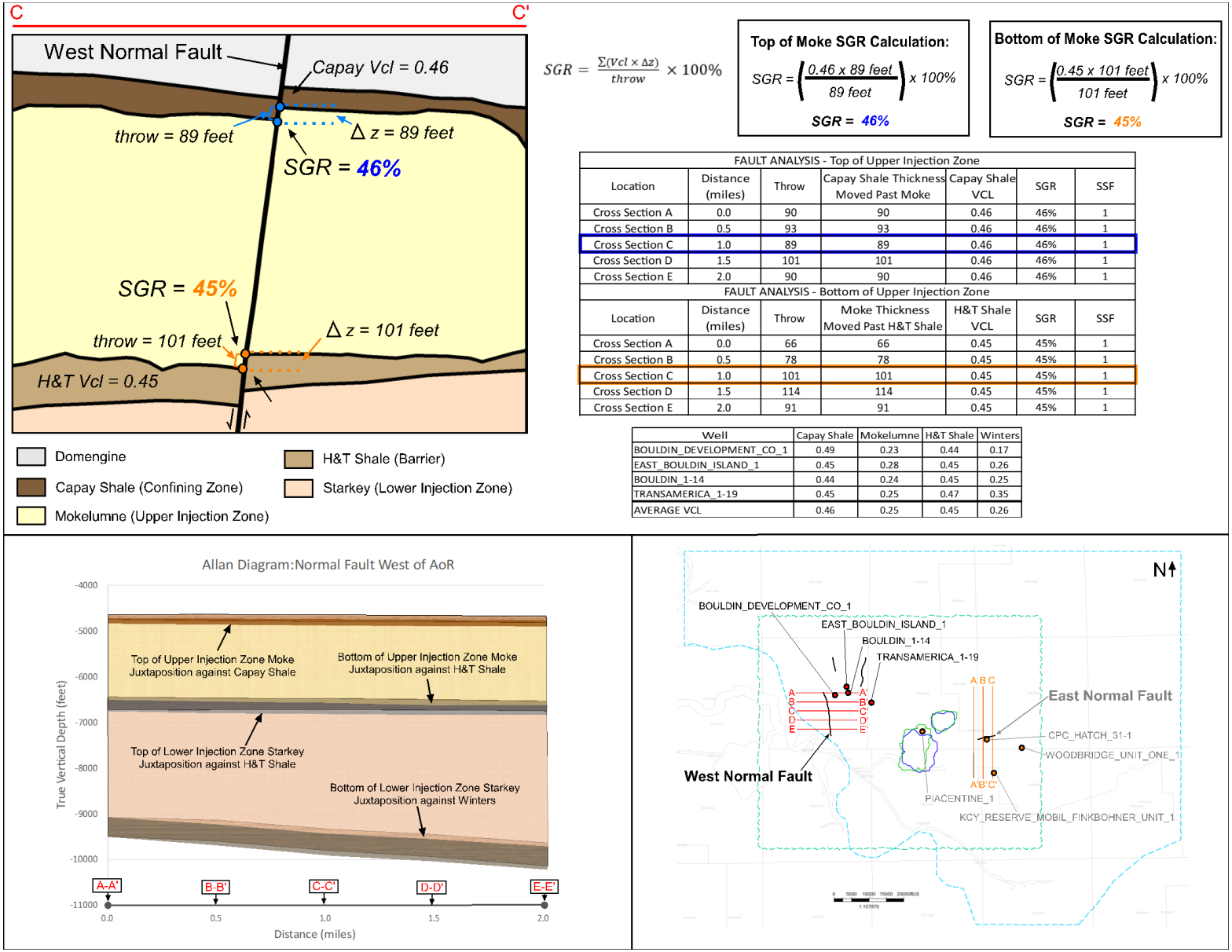

FAULT ANALYSIS - Top of Upper Injection Zone						
Location	Distance (miles)	Throw	Capay Shale Thickness Moved Past Moke	Capay Shale VCL	SGR	SSF
Cross Section A	0.0	90	90	0.46	46%	1
Cross Section B	0.5	93	93	0.46	46%	1
Cross Section C	1.0	89	89	0.46	46%	1
Cross Section D	1.5	101	101	0.46	46%	1
Cross Section E	2.0	90	90	0.46	46%	1
FAULT ANALYSIS - Bottom of Upper Injection Zone						
Location	Distance (miles)	Throw	Moke Thickness Moved Past H&T Shale	H&T Shale VCL	SGR	SSF
Cross Section A	0.0	66	66	0.45	45%	1
Cross Section B	0.5	78	78	0.45	45%	1
Cross Section C	1.0	101	101	0.45	45%	1
Cross Section D	1.5	114	114	0.45	45%	1
Cross Section E	2.0	91	91	0.45	45%	1

Well	Capay Shale	Mokelumne	H&T Shale	Winters
BOULDIN_DEVELOPMENT_CO_1	0.49	0.23	0.44	0.17
EAST_BOULDIN_ISLAND_1	0.45	0.28	0.45	0.26
BOULDIN_1-14	0.44	0.24	0.45	0.25
TRANSAMERICA_1-19	0.45	0.25	0.47	0.35
AVERAGE VCL	0.46	0.25	0.45	0.26

Figure 2.3-6. West Normal Fault Shale Gouge Ratio (SGR) calculation for the Upper Injection Zone (Mokelumne Formation).

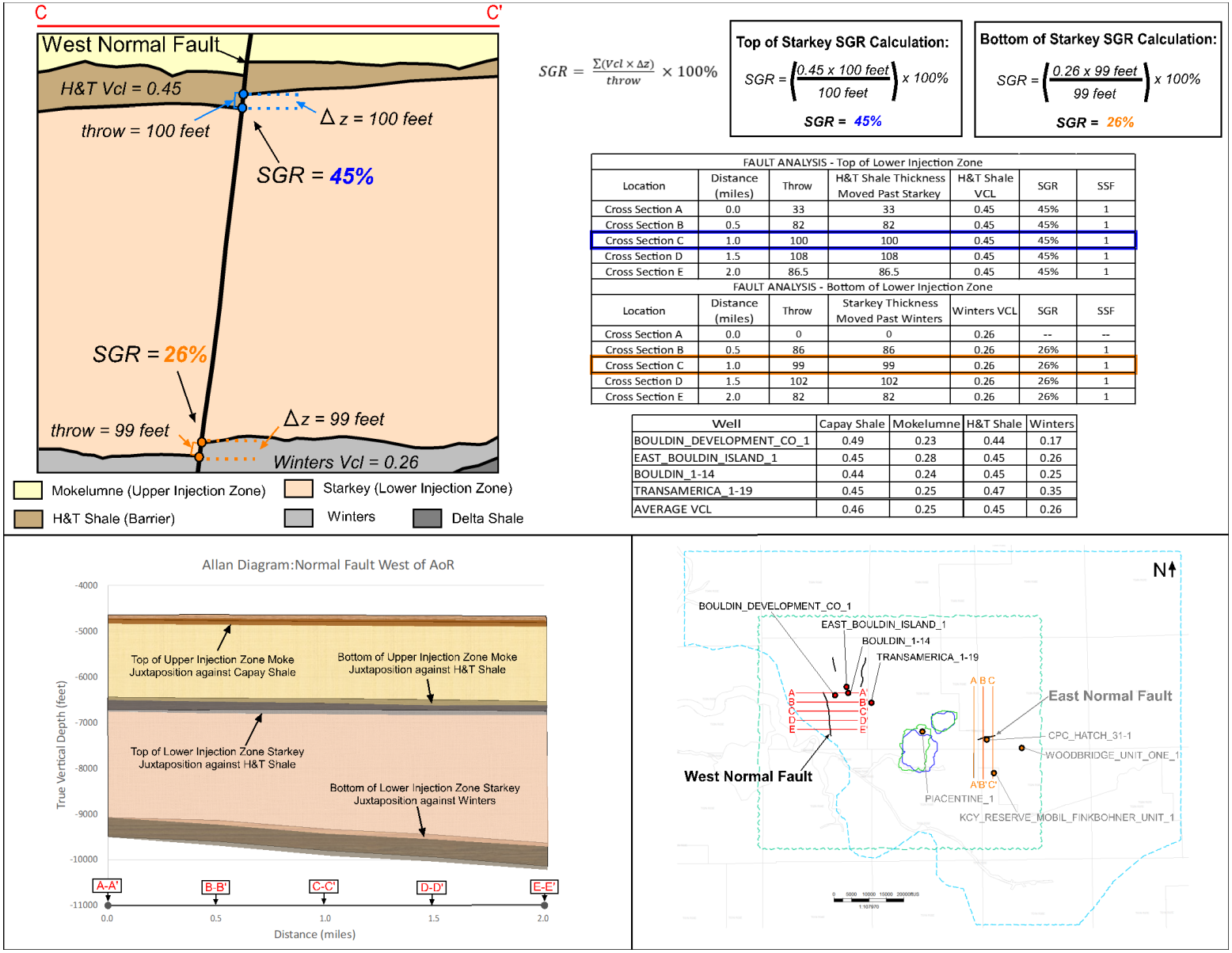

FAULT ANALYSIS - Top of Lower Injection Zone						
Location	Distance (miles)	Throw	H&T Shale Thickness Moved Past Starkey	H&T Shale VCL	SGR	SSF
Cross Section A	0.0	33	33	0.45	45%	1
Cross Section B	0.5	82	82	0.45	45%	1
Cross Section C	1.0	100	100	0.45	45%	1
Cross Section D	1.5	108	108	0.45	45%	1
Cross Section E	2.0	86.5	86.5	0.45	45%	1
FAULT ANALYSIS - Bottom of Lower Injection Zone						
Location	Distance (miles)	Throw	Starkey Thickness Moved Past Winters	Winters VCL	SGR	SSF
Cross Section A	0.0	0	0	0.26	--	--
Cross Section B	0.5	86	86	0.26	26%	1
Cross Section C	1.0	99	99	0.26	26%	1
Cross Section D	1.5	102	102	0.26	26%	1
Cross Section E	2.0	82	82	0.26	26%	1

Well	Capay Shale	Mokelumne	H&T Shale	Winters
BOULDIN_DEVELOPMENT_CO_1	0.49	0.23	0.44	0.17
EAST_BOULDIN_ISLAND_1	0.45	0.28	0.45	0.26
BOULDIN_1-14	0.44	0.24	0.45	0.25
TRANSAMERICA_1-19	0.45	0.25	0.47	0.35
AVERAGE VCL	0.46	0.25	0.45	0.26

Figure 2.3-7. West Normal Fault Shale Gouge Ratio (SGR) calculation for the Lower Injection Zone (Starkey Formation).

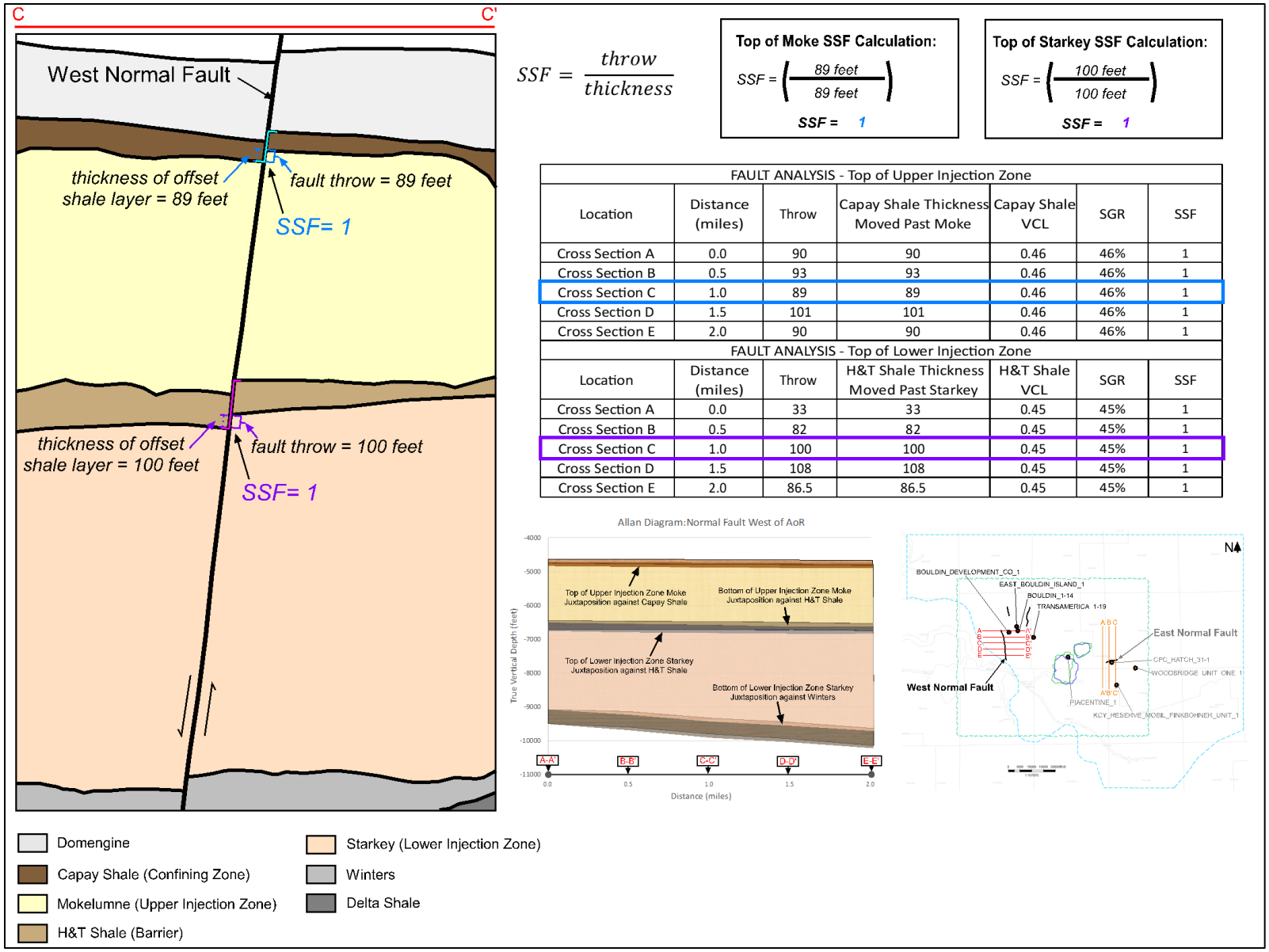

FAULT ANALYSIS - Top of Upper Injection Zone

Location	Distance (miles)	Throw	Capay Shale Thickness Moved Past Moke	Capay Shale VCL	SGR	SSF
Cross Section A	0.0	90	90	0.46	46%	1
Cross Section B	0.5	93	93	0.46	46%	1
Cross Section C	1.0	89	89	0.46	46%	1
Cross Section D	1.5	101	101	0.46	46%	1
Cross Section E	2.0	90	90	0.46	46%	1

FAULT ANALYSIS - Top of Lower Injection Zone

Location	Distance (miles)	Throw	H&T Shale Thickness Moved Past Starkey	H&T Shale VCL	SGR	SSF
Cross Section A	0.0	33	33	0.45	45%	1
Cross Section B	0.5	82	82	0.45	45%	1
Cross Section C	1.0	100	100	0.45	45%	1
Cross Section D	1.5	108	108	0.45	45%	1
Cross Section E	2.0	86.5	86.5	0.45	45%	1

Figure 2.3-8. West Normal Fault Shale Smear Factor (SSF) calculation for the Upper and Lower Injection Zones.

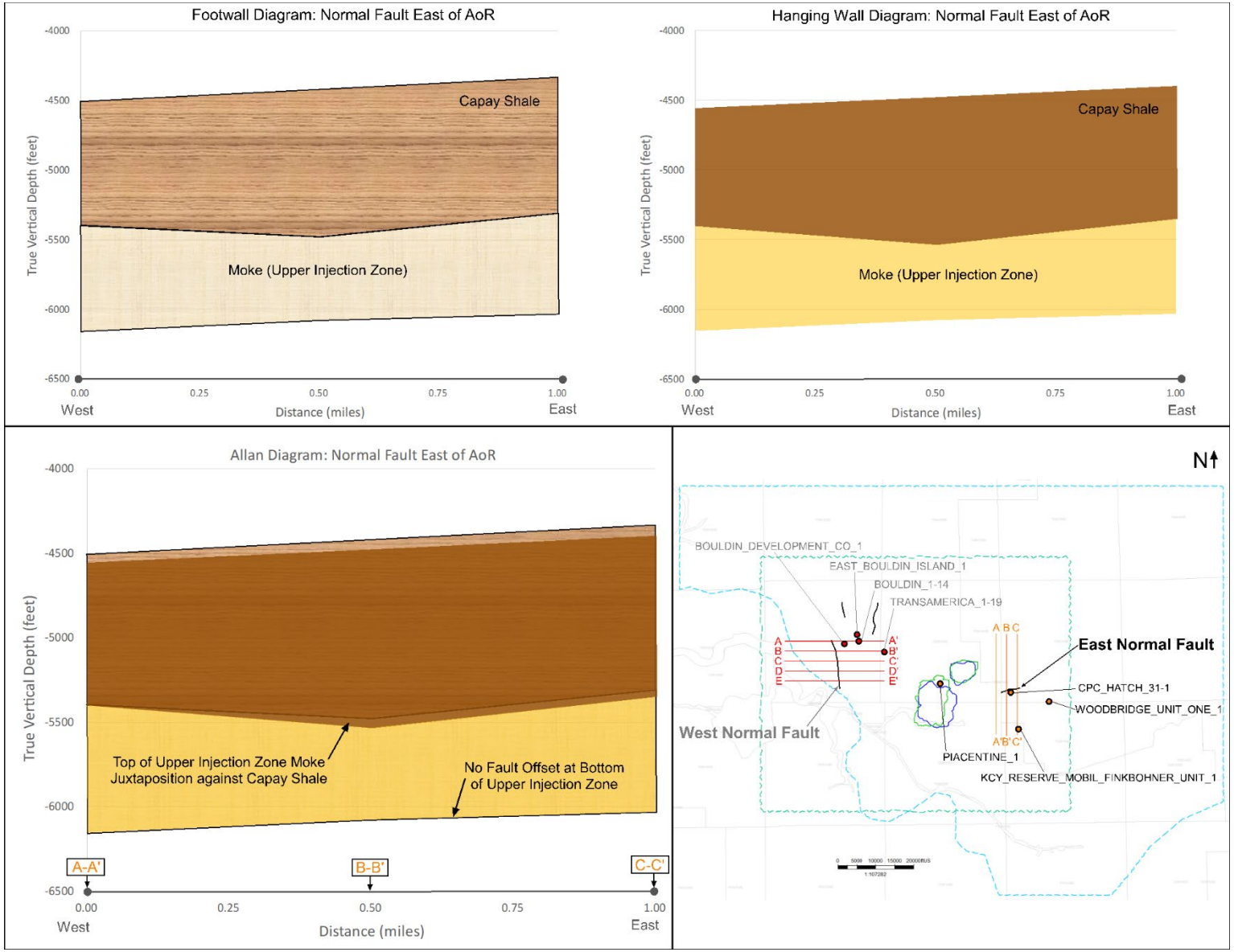

Figure 2.3-9. East Normal Fault Allan Diagram.

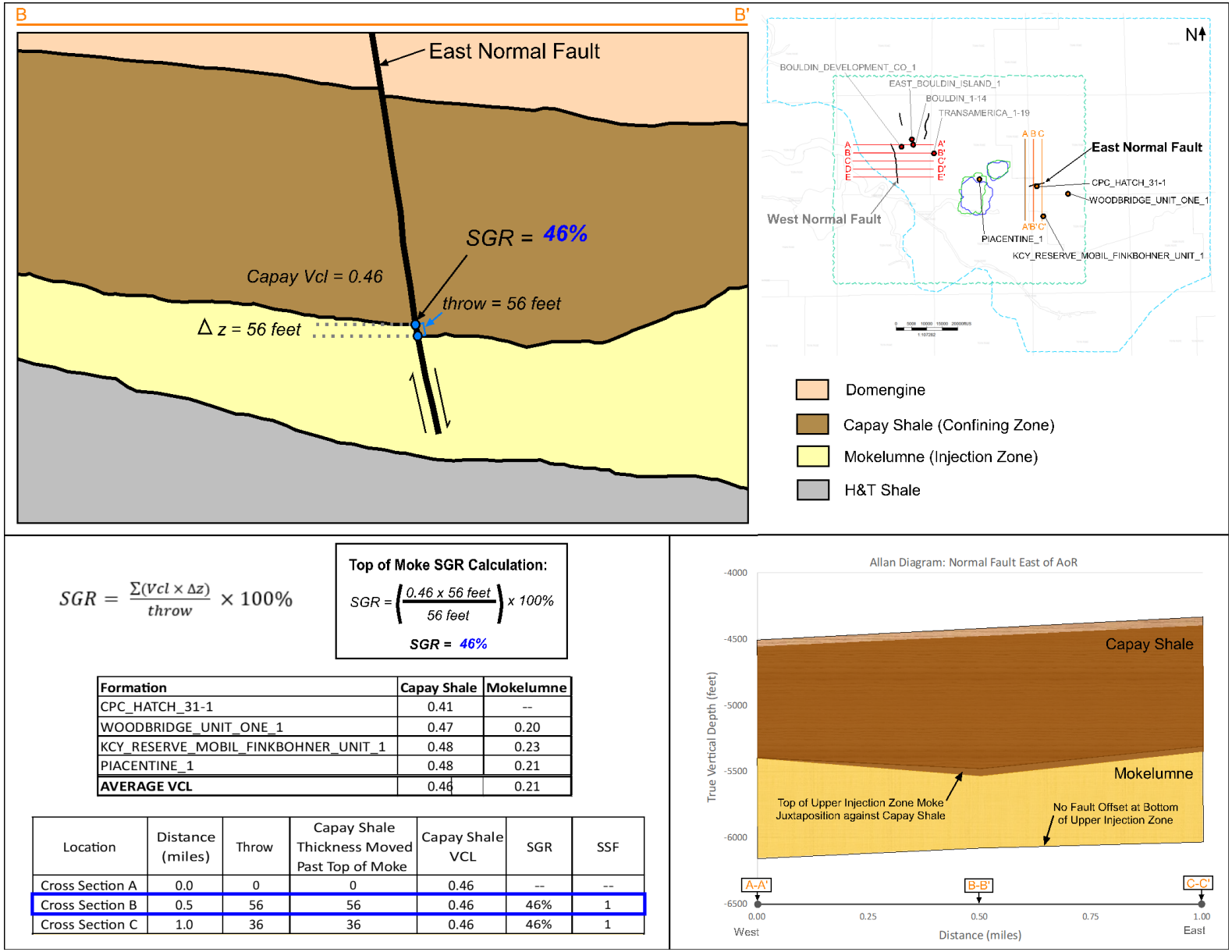

Formation	Capay Shale	Mokelumne
CPC_HATCH_31-1	0.41	--
WOODBRIDGE_UNIT_ONE_1	0.47	0.20
KCY_RESERVE_MOBIL_FINKBOHNER_UNIT_1	0.48	0.23
PIACENTINE_1	0.48	0.21
AVERAGE VCL	0.46	0.21

Location	Distance (miles)	Throw	Capay Shale Thickness Moved Past Top of Moke	Capay Shale VCL	SGR	SSF
Cross Section A	0.0	0	0	0.46	--	--
Cross Section B	0.5	56	56	0.46	46%	1
Cross Section C	1.0	36	36	0.46	46%	1

Figure 2.3-10. East Normal Fault Shale Gouge Ratio (SGR) calculation for the Upper Injection Zone (Mokelumne Formation).

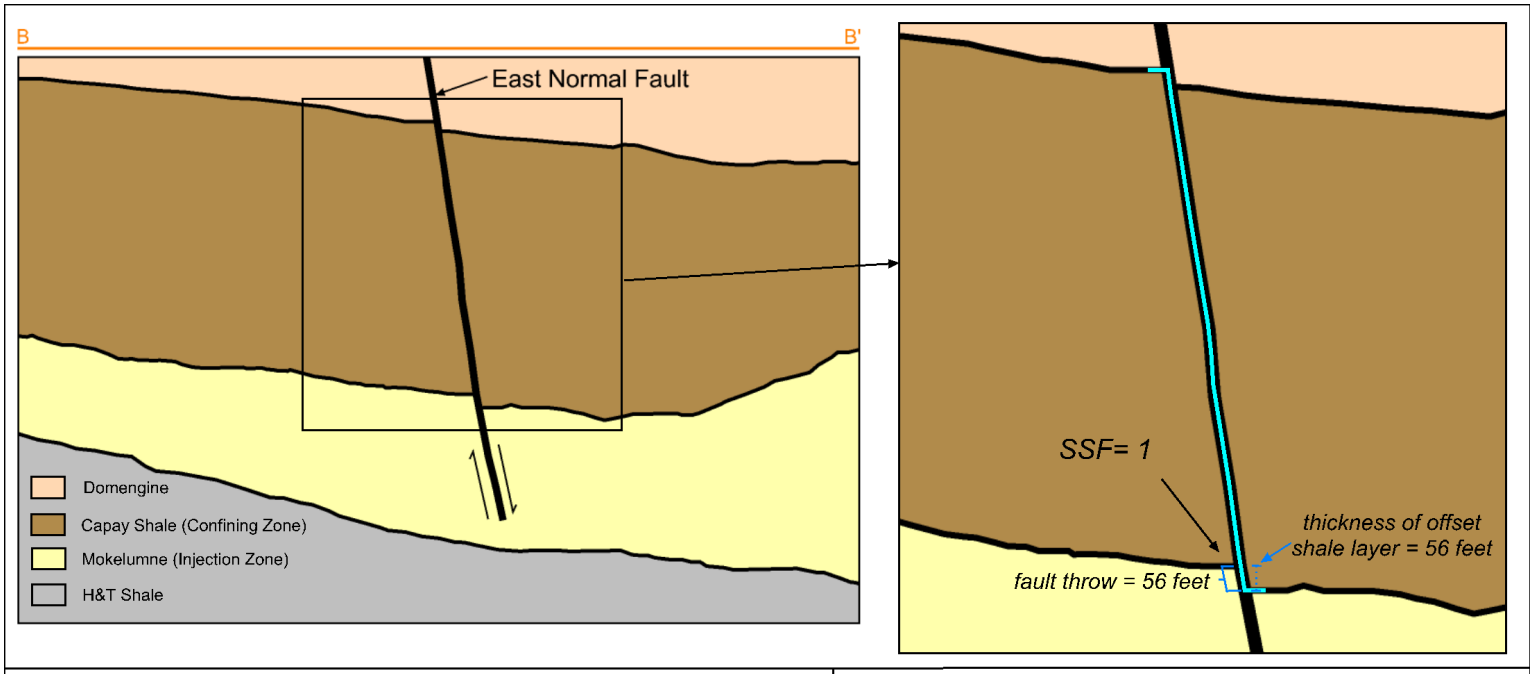

$$SSF = \frac{throw}{thickness}$$

Top of Moke SSF Calculation:

$$SSF = \left(\frac{56\ feet}{56\ feet}\right)$$

$$SSF = 1$$

Formation	Capay Shale	Mokelumne
CPC_HATCH_31-1	0.41	--
WOODBRIDGE_UNIT_ONE_1	0.47	0.20
KCY_RESERVE_MOBIL_FINKBOHNER_UNIT_1	0.48	0.23
PIACENTINE_1	0.48	0.21
AVERAGE VCL	0.46	0.21

Location	Distance (miles)	Throw	Capay Shale Thickness Moved Past Top of Moke	Capay Shale VCL	SGR	SSF
Cross Section A	0.0	0	0	0.46	--	--
Cross Section B	0.5	56	56	0.46	46%	1
Cross Section C	1.0	36	36	0.46	46%	1

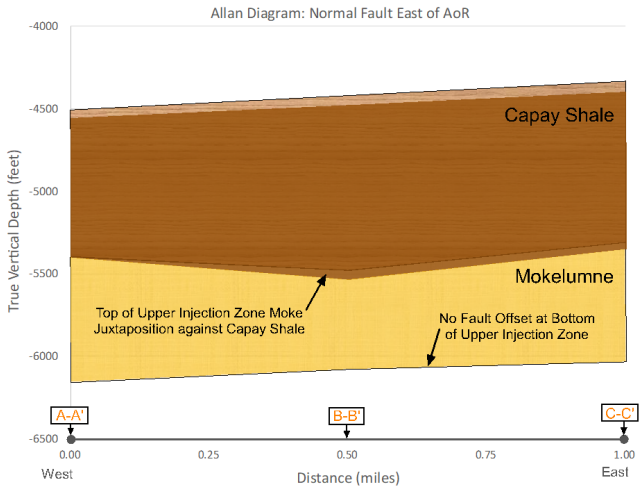

Figure 2.3-11. East Normal Fault Shale Smear Factor (SSF) calculation for the Upper Injection Zone (Mokelumne Formation).

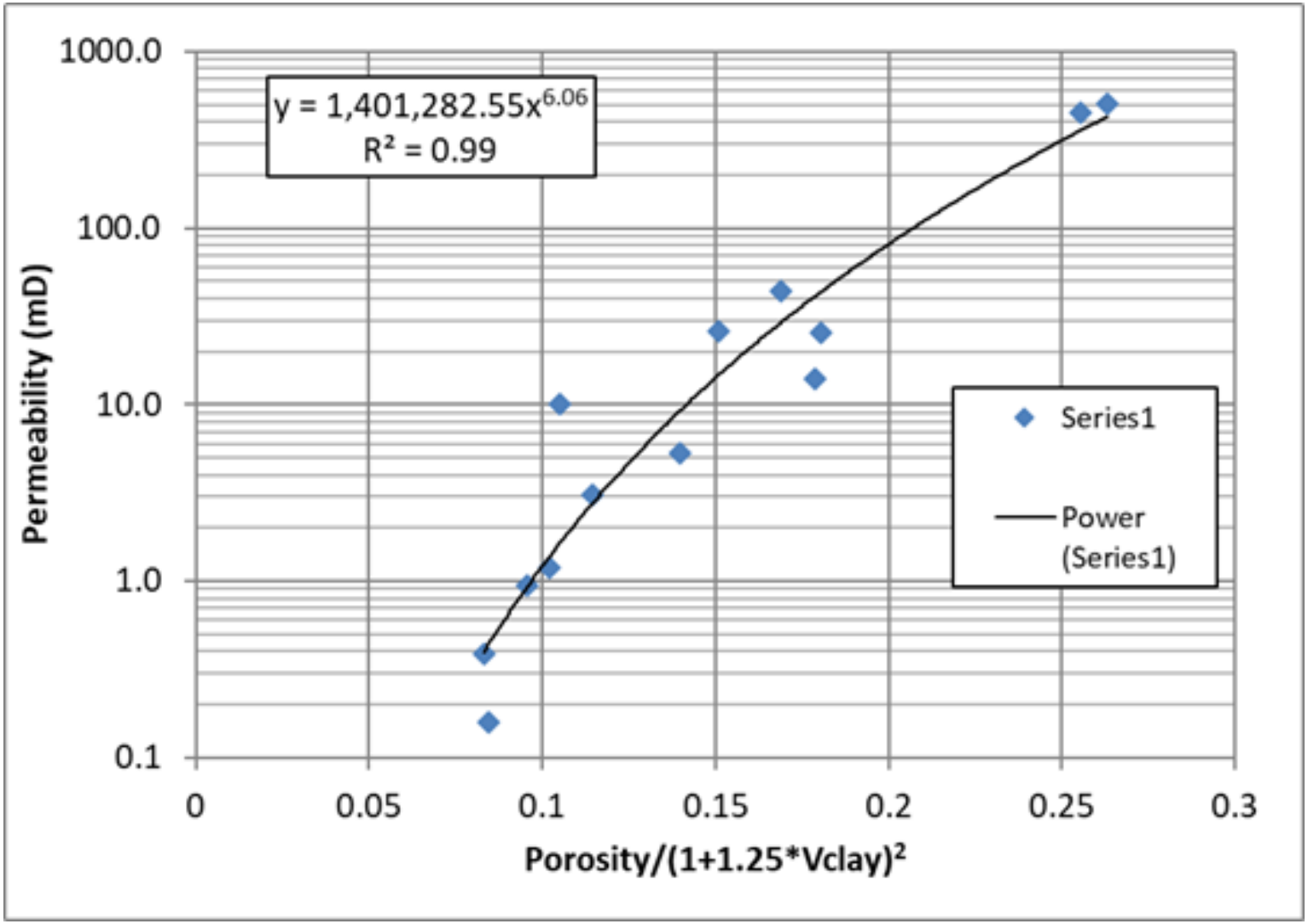

Figure 2.4-1. Permeability transform for Sacramento basin zones.

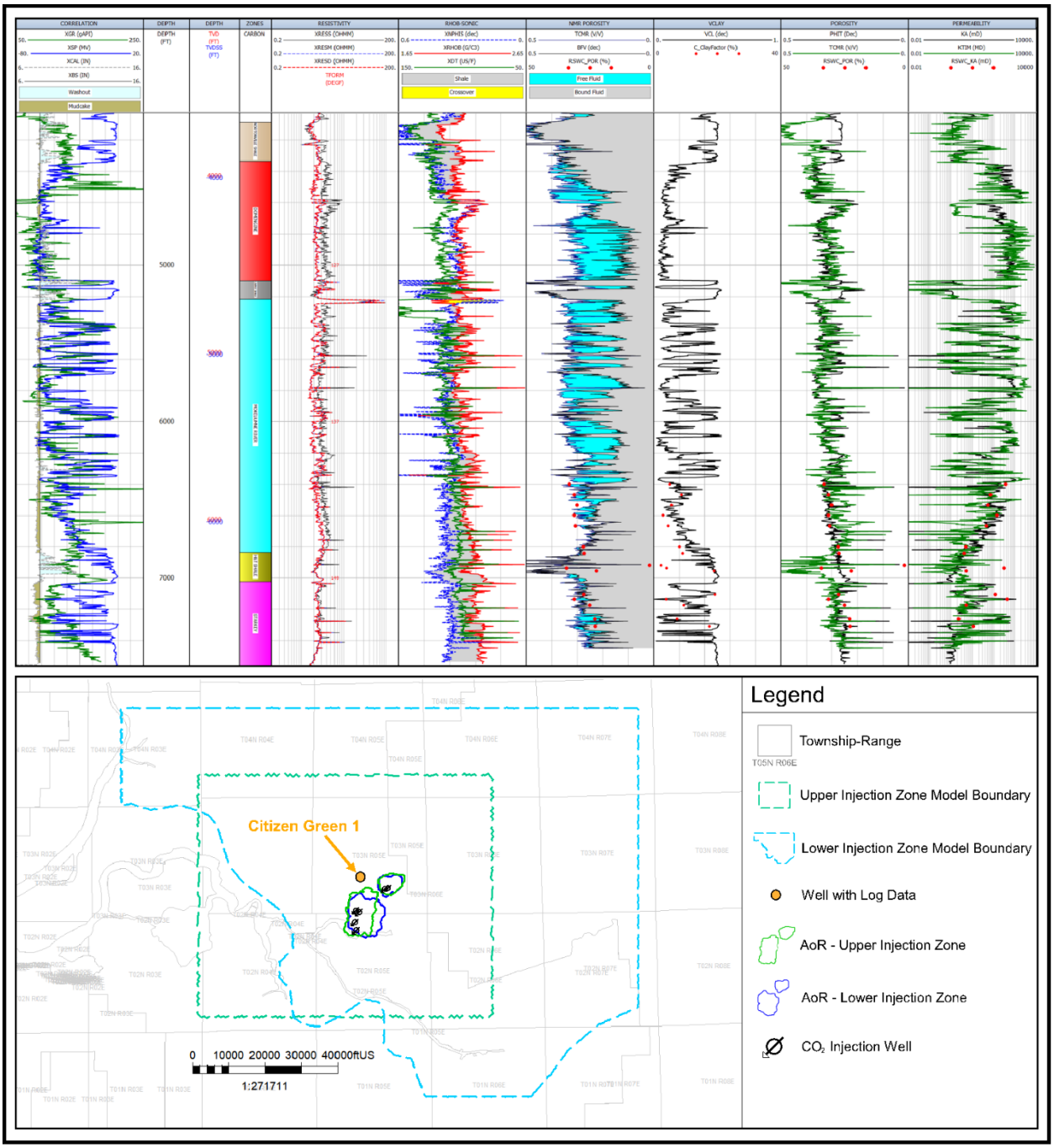

Figure 2.4-2. Example log from the Citizen_Green_1 well in King Island Gas Field. The last track shows a comparison of the permeability calculated from the transform (black) shown in **Figure 2.4-1** to permeability calculated from an NMR log (green) and rotary sidewall core permeability (red dots). Track 1: Correlation and caliper logs. Track 2: Measured depth. Track 3: Vertical depth and vertical subsea depth. Track 4: Zones. Track 5: Resistivity. Track 6: Compressional sonic, density, and neutron logs. Track 7: NMR total porosity and bound fluid. Track 8: Volume of clay. Track 9: Porosity calculated from density and NMR total porosity (green). Track 10: Permeability calculated using permeability transform and NMR Timur-Coates permeability (green).

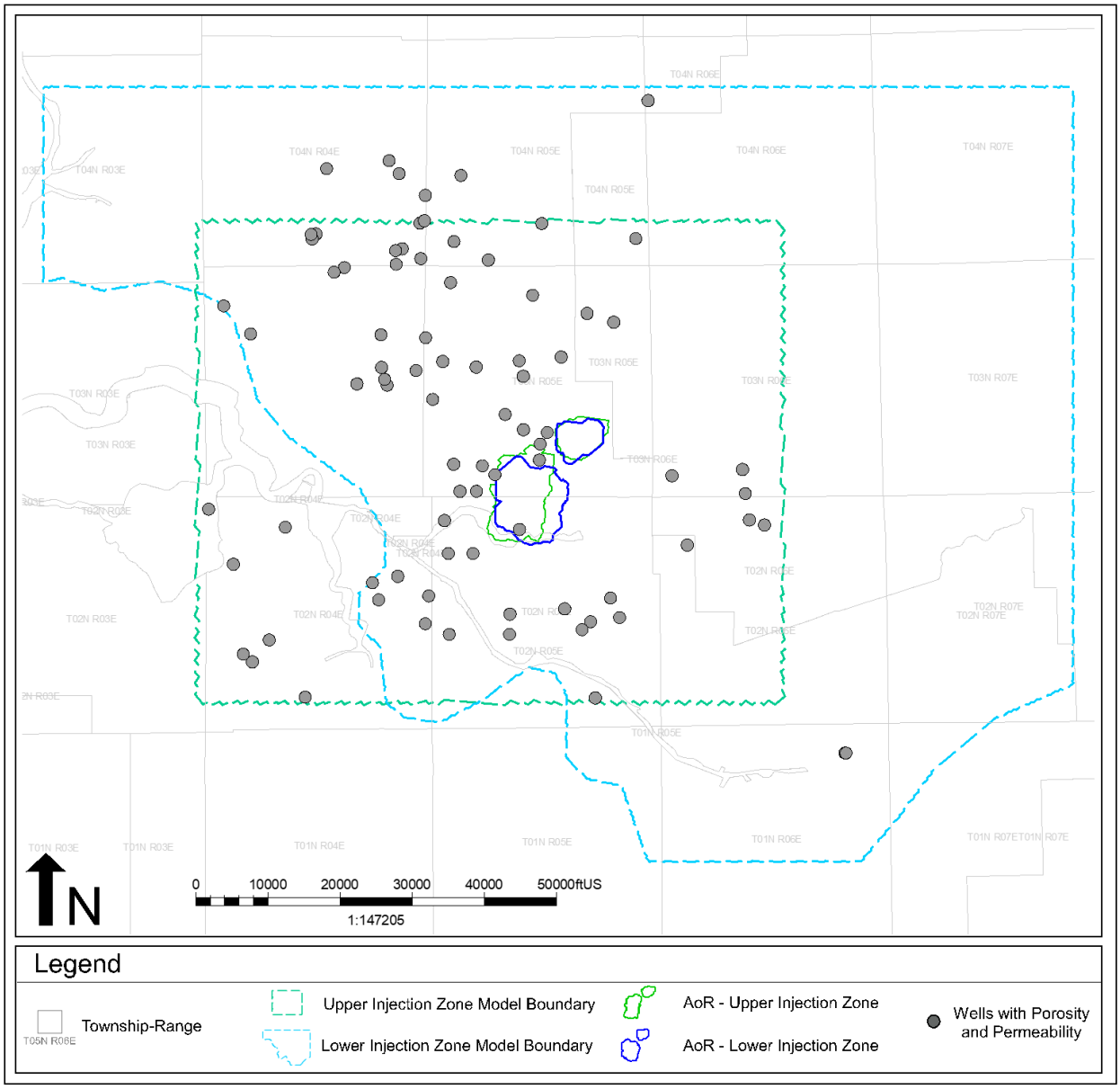

Figure 2.4-3. Map of wells with porosity and permeability data.

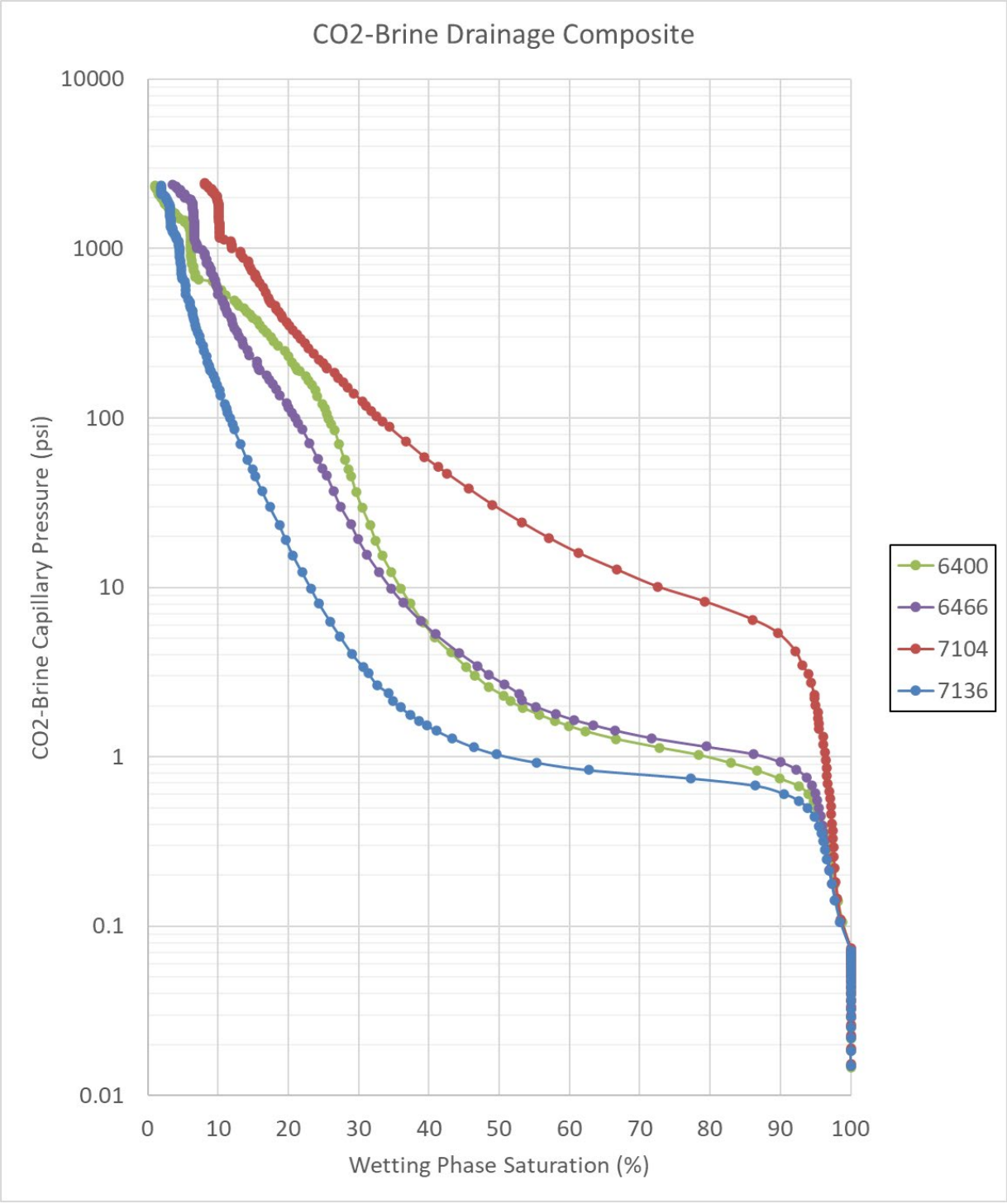

Figure 2.4-4. Capillary pressure versus wetting phase saturation for core data from the Citizen_Green_1 well. Samples are labeled by their depth.

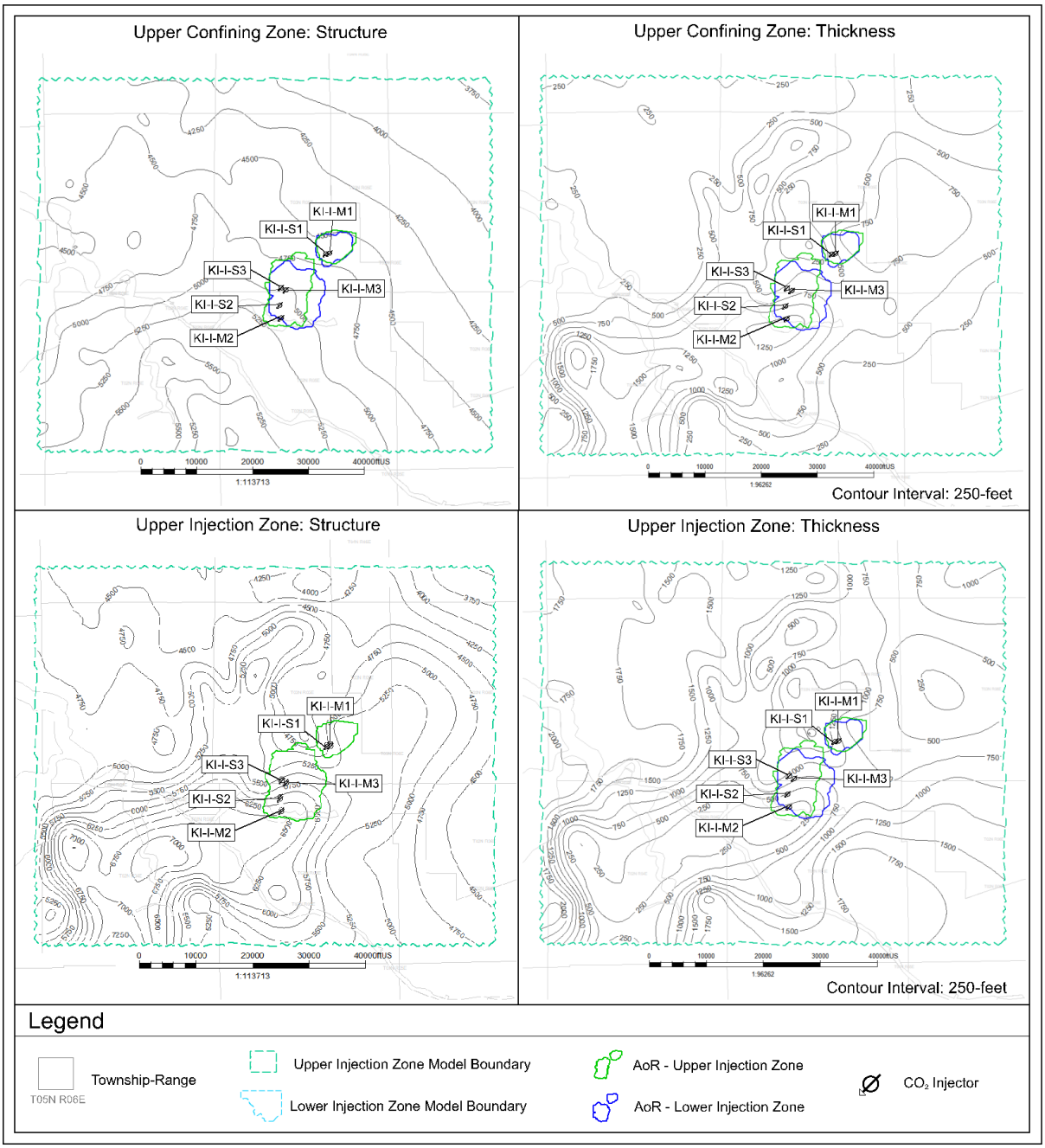

Figure 2.4-5. Thickness and structure maps for Upper Confining Zone, Upper Injection Zone.

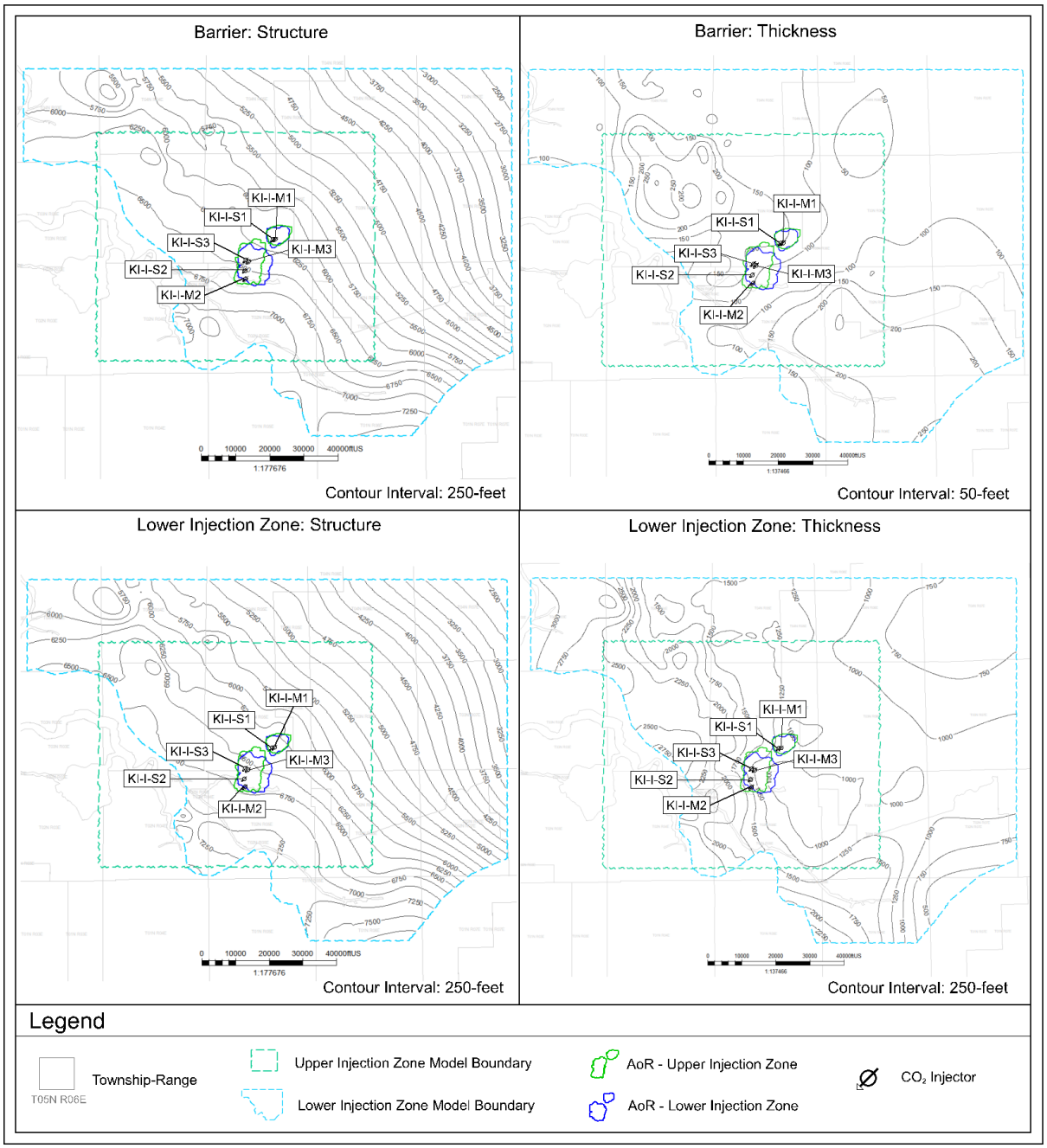

Figure 2.4-6. Thickness and structure maps for Barrier and Lower Injection Zone.

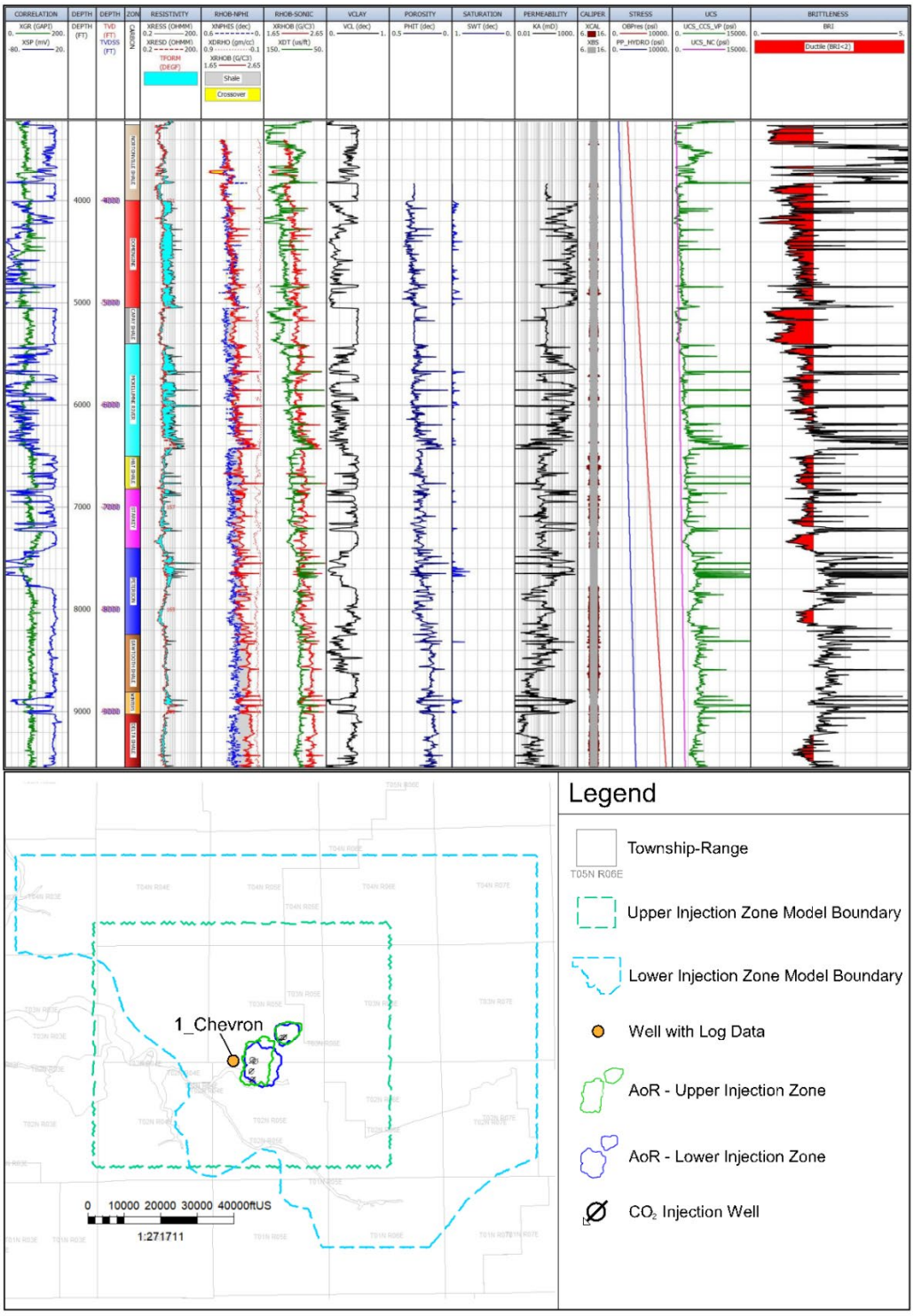

Figure 2.5-1. Unconfined compressive strength and ductility calculations for well 1_Chevron. The ductility is less than two for all of the upper confining zone, secondary confining zone, and the internal barrier. Track 1: Correlation logs. Track 2: Measured depth. Track 3: Vertical depth and vertical subsea depth. Track 4: Zones. Track 5: Resistivity. Track 6: Density and neutron logs. Track 7: Density and compressional sonic logs. Track 8: Volume of clay. Track 9: Porosity calculated from density. Track 10: Water saturation. Track 11: Permeability. Track 12: Caliper. Track 13: Overburden pressure and hydrostatic pore pressure. Track 14: UCS and UCS_NC. Track 15: Brittleness.

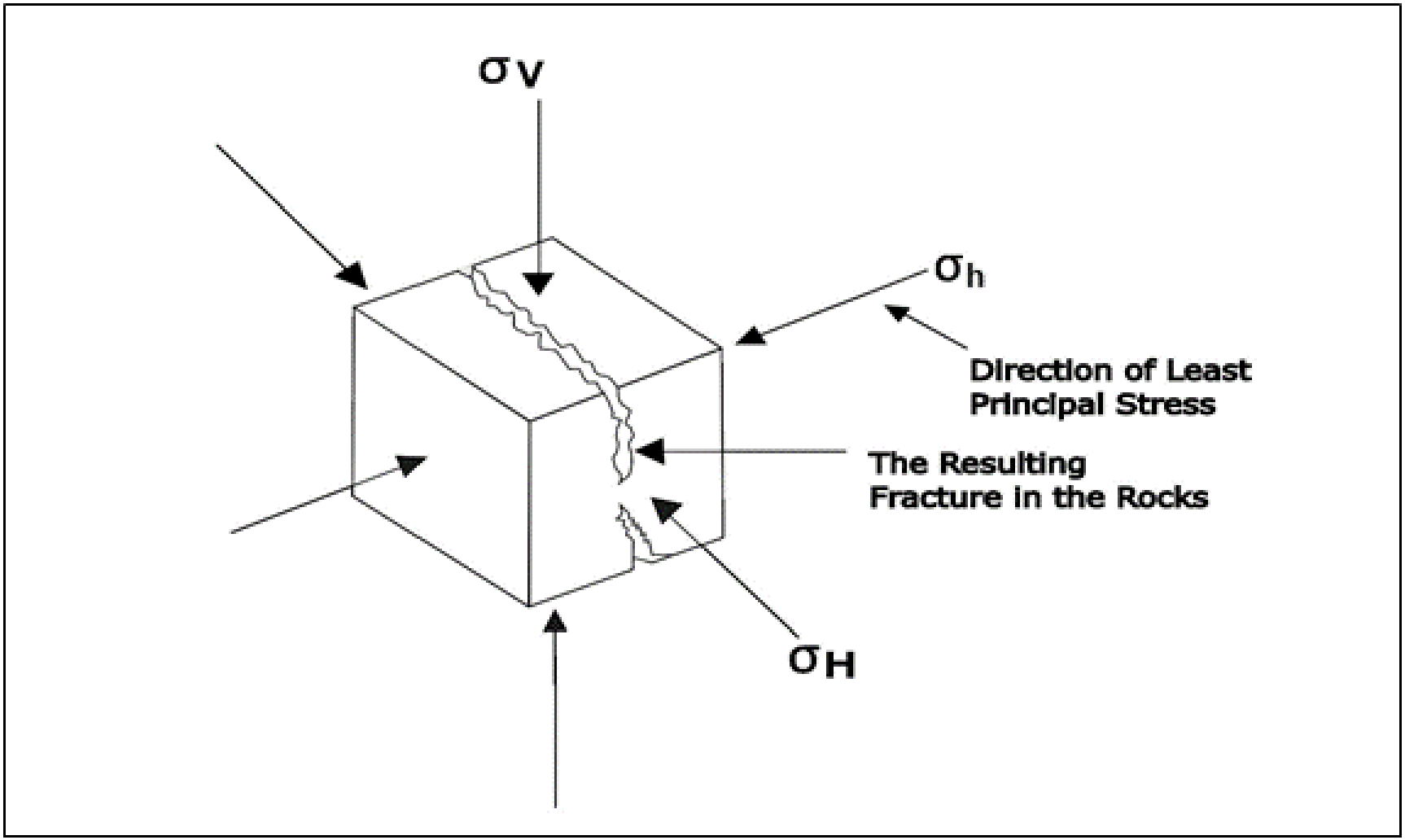

Figure 2.5-2. Stress diagram showing the three principal stresses and the fracturing that will occur perpendicular to the minimum principal stress.

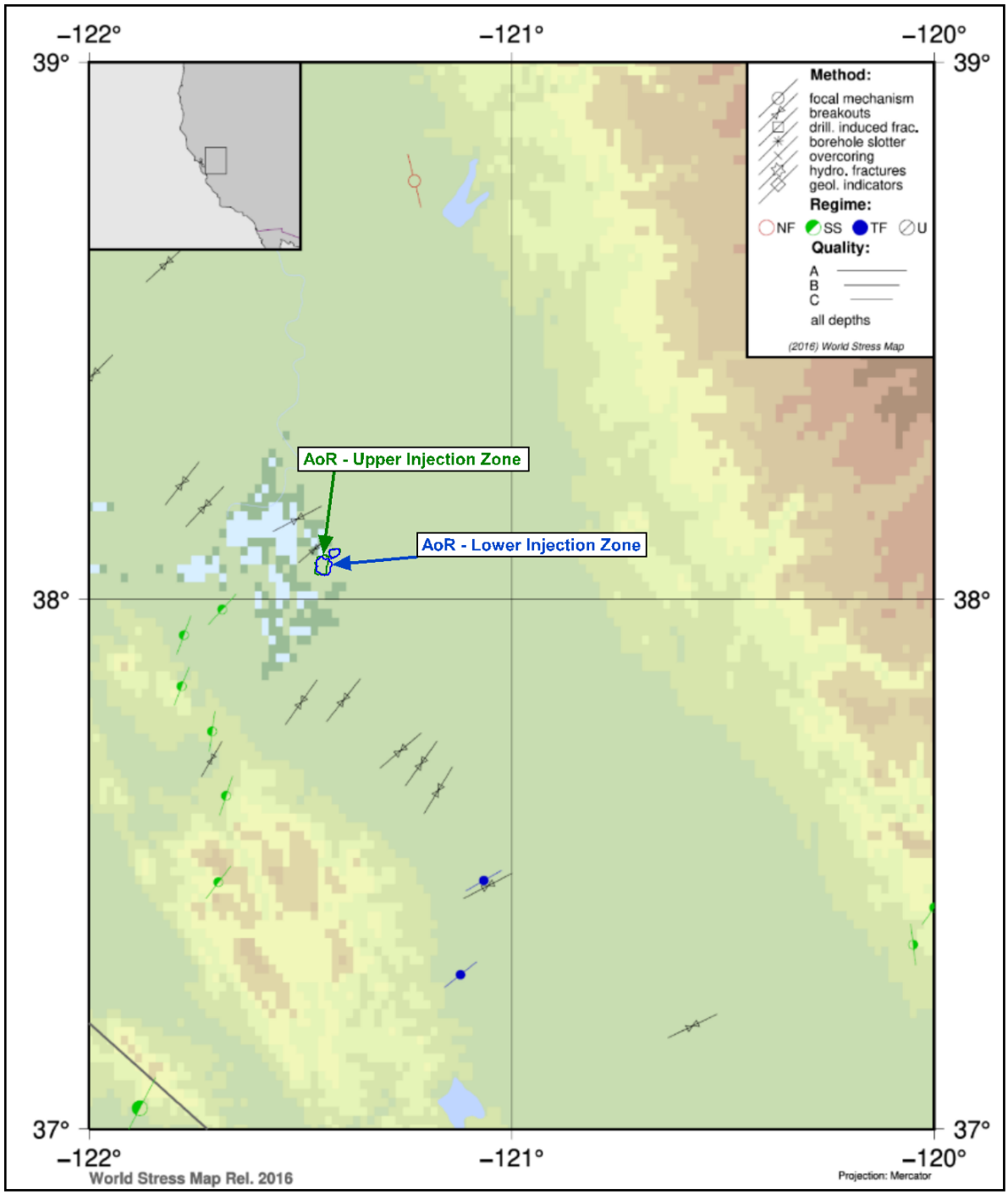

Figure 2.5-3. World Stress Map output showing S_{Hmax} azimuth indicators and earthquake faulting styles in the Sacramento Basin (Heidbach et al., 2016). The background coloring represents topography.

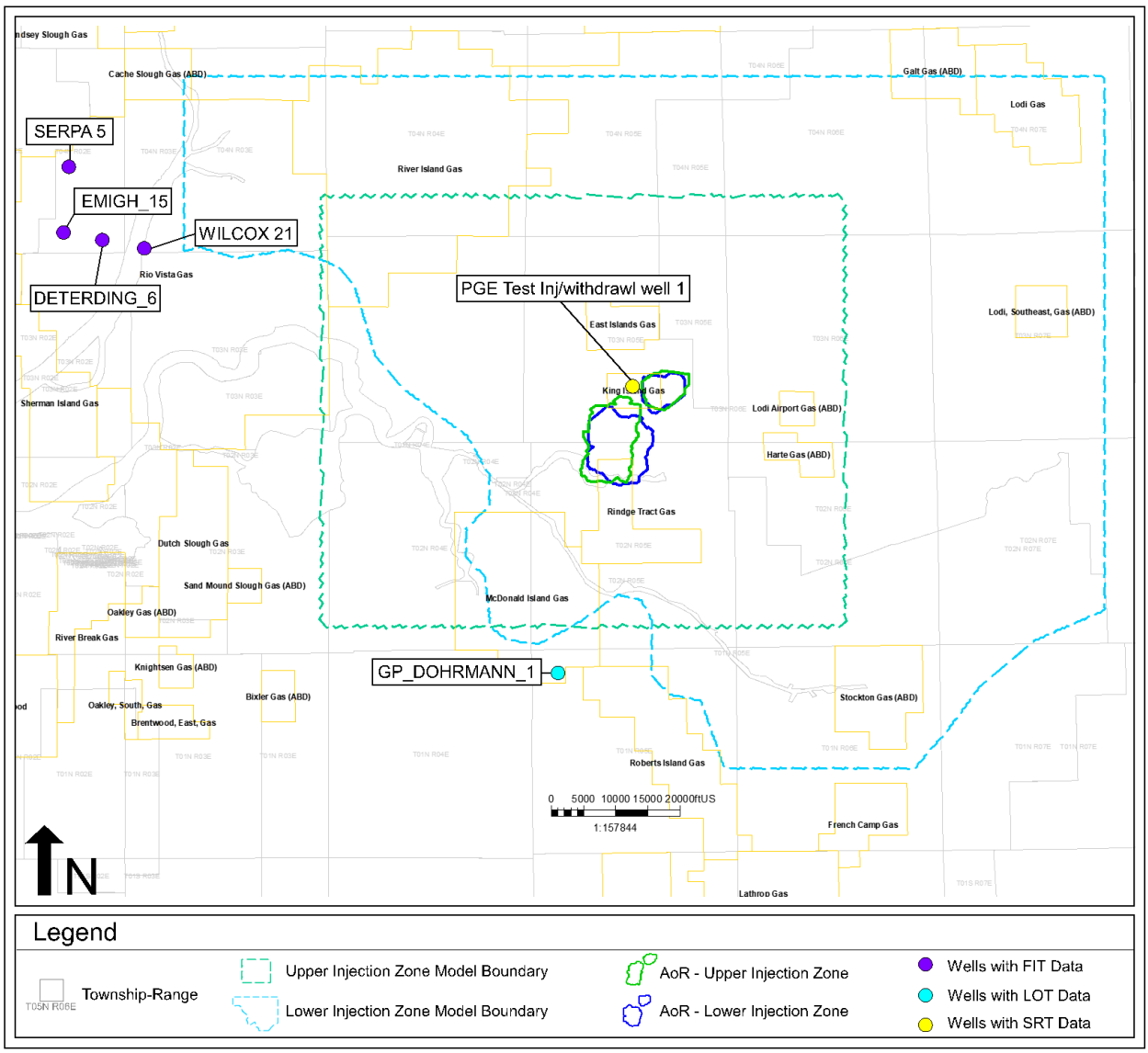

Figure 2.5-4. Map showing the location of wells with formation integrity tests (FIT).

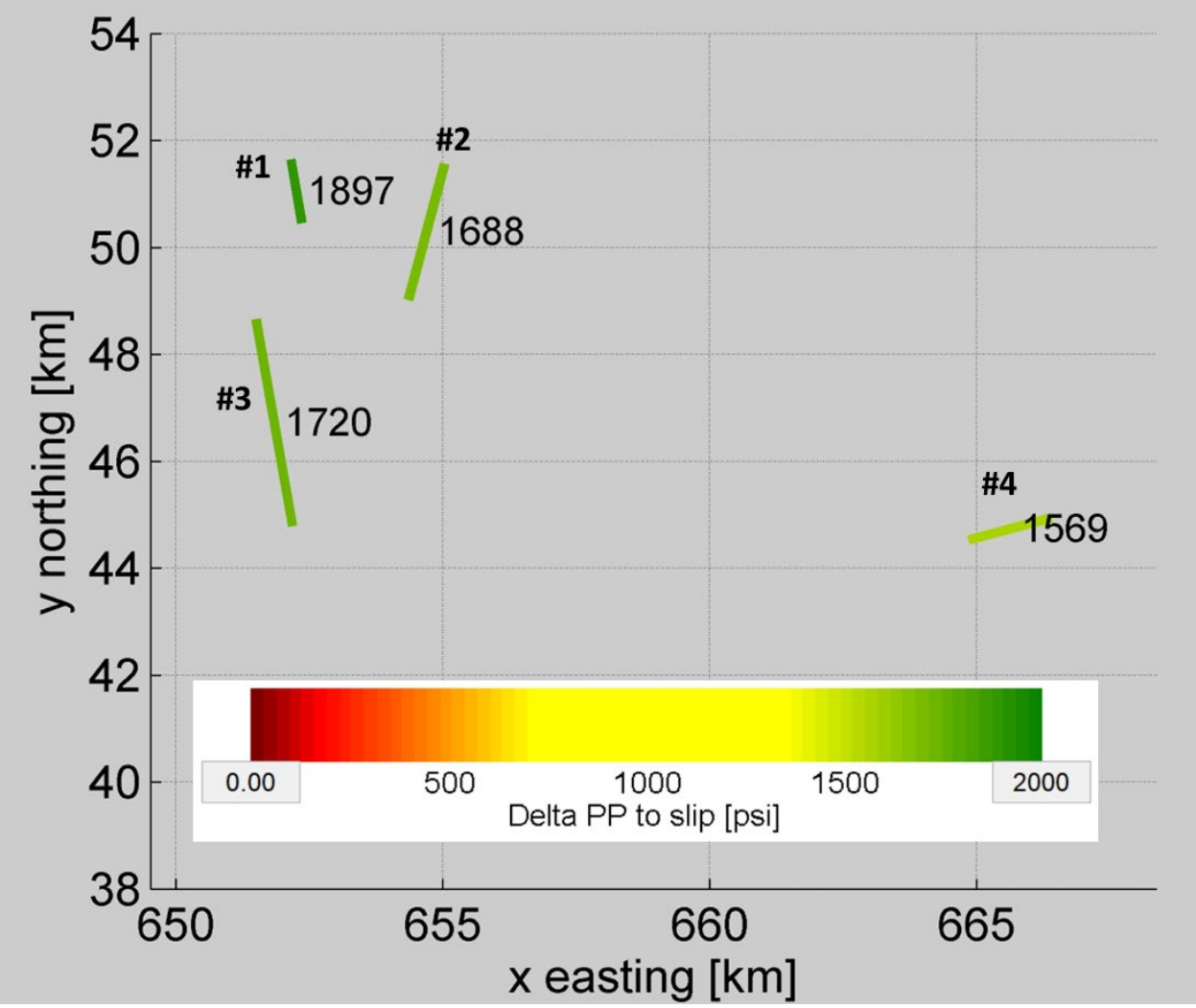

Figure 2.5-5. Map showing the four modeled faults for the Mokelumne River Formation. The numbers on the plot next to each fault represent the necessary increase in pore pressure above present day conditions to cause failure on that fault segment.

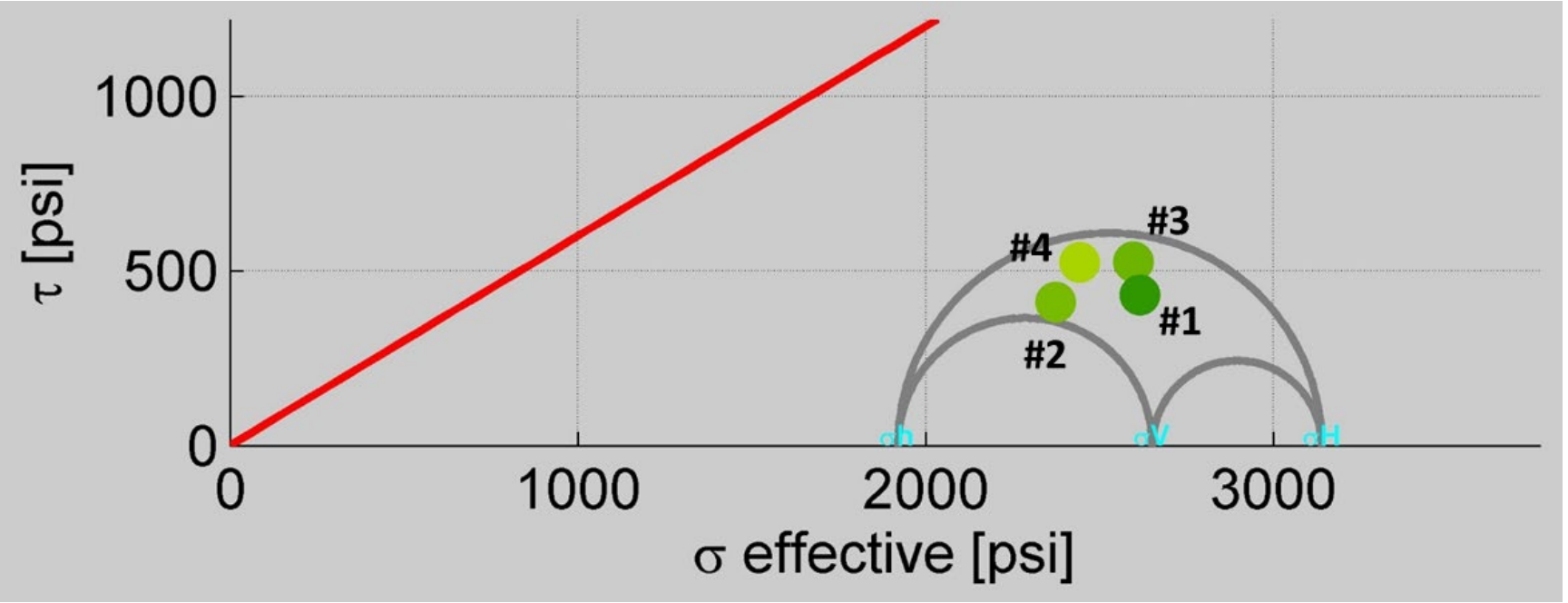

Figure 2.5-6. Mohr circle of the Mokelumne River Formation at present-day conditions. The effective normal stress (x-axis) and shear stress (y-axis) on the four modeled faults are represented by the green dots. The red line represents the Mohr coulomb failure surface assuming a coefficient of friction of 0.6 and a fault cohesion of 0 psi.

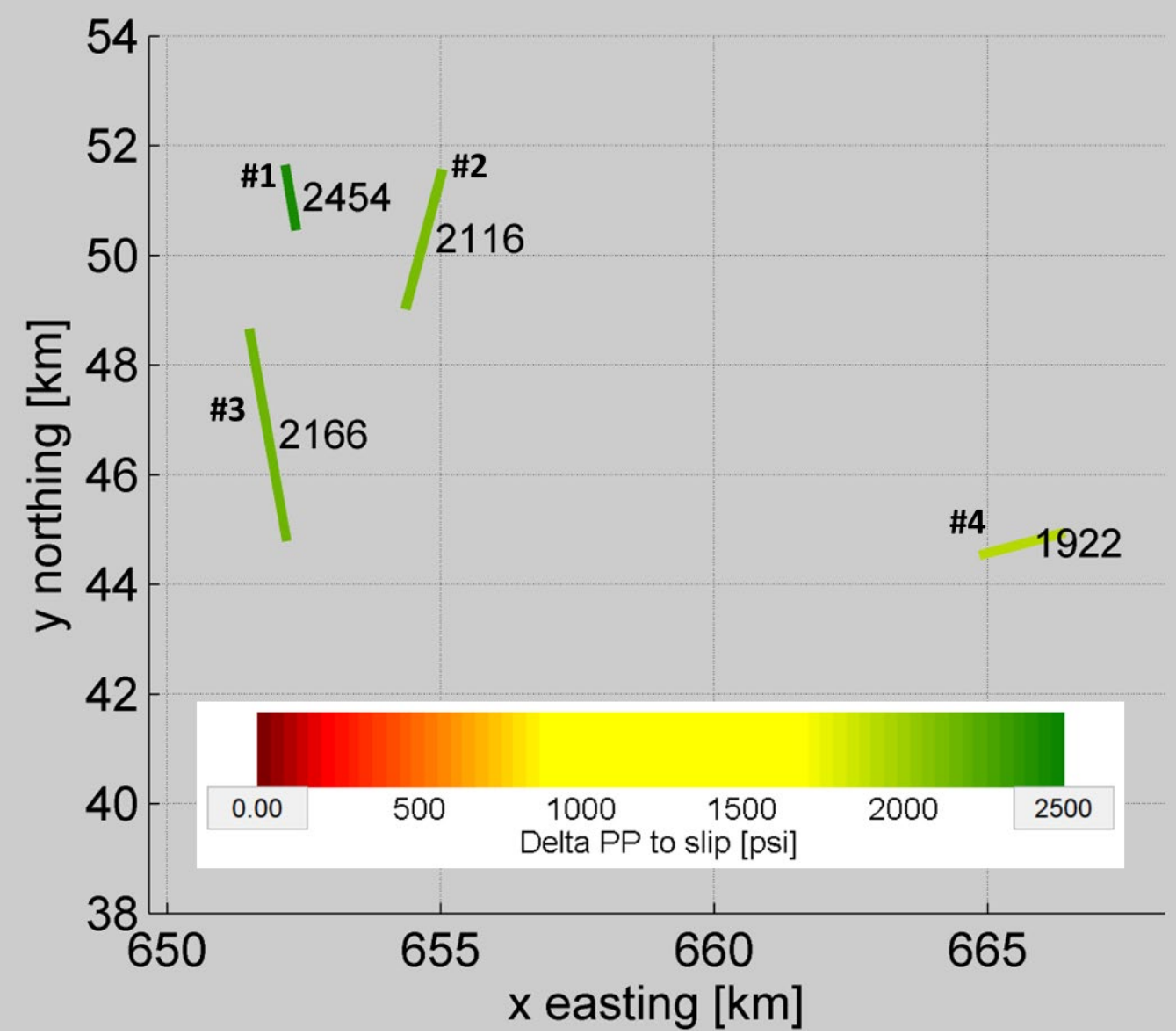

Figure 2.5-7. Map showing the four modeled faults for the Starkey Formation. The numbers on the plot next to each fault represent the necessary increase in pore pressure above present day conditions to cause failure on that fault segment.

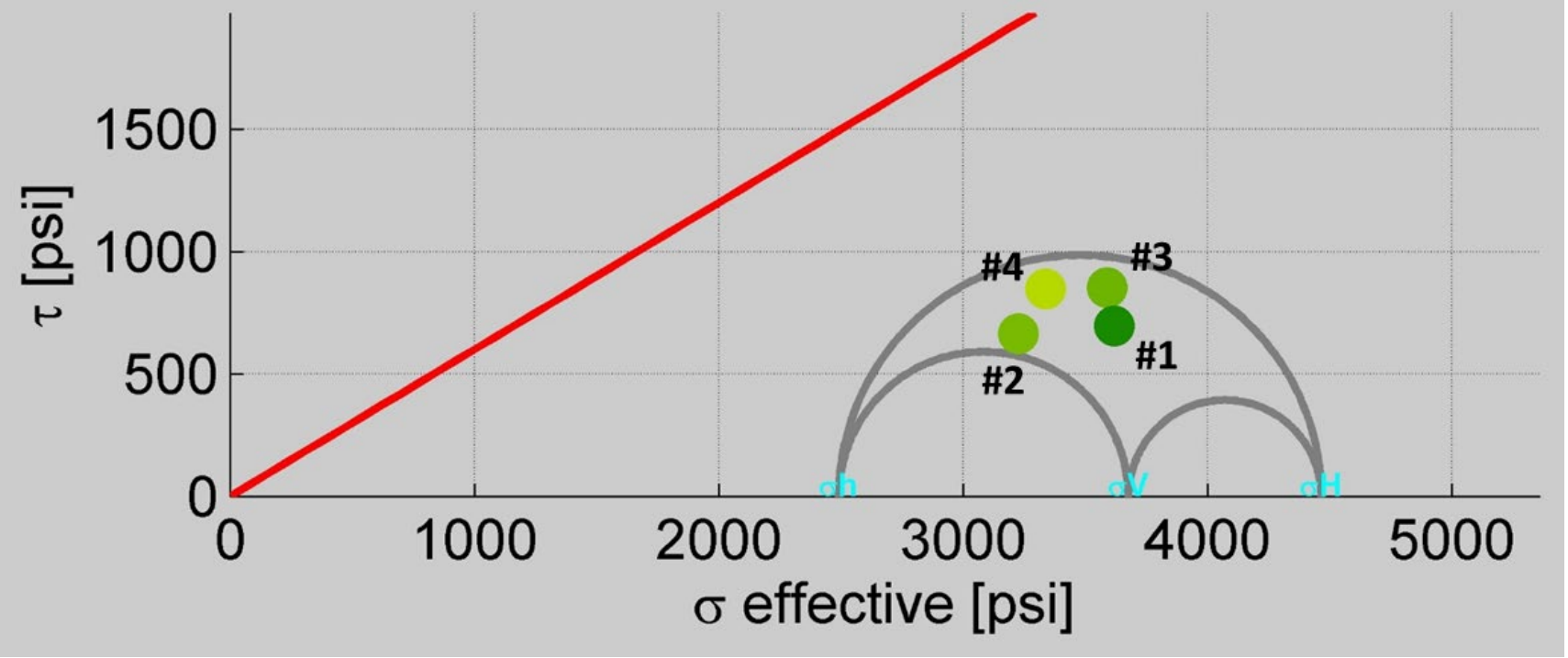

Figure 2.5-8. Mohr circle of the Starkey Formation at present-day conditions. The effective normal stress (x-axis) and shear stress (y-axis) on the four modeled faults are represented by the green dots. The red line represents the Mohr coulomb failure surface assuming a coefficient of friction of 0.6 and a fault cohesion of 0 psi.

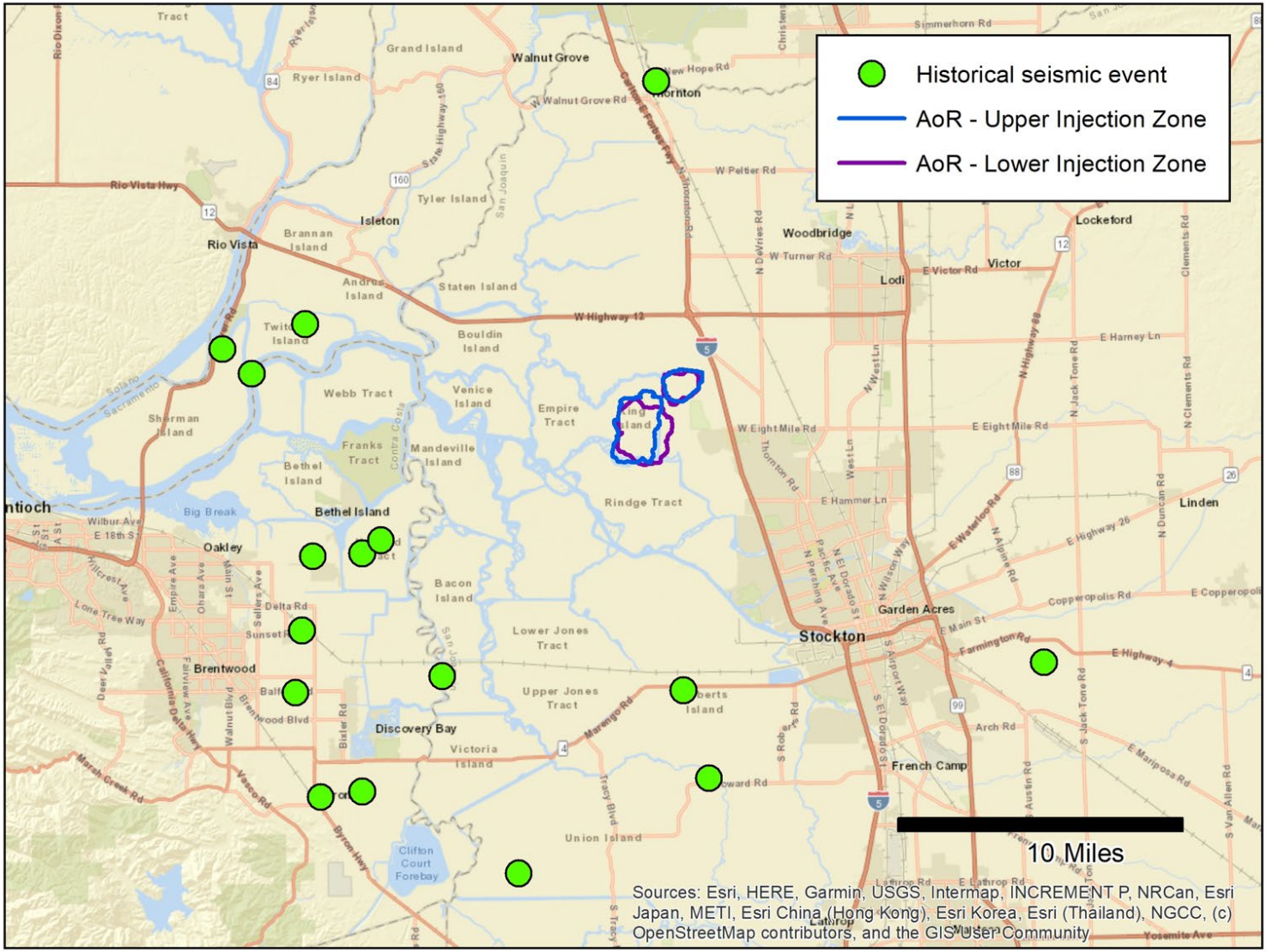

Figure 2.6-1. Historical earthquakes from the USGS catalog tool for the greater area. Data from these events are compiled in **Table 2.6-1**. (https://earthquake.usgs.gov/earthquakes/search/)

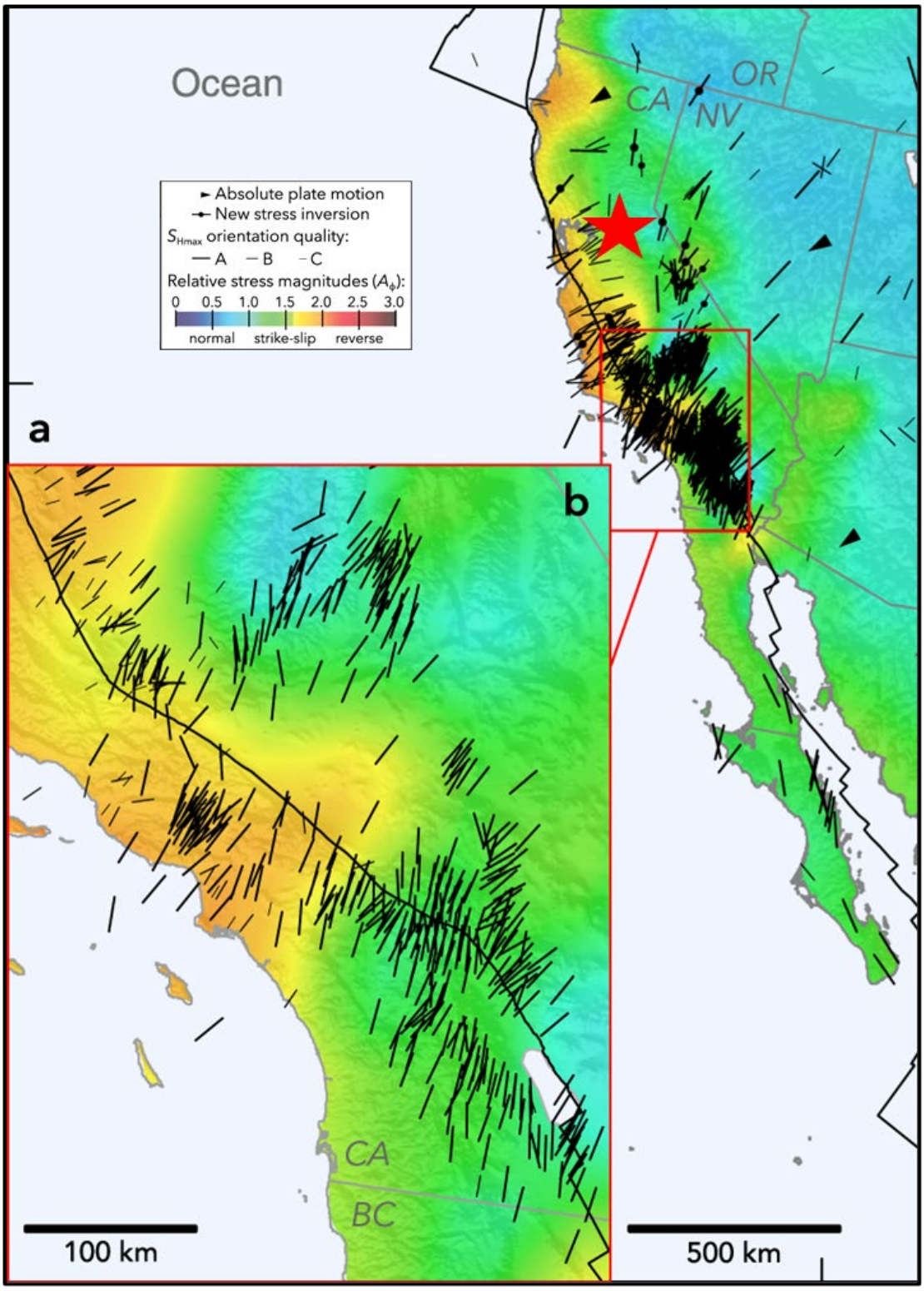

Figure 2.6-2. Image modified from Lund-Snee and Zoback (2020) showing relative stress magnitudes across California. Red star indicates the CTV V site area.

Figure 1-5: Neighboring Groundwater Subbasins

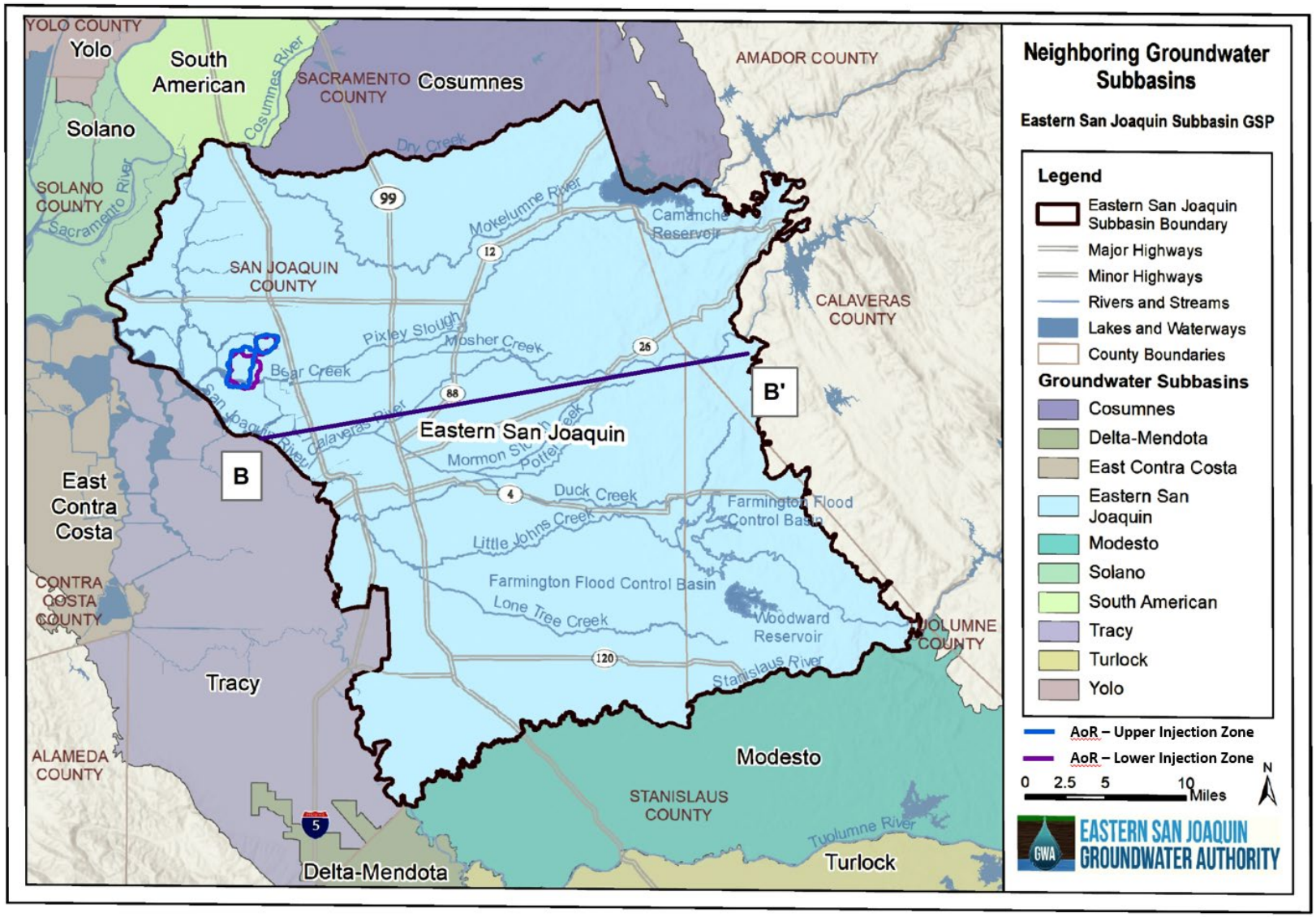

Figure 2.7-1 Map of the project AoR, groundwater subbasins, the surrounding areas

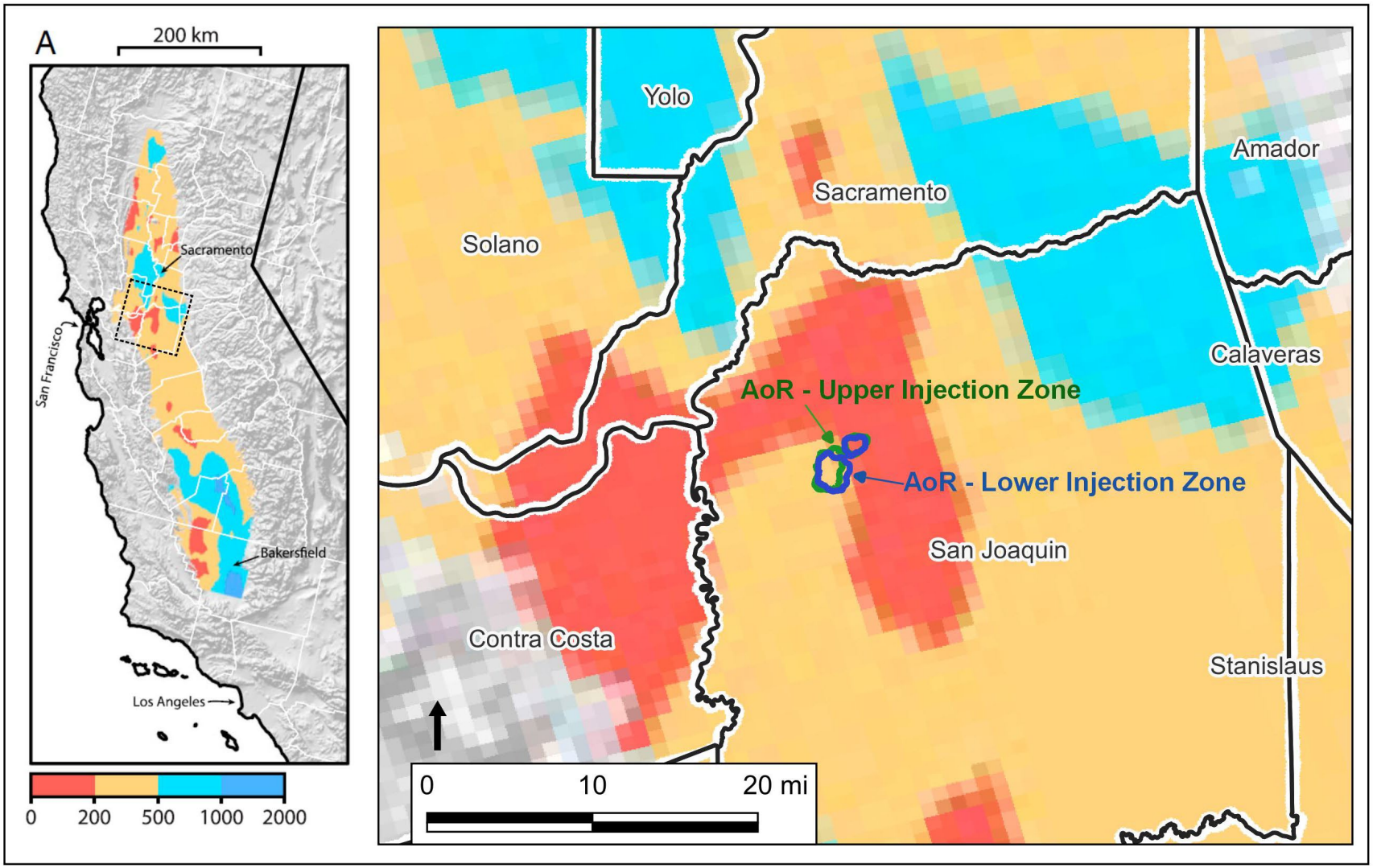

Figure 2.7-2. Elevation (meters below land surface) of the Estimated Base of Fresh Water (2,000 mg/L TDS) from Kang et al., 2020.

Figure 2-18: Base of Fresh Water Elevation and Stockton Fault

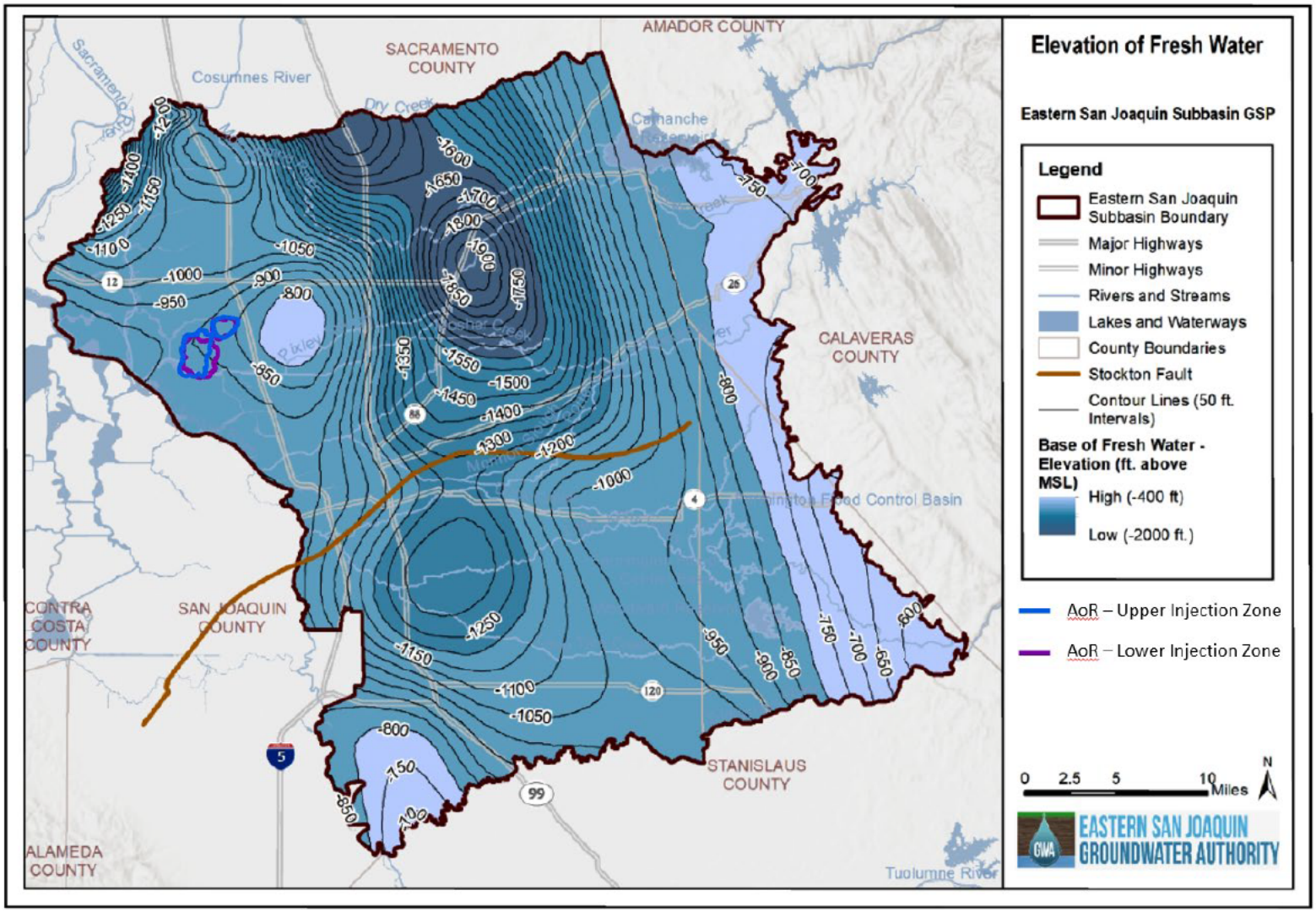

Figure 2.7-3 Base of fresh water map (ESJGA, 2019).

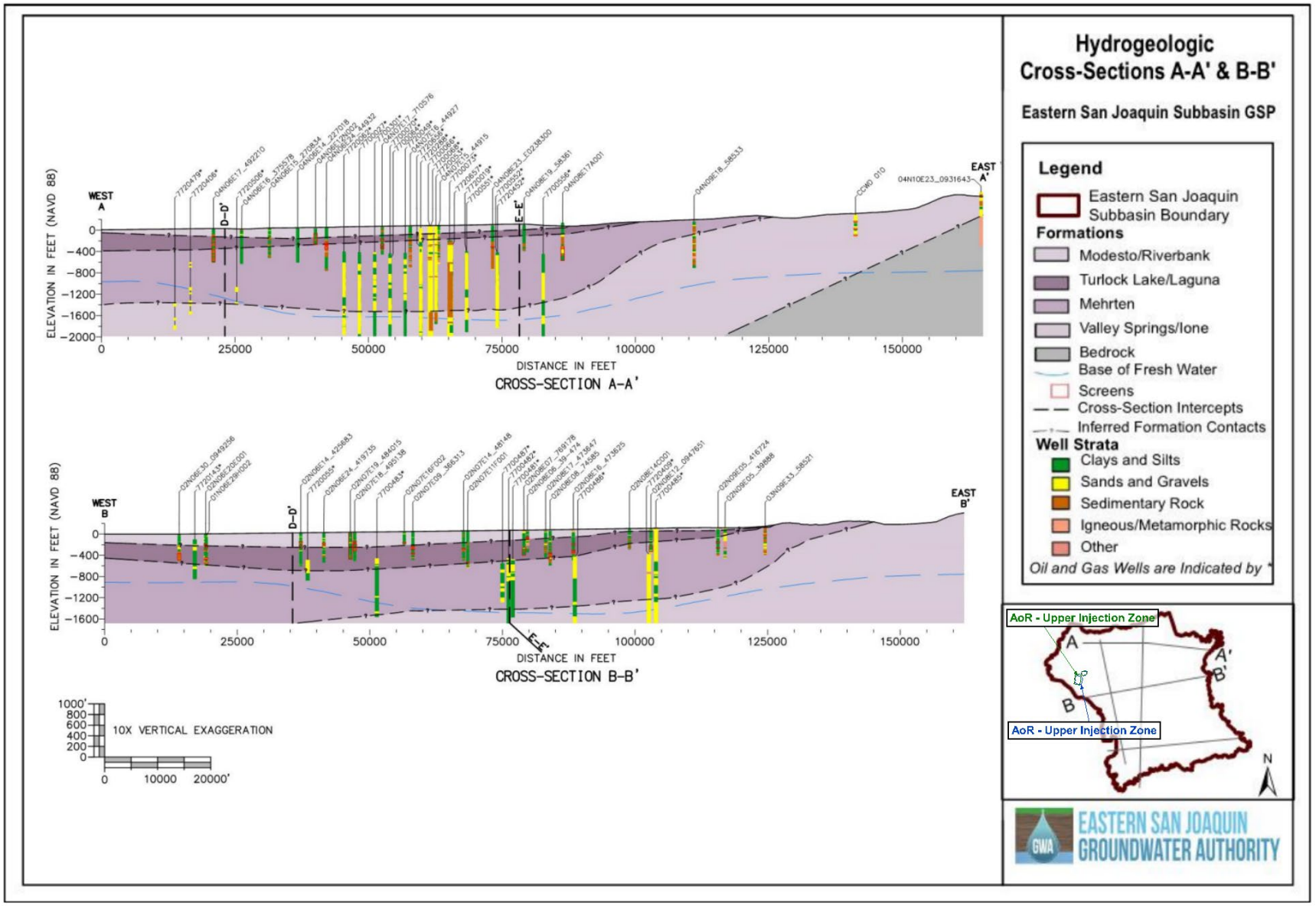

Figure 2.7-4 Geologic Cross Section B-B' showing Base of Fresh Water (ESJGA, 2019)

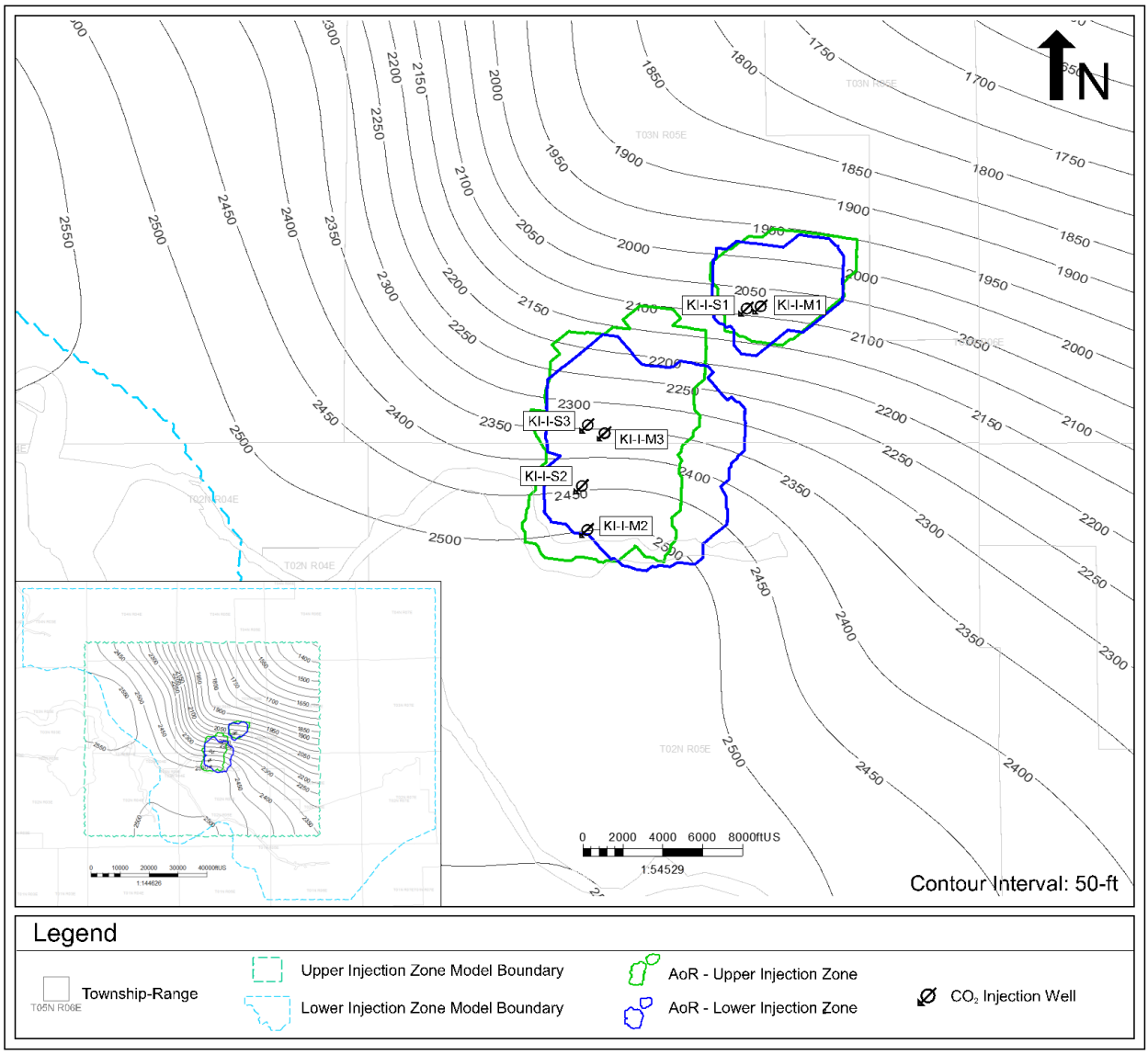

Figure 2.7-5. Depth to the base of the lowermost USDW (feet TVD) based on the calculation of salinity from logs inthe vicinity of the AoR.

Figure 2-38: Fourth Quarter 2017 Groundwater Levels

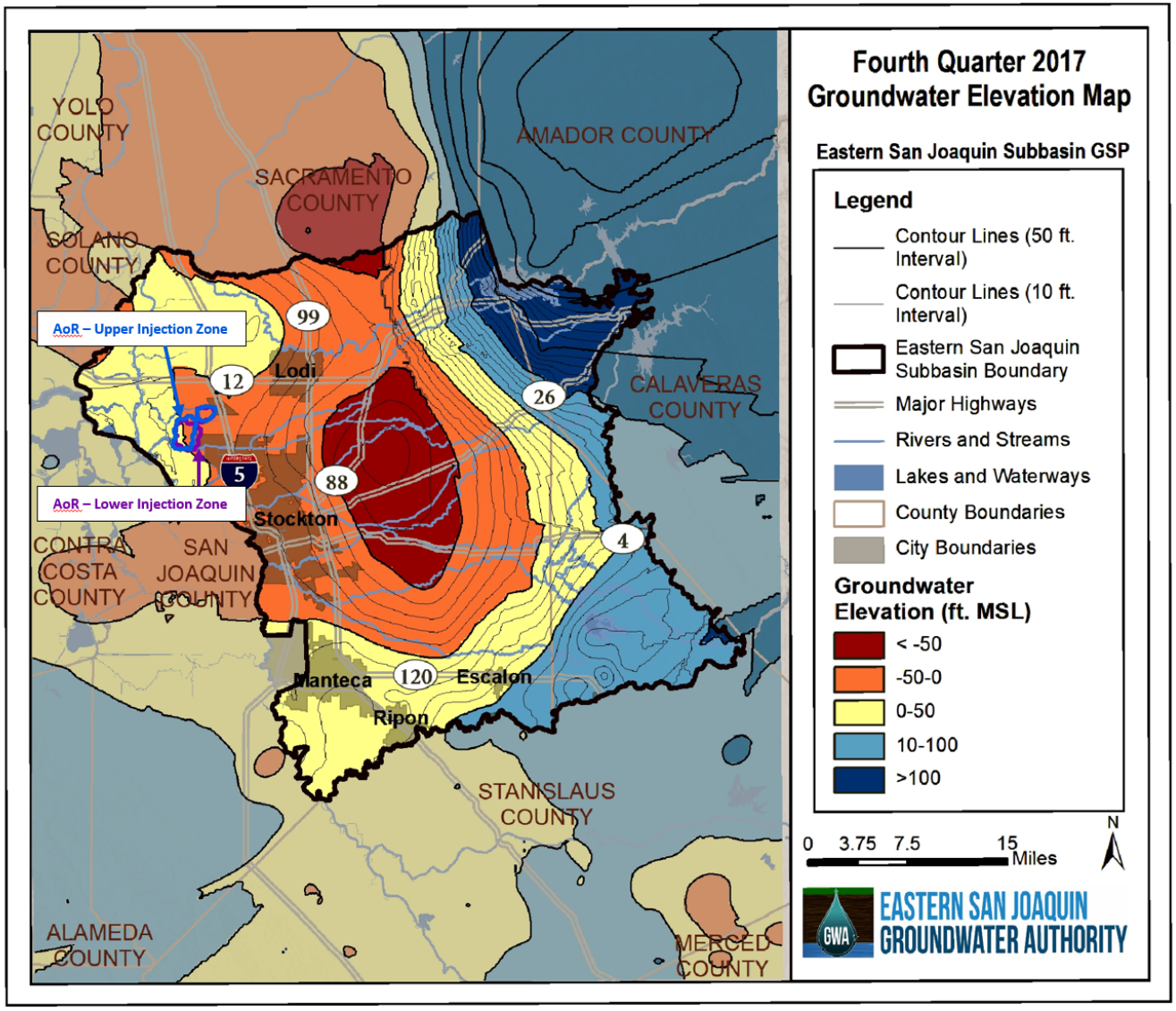

Figure 2.7-6 Groundwater level contours, 4th Quarter 2017 (ESJGA, 2019).

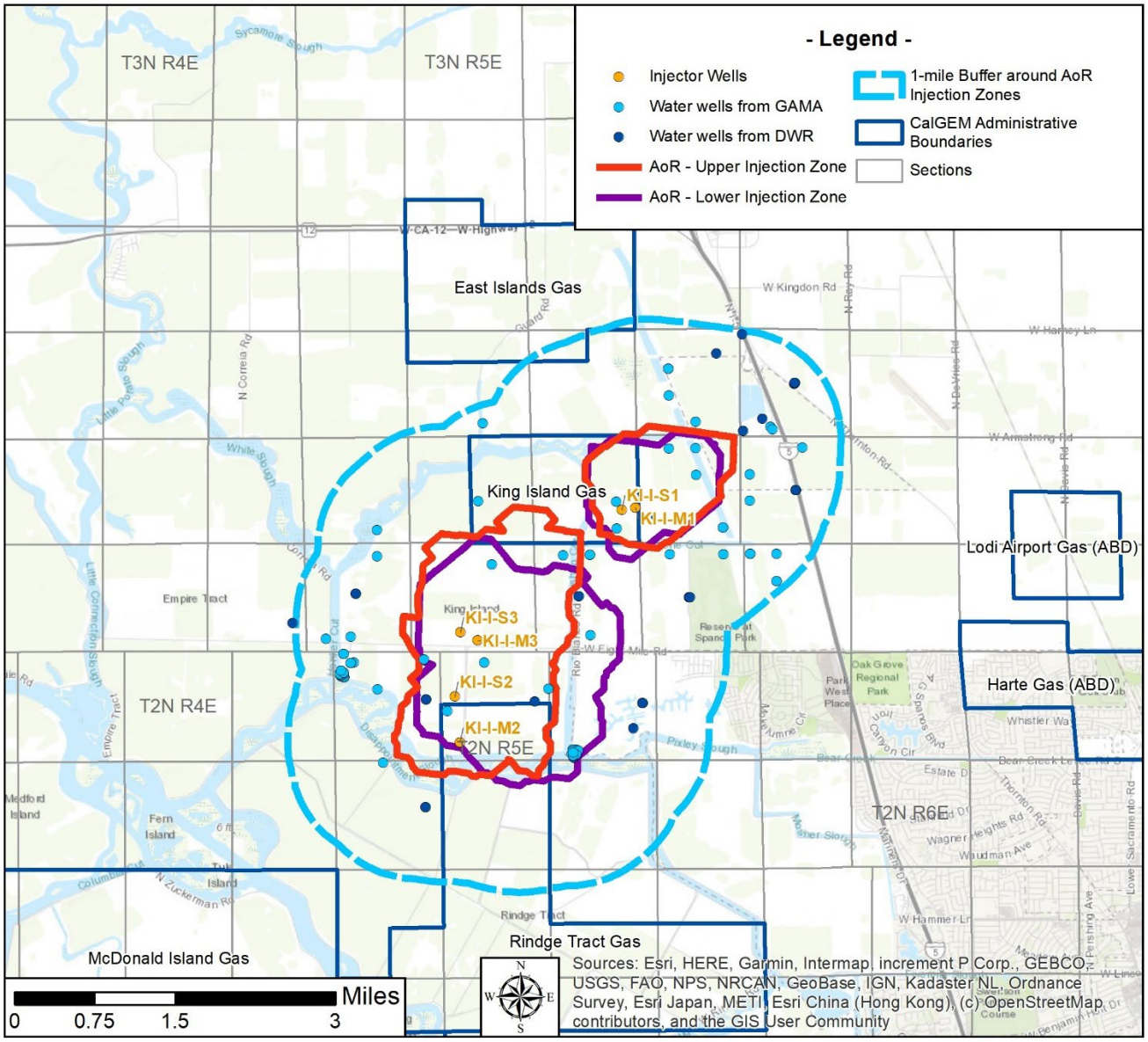

Figure 2.7-7 Water well location map.

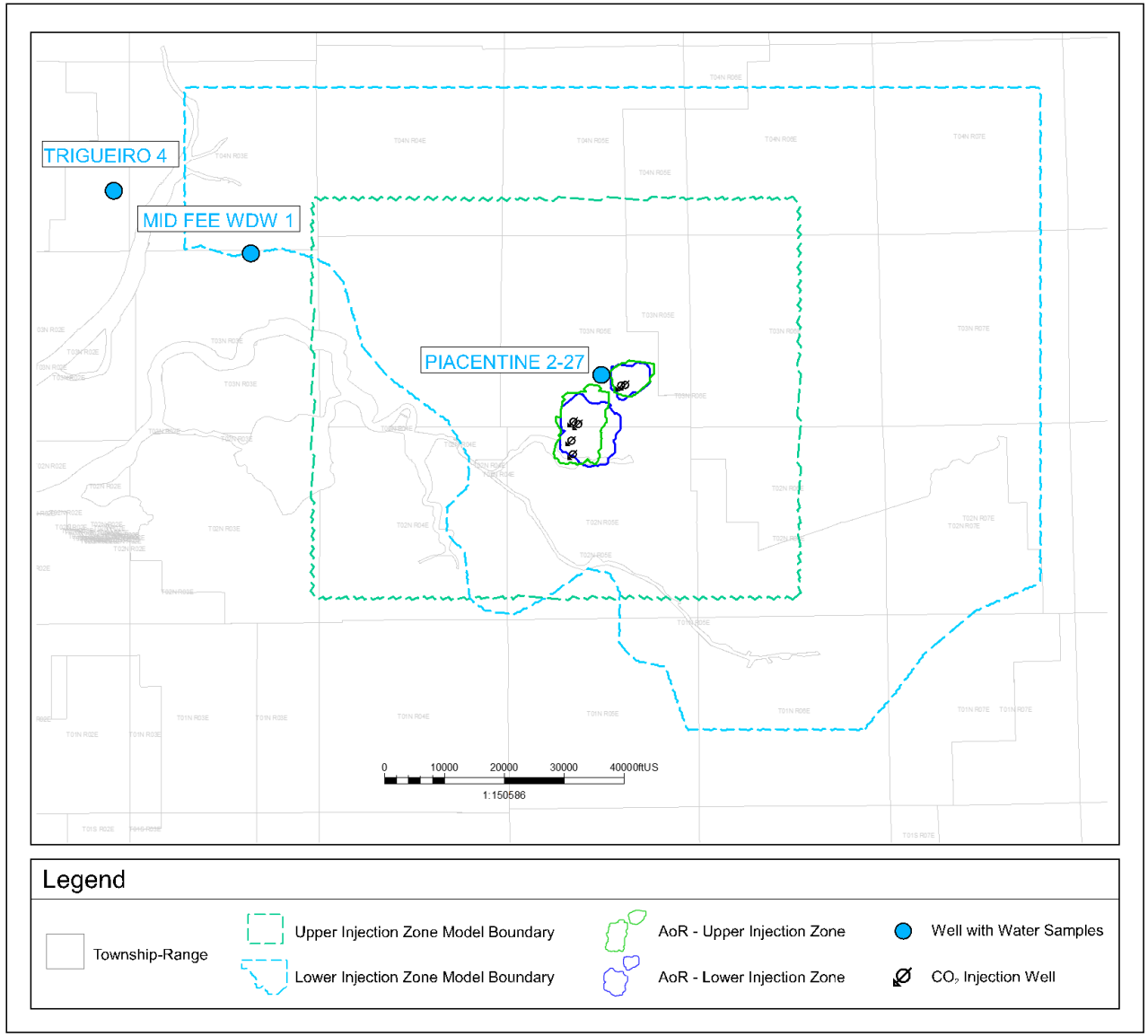

Figure 2.8-1. Map of wells with water samples.

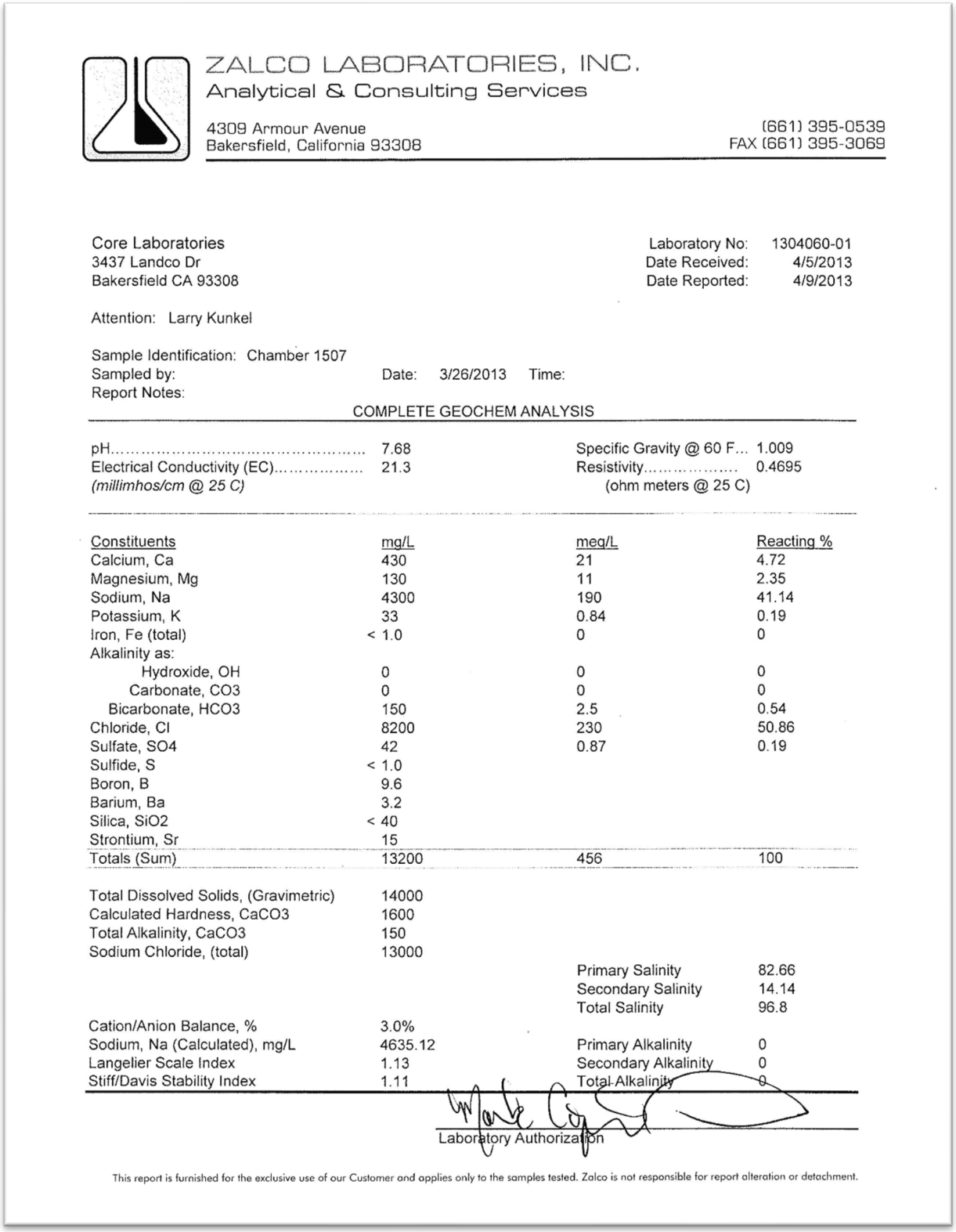

ZALCO LABORATORIES, INC.
Analytical & Consulting Services

4309 Armour Avenue
Bakersfield, California 93308

(661) 395-0539
FAX (661) 395-3069

Core Laboratories
3437 Landco Dr
Bakersfield CA 93308

Laboratory No: 1304060-01
Date Received: 4/5/2013
Date Reported: 4/9/2013

Attention: Larry Kunkel

Sample Identification: Chamber 1507
Sampled by: Date: 3/26/2013 Time:
Report Notes:

COMPLETE GEOCHEM ANALYSIS

pH	7.68	Specific Gravity @ 60 F...	1.009
Electrical Conductivity (EC) *(millimhos/cm @ 25 C)*	21.3	Resistivity (ohm meters @ 25 C)	0.4695

Constituents	mg/L	meq/L	Reacting %
Calcium, Ca	430	21	4.72
Magnesium, Mg	130	11	2.35
Sodium, Na	4300	190	41.14
Potassium, K	33	0.84	0.19
Iron, Fe (total)	< 1.0	0	0
Alkalinity as:			
Hydroxide, OH	0	0	0
Carbonate, CO3	0	0	0
Bicarbonate, HCO3	150	2.5	0.54
Chloride, Cl	8200	230	50.86
Sulfate, SO4	42	0.87	0.19
Sulfide, S	< 1.0		
Boron, B	9.6		
Barium, Ba	3.2		
Silica, SiO2	< 40		
Strontium, Sr	15		
Totals (Sum)	13200	456	100

Total Dissolved Solids, (Gravimetric)	14000		
Calculated Hardness, CaCO3	1600		
Total Alkalinity, CaCO3	150		
Sodium Chloride, (total)	13000		
		Primary Salinity	82.66
		Secondary Salinity	14.14
		Total Salinity	96.8
Cation/Anion Balance, %	3.0%		
Sodium, Na (Calculated), mg/L	4635.12	Primary Alkalinity	0
Langelier Scale Index	1.13	Secondary Alkalinity	0
Stiff/Davis Stability Index	1.11	Total Alkalinity	0

Laboratory Authorization

This report is furnished for the exclusive use of our Customer and applies only to the samples tested. Zalco is not responsible for report alteration or detachment.

Figure 2.8-2. Water geochemistry for the Piacentine_2-27 well (Upper Injection Zone in AoR).

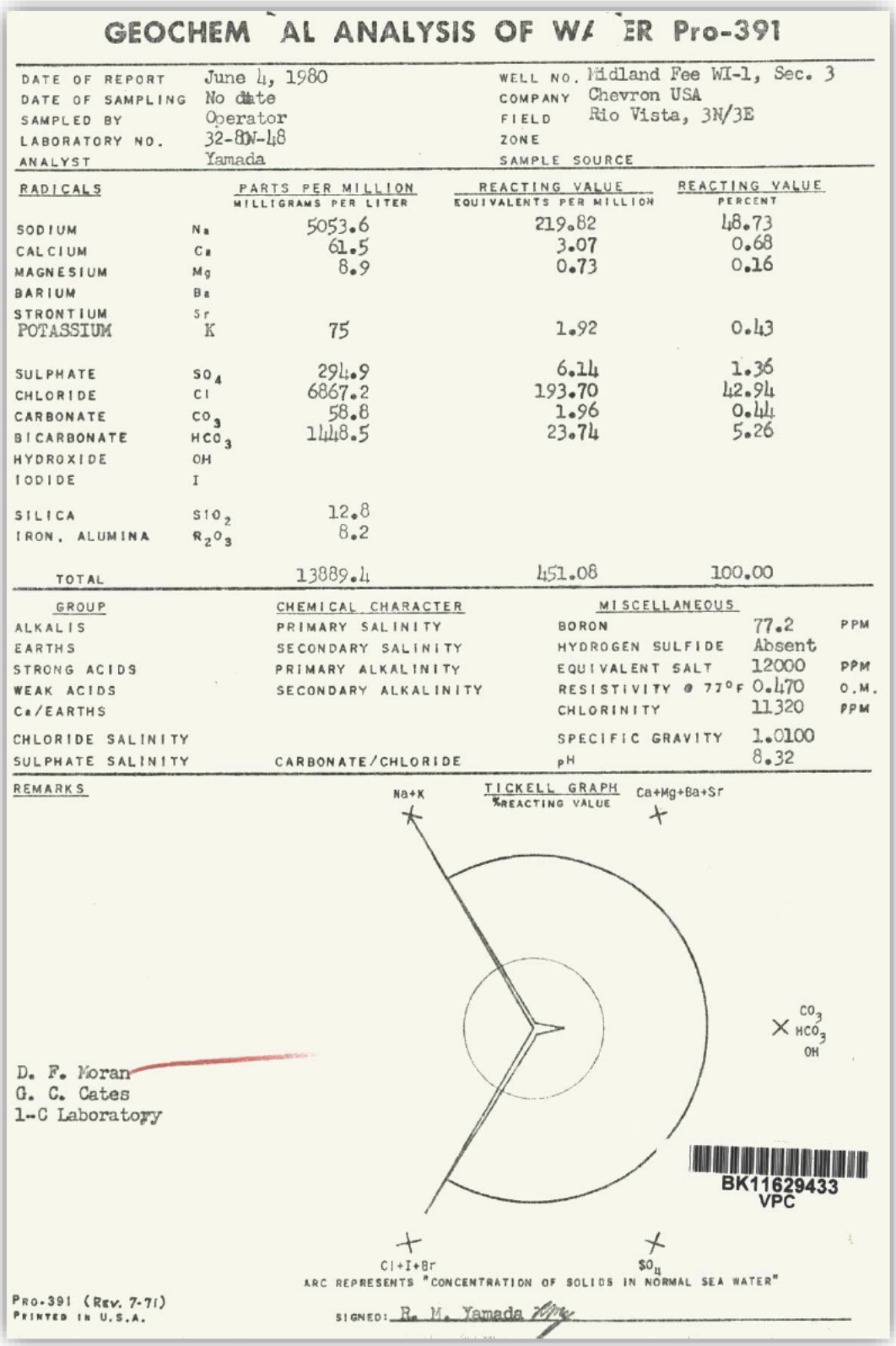

GEOCHEMICAL ANALYSIS OF WATER Pro-391

DATE OF REPORT	June 4, 1980		WELL NO.	Midland Fee WI-1, Sec. 3
DATE OF SAMPLING	No date		COMPANY	Chevron USA
SAMPLED BY	Operator		FIELD	Rio Vista, 3N/3E
LABORATORY NO.	32-8N-4E		ZONE	
ANALYST	Yamada		SAMPLE SOURCE	

RADICALS		PARTS PER MILLION MILLIGRAMS PER LITER	REACTING VALUE EQUIVALENTS PER MILLION	REACTING VALUE PERCENT
SODIUM	Na	5053.6	219.82	48.73
CALCIUM	Ca	61.5	3.07	0.68
MAGNESIUM	Mg	8.9	0.73	0.16
BARIUM	Ba			
STRONTIUM	Sr			
POTASSIUM	K	75	1.92	0.43
SULPHATE	SO_4	294.9	6.14	1.36
CHLORIDE	Cl	6867.2	193.70	42.94
CARBONATE	CO_3	58.8	1.96	0.44
BICARBONATE	HCO_3	1448.5	23.74	5.26
HYDROXIDE	OH			
IODIDE	I			
SILICA	SiO_2	12.8		
IRON, ALUMINA	R_2O_3	8.2		
TOTAL		13889.4	451.08	100.00

GROUP	CHEMICAL CHARACTER	MISCELLANEOUS		
ALKALIS	PRIMARY SALINITY	BORON	77.2	PPM
EARTHS	SECONDARY SALINITY	HYDROGEN SULFIDE	Absent	
STRONG ACIDS	PRIMARY ALKALINITY	EQUIVALENT SALT	12000	PPM
WEAK ACIDS	SECONDARY ALKALINITY	RESISTIVITY @ 77°F	0.470	O.M.
Ca/EARTHS		CHLORINITY	11320	PPM
CHLORIDE SALINITY		SPECIFIC GRAVITY	1.0100	
SULPHATE SALINITY	CARBONATE/CHLORIDE	pH	8.32	

REMARKS

D. F. Moran
G. C. Cates
1-C Laboratory

TICKELL GRAPH
%REACTING VALUE

Na+K
Ca+Mg+Ba+Sr
CO_3 HCO_3 OH
Cl+I+Br
SO_4

ARC REPRESENTS "CONCENTRATION OF SOLIDS IN NORMAL SEA WATER"

BK11629433
VPC

PRO-391 (REV. 7-71)
PRINTED IN U.S.A.

SIGNED: R. M. Yamada

Figure 2.8-3. Water geochemistry for the Midland_Fee_Water_Injection_1 well (Upper Injection Zone outside of the AoR).

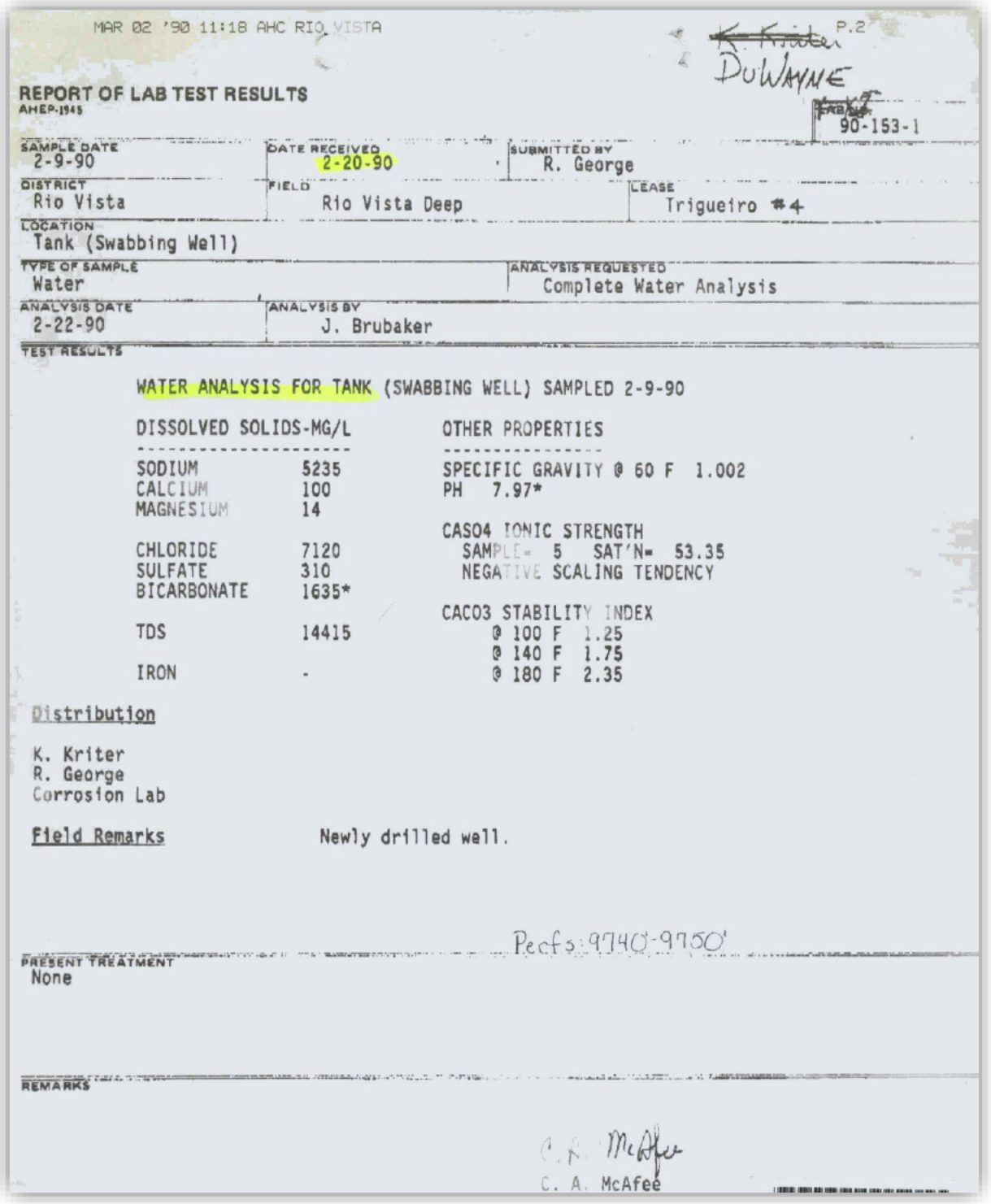

MAR 02 '90 11:18 AHC RIO VISTA P.2

REPORT OF LAB TEST RESULTS
AHEP-1945

~~K. Kriter~~ DoWAYNE

90-153-1

SAMPLE DATE	DATE RECEIVED	SUBMITTED BY
2-9-90	2-20-90	R. George

DISTRICT	FIELD	LEASE
Rio Vista	Rio Vista Deep	Trigueiro #4

LOCATION: Tank (Swabbing Well)

TYPE OF SAMPLE	ANALYSIS REQUESTED
Water	Complete Water Analysis

ANALYSIS DATE	ANALYSIS BY
2-22-90	J. Brubaker

TEST RESULTS

WATER ANALYSIS FOR TANK (SWABBING WELL) SAMPLED 2-9-90

DISSOLVED SOLIDS-MG/L		OTHER PROPERTIES
SODIUM	5235	SPECIFIC GRAVITY @ 60 F 1.002
CALCIUM	100	PH 7.97*
MAGNESIUM	14	
		CASO4 IONIC STRENGTH
CHLORIDE	7120	SAMPLE= 5 SAT'N= 53.35
SULFATE	310	NEGATIVE SCALING TENDENCY
BICARBONATE	1635*	
		CACO3 STABILITY INDEX
TDS	14415	@ 100 F 1.25
		@ 140 F 1.75
IRON	-	@ 180 F 2.35

Distribution

K. Kriter
R. George
Corrosion Lab

Field Remarks: Newly drilled well.

Perfs: 9740-9750'

PRESENT TREATMENT
None

REMARKS

C. A. McAfee

C. A. McAfee

Figure 2.8-4. Water geochemistry for the Trigueiro_4 well. (Lower Injection Zone outside of the AoR).

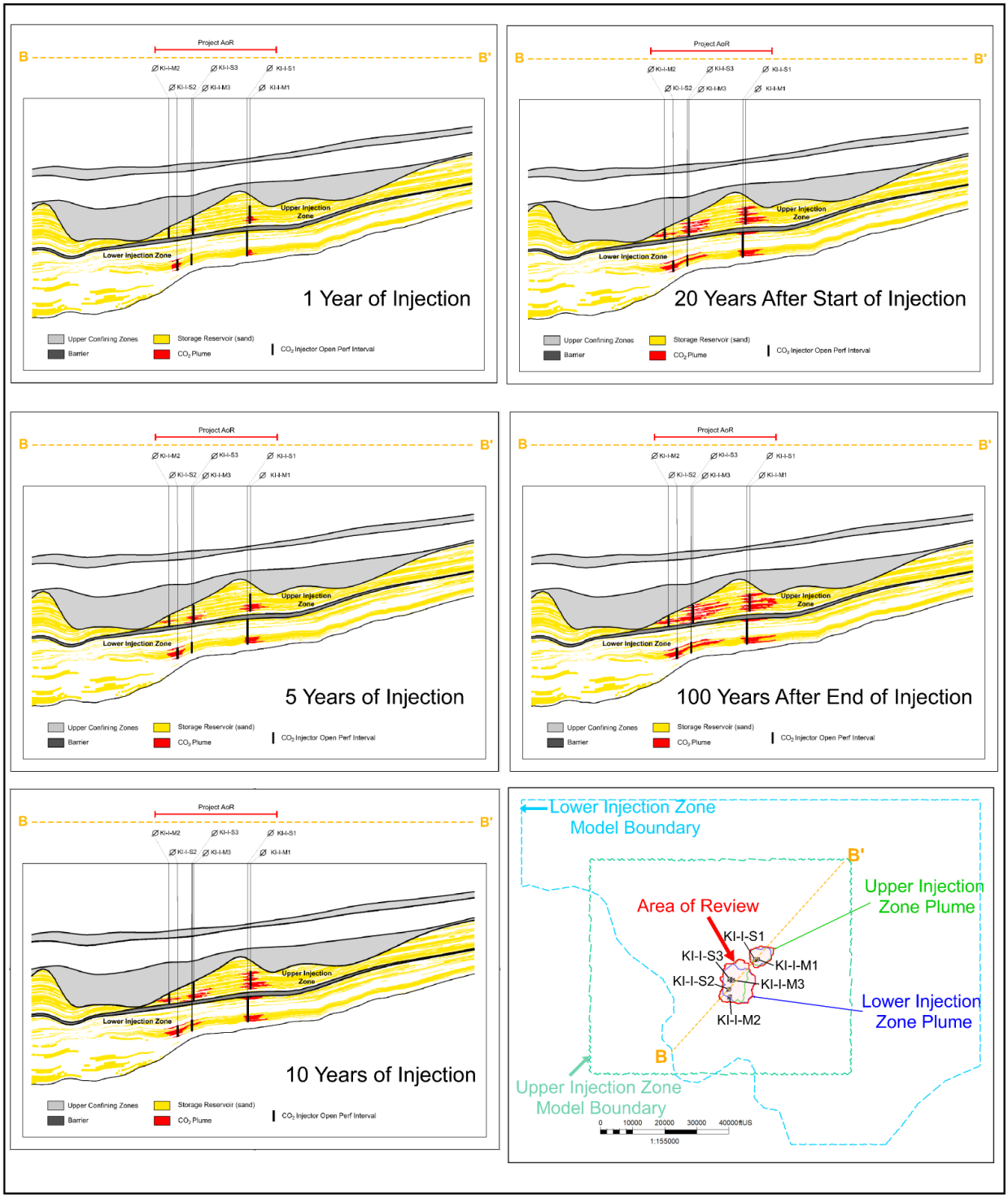

Figure 2.10-1. Lateral dispersion and development of CO_2 plumes through time and confinement under the Upper Confining Zone.

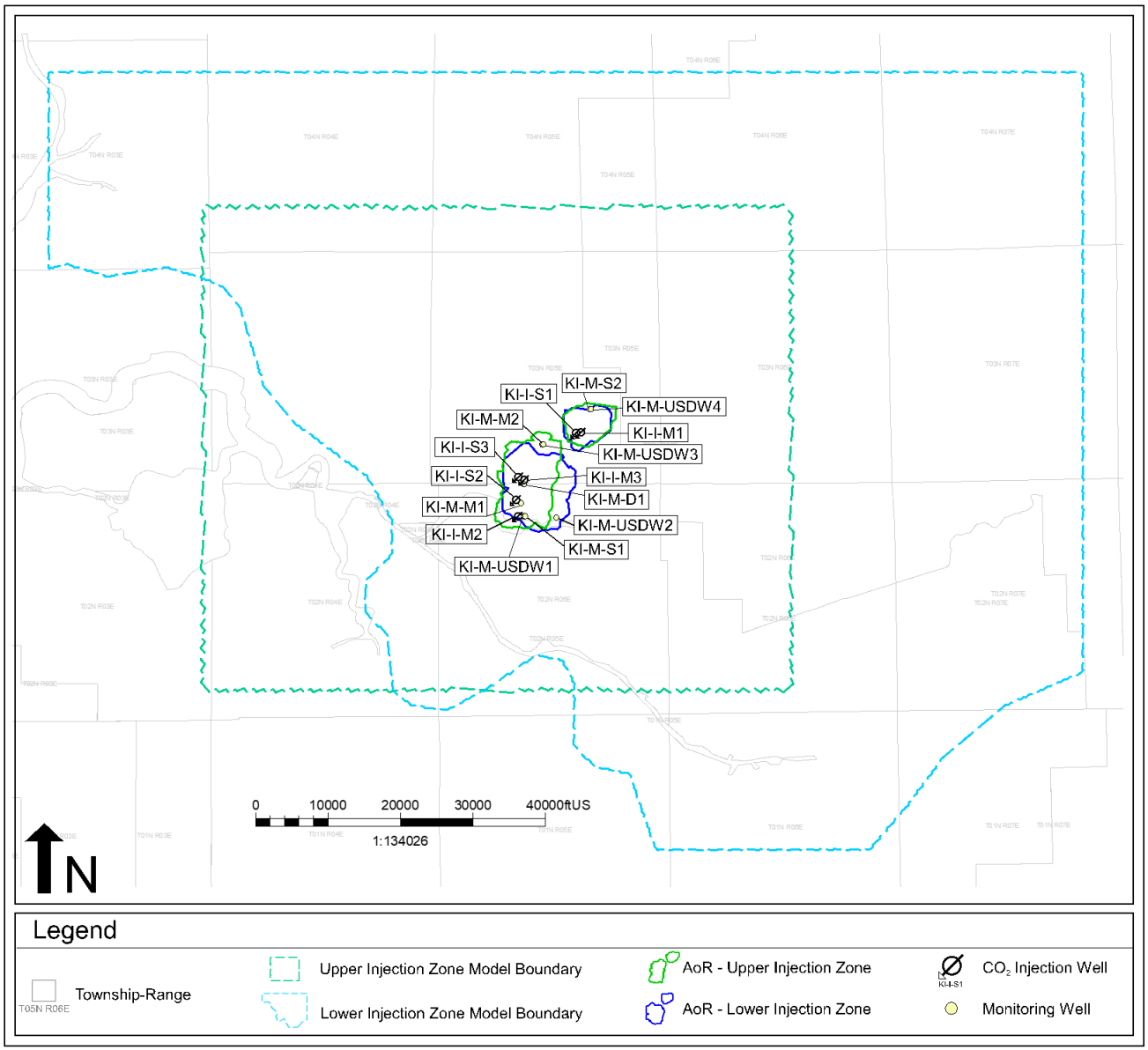

Figure 5.0-1. Map showing the location of injection wells and monitoring wells.

Tables

Table 2.2-1. Reference list of Water Supply Wells in the AoR

Well Number	Well ID	Dataset	Type
1	AGW080018293-KING	WB_ILRP	Domestic
2	CA3901130_001_001	DDW	Municipal
3	77694	DPR	Irrigation/Industrial
4	78503	DPR	Domestic
5	03N05E26C008M	DWR	Water Supply, Other
6	03N05E23N002M	DWR	Water Supply, Other
7	03N05E27G001M	DWR	Water Supply, Other
8	03N05E27K001M	DWR	Water Supply, Other
9	03N05E27N001M	DWR	Water Supply, Other
10	03N05E34L001M	DWR	Water Supply, Other
11	03N05E23P002M	DWR	Water Supply, Other
12	03N05E33P001M	DWR	Water Supply, Other
13	T10000007741-MWP-10	WB_CLEANUP	Monitoring
14	T10000007741-MWP-4	WB_CLEANUP	Monitoring
15	T10000007741-MWP-11	WB_CLEANUP	Monitoring
16	T10000007741-MWP-3	WB_CLEANUP	Monitoring
17	T10000007741-MWP-1	WB_CLEANUP	Monitoring
18	T10000007741-MWP-2	WB_CLEANUP	Monitoring
19	T10000007741-MWP-9	WB_CLEANUP	Monitoring
20	T10000007741-MWP-8	WB_CLEANUP	Monitoring
21	WCR2014-015527	DWR	Water Supply Domestic
22	WCR2017-011011	DWR	Monitoring
23	WCR2017-011012	DWR	Monitoring
24	WCR0100384	DWR	NA
25	WCR1994-004385	DWR	Water Supply Domestic
26	WCR0203653	DWR	NA
27	WCR0263575	DWR	NA
28	WCR1986-004210	DWR	Water Supply Public
29	WCR2017-009654	DWR	Monitoring
30	WCR0288639	DWR	Water Supply Domestic

NA= Data are not available or not applicable

Table 2.2-2. Reference list of Oil and Gas Wells in the AoR

Well Number	API	Well Name	Status	Well Type
31	407720686	King Island 33-1	Plugged	Dry Gas
32	407720630	Jackson et al 1	Plugged	Dry Gas
33	407720172	Rio Blanco 1	Plugged	Dry Hole
34	407700467	Victor Leonardini et al 1	Plugged	Dry Hole
35	407700516	McCulloch-Stefani 1	Plugged	Dry Hole
36	407700515	Piacentine 1	Plugged	Dry Hole

Table 2.4-1. Formation mineralogy from x-ray diffraction (XRD) and Fourier-transform infrared spectroscopy (FTIR) in eight wells

Well	Zone	Depth (feet)	Quartz	Chert	Plagioclase	K-Feldspar	Feldspar	Albite	Oligoclase	Andesine	Labrodorite	Calcite	Dolomite	Amphibole	Siderite	Glauconite	Apatite	Barite	Pyrite	Kaolinite	Chlorite	Illite & Mica	Smectite	MXL I/S	Total Clay
RVGU_209	Capay	4,442.5	26.0			17.0		14.0	0.0	11.0		1.0	0.0							5.0	3.0			23.0	31.0
RVGU_209	Capay	4,454.5	30.0			15.0		8.0	15.0	6.0		0.0	0.0							2.0	6.0			18.0	26.0
RVGU_209	Capay	4,476.5	30.0			18.0		13.0	4.0	6.0		0.0	0.0							5.0	9.0			15.0	29.0
RVGU_209	Capay	4,480.5	26.0			20.0		13.0	0.0	10.0		0.0	0.0							0.0	6.0			25.0	31.0
RVGU_209	Capay	4,498.5	34.0			19.0		13.0	0.0	13.0		0.0	0.0							1.0	2.0			18.0	21.0
RVGU_209	Capay	4,500.5	28.0			19.0		0.0	19.0	0.0		0.0	0.0							0.0	12.0			22.0	34.0
RVGU_248	Capay	4,425.5	35.0		25.0	15.0														5.0	5.0	5.0	10.0		25.0
Wilcox_20	Capay	4,622.0	42.2		18.7	10.7						0.0	0.0						0.6	9.4	3.4	4.5		10.5	27.8
Wilcox_20	Capay	4,905.0	34.9		20.7	10.2						0.7	0.0						1.1	15.2	5.8	5.8		5.5	32.3
Citizen_Green_1	Mokelumne	5247	27.8			16.2		34		0	0			0			0.8		0	3.6	17	0	1.1		21.7
Citizen_Green_1	Mokelumne	5249	17			32.7		6.5		0	0			0					0	34.9	0	8.4	0.5		43.8
Citizen_Green_1	Mokelumne	6400	40.3			17.1		0		3.6	29.2			0.17					0	5.2	4.0	0.4	0		9.6
Citizen_Green_1	Mokelumne	6466	36.3			12.6		0.23		0	36.6			0.57					0.7	2.7	5.4	5.0	0		13.0
Citizen_Green_1	Mokelumne	6532	34.2			24.1		0		31	0			1.1					0.5	2.9	2	4.2			9.1
Citizen_Green_1	Mokelumne	6598	33.9			22.0		0		34.5	0			0.23					0.2	3.6	5.4	0.1	0		9.2
Speckman_Decarli_1	H&T Shale	8,828.0	23.0			9.0		12.0	0.0	9.0		3.0	0.0			0.0			1.0	12.0	5.0			26.0	43.0
Speckman_Decarli_1	H&T Shale	8,830.0	30.0		17.0	11.0						0.0	0.0						4.0	3.4	14.4	6.1	14.1		38.0
Speckman_Decarli_1	H&T Shale	8,909.0	20.0			13.0		10.0	0.0	10.0		0.0	0.0			2.0			2.0	5.0	3.0			35.0	43.0
Speckman_Decarli_1	H&T Shale	8,937.0	20.0			8.0		7.0	0.0	5.0		0.0	0.0			0.0			2.0	14.0	6.0			38.0	58.0
Speckman_Decarli_1	H&T Shale	8,939.0	24.0		18.0	11.0						1.0	0.0						3.0	3.0	15.5	7.7	16.8		43.0
Speckman_Decarli_1	H&T Shale	8,940.0	23.0			12.0		14.0	0.0	15.0		0.0	0.0			0.0			0.0	4.0	5.0			27.0	36.0
Speckman_Decarli_1	H&T Shale	8,942.0	23.0			10.0		9.0	0.0	6.0		0.0	0.0			0.0			2.0	12.0	5.0			33.0	50.0
Speckman_Decarli_1	H&T Shale	9,439.0	20.0			9.0		7.0	0.0	7.0		0.0	0.0			0.0			1.0	0.0	5.0			51.0	56.0
Speckman_Decarli_1	H&T Shale	9,441.0	21.0			12.0		10.0	0.0	9.0		2.0	0.0			0.0			3.0	0.0	0.0			43.0	43.0
Citizen_Green_1	Starkey	7104	39.9			6.5		0		27.4	0			0					1.2	1.3	5.7	8.5	9.5		23.7
Citizen_Green_1	Starkey	7136	42.8			8.7		0		39.6	0								0.5	0	1.4	4.7	2.4		8.5
Citizen_Green_1	Starkey	7146	37.5			11.1		34.2									5.3		1.1		1.8	1.3	7.7		10.8
Lopes_Transamerica_1	Winters	7,926.3	59.1		21.0	10.0						0.0			0.0	0.0	0.0	8.0	0.0	0.1	0.0	0.1	1.7		1.9
Lopes_Transamerica_1	Winters	7,929.3	24.6		15.1	9.8						0.0			0.0	0.0	0.0	0.0	1.8	4.4	27.6	7.1	9.6		48.7
Lopes_Transamerica_1	Winters	7,932.5	8.9		4.9	0.0						76.2			0.0	0.0	3.0	0.0	2.0	4.9	0.0	0.0	0.0		5.0
Lopes_Transamerica_1	Winters	7,935.3	27.4		18.2	10.5						0.0			0.0	0.0	0.0	0.0	1.9	4.8	27.5	7.0	2.6		41.9
Lopes_Transamerica_1	Winters	7,938.3	28.9		17.3	11.6						0.0			0.0	0.0	0.0	0.0	1.9	4.8	27.6	5.1	2.7		40.3
Lopes_Transamerica_1	Winters	7,941.3	29.4		17.9	11.3						0.0			0.0	0.0	0.0	1.9	0.9	0.0	26.7	5.0	6.9		38.6

Well	Zone	Depth (feet)	Quartz	Chert	Plagioclase	K-Feldspar	Feldspar	Albite	Oligoclase	Andesine	Labrodorite	Calcite	Dolomite	Amphibole	Siderite	Glauconite	Apatite	Barite	Pyrite	Kaolinite	Chlorite	Illite & Mica	Smectite	MXL I/S	Total Clay
Lopes_Transamerica_1	Winters	7,944.3	23.1		16.3	10.0						0.0			0.0	0.0	0.0	3.6	1.8	0.0	25.6	4.9	14.6		45.1
Lopes_Transamerica_1	Winters	7,947.3	22.2		17.3	9.1						0.0			0.0	0.0	0.0	5.5	1.8	0.0	24.8	6.7	12.6		44.1
Lopes_Transamerica_1	Winters	7,950.3	20.2		16.0	7.6						0.0			2.5	0.0	0.0	1.7	1.7	0.0	26.2	9.3	14.7		50.2
Lopes_Transamerica_1	Winters	7,953.3	38.5		19.9	8.5						0.0			4.7	0.0	0.0	0.0	0.0	0.0	18.8	5.1	4.4		28.3
Lopes_Transamerica_1	Winters	7,960.7	27.1		15.4	10.8						0.0			0.0	0.0	0.0	0.0	1.8	4.5	26.4	5.2	8.8		44.9
Lopes_Transamerica_1	Winters	7,962.7	22.8		16.6	9.2						0.0			0.0	0.0	0.0	0.0	1.8	0.0	24.4	9.8	15.3		49.5
Lopes_Transamerica_1	Winters	7,965.7	28.1		18.2	11.8						0.0			0.0	0.0	0.0	0.0	0.9	0.0	27.3	5.2	8.5		41.0
Lopes_Transamerica_1	Winters	7,968.7	14.7		6.5	4.6						46.4			0.0	0.0	0.0	0.0	0.9	0.3	18.4	5.0	3.1		26.8
Lopes_Transamerica_1	Winters	7,971.7	26.1		18.9	11.7						0.0			0.0	0.0	0.0	0.0	1.8	0.0	27.6	6.4	7.6		41.6
Lopes_Transamerica_1	Winters	7,974.7	22.4		16.4	10.3						0.0			2.6	0.0	0.0	0.0	1.7	0.0	31.9	7.8	6.9		46.6
Lopes_Transamerica_1	Winters	7,977.7	26.0		17.9	9.0						0.0			0.0	0.0	0.0	0.0	2.7	0.0	31.2	13.3	0.0		44.4
Lopes_Transamerica_1	Winters	7,980.7	17.9		15.2	9.3						0.0			0.0	0.0	0.0	0.0	1.7	0.0	30.5	11.0	14.4		55.8
Lopes_Transamerica_1	Winters	7,983.7	24.8		15.3	9.0						0.0			0.0	0.0	0.0	0.0	1.8	0.0	26.4	12.7	10.0		49.1
Lopes_Transamerica_1	Winters	7,986.7	22.7		17.6	10.7						0.0			0.0	0.0	0.0	0.0	2.0	0.0	23.7	11.9	11.5		47.1
Lopes_Transamerica_1	Winters	7,989.7	17.8		16.3	8.6						0.0			0.0	0.0	0.0	0.0	1.9	0.0	27.9	12.8	14.8		55.4
Lopes_Transamerica_1	Winters	7,992.7	22.0		18.0	9.5						0.0			2.8	0.0	0.0	0.0	1.9	0.0	23.4	11.9	10.6		45.9
Lopes_Transamerica_1	Sacramento Shale	8,200.0	20.1		18.0	9.0						0.0						0.0	0.9		24.2	11.9	16.0		52.1
Lopes_Transamerica_1	Sacramento Shale	8,200.7	21.6		17.8	8.9						0.0						0.0	0.9		24.1	11.5	15.3		50.8
Lopes_Transamerica_1	Sacramento Shale	8,203.7	21.6		17.4	8.3						0.0						4.6	0.0		21.8	10.6	15.7		48.1
Lopes_Transamerica_1	Sacramento Shale	8,206.7	22.6		16.1	8.5						1.7						2.5	0.8		19.6	11.8	16.3		47.8
Lopes_Transamerica_1	Sacramento Shale	8,209.7	21.2		21.0	11.3						0.0						0.0	1.8		9.9	8.6	26.2		44.7
Lopes_Transamerica_1	Sacramento Shale	8,212.7	21.4		20.0	10.0						0.0						0.0	1.8		10.1	9.6	27.1		46.8
Lopes_Transamerica_1	Sacramento Shale	8,215.7	23.9		19.0	9.0						0.0						4.3	1.7		10.3	9.3	22.6		42.1
Lopes_Transamerica_1	Sacramento Shale	8,218.7	17.8		16.8	8.0						0.8						0.0	1.6		10.2	9.0	35.7		55.0
Lopes_Transamerica_1	Sacramento Shale	8,221.7	25.3		17.5	8.8						0.9						4.4	0.9		8.5	8.6	25.1		42.3
Lopes_Transamerica_1	Sacramento Shale	8,225.0	25.1		18.2	9.1						0.0						6.4	1.8		7.3	8.7	23.5		39.5

Table 2.4-2. Sonic porosity equations by zone

Zones	Sonic Porosity Equation	Wyllie Compaction Factor
Nortonville Shale-Domengine	Wyllie	1.3
Capay Shale – Mokelumne River Formation	Wyllie	1.2
H&T Shale-Sawtooth Shale	Wyllie	1.0

Table 2.4-3. Core samples from in the Upper Injection Zone

Well	Sample Depth (feet)	Porosity (%)	Permeability Horizontal (mD)	Permeability Vertical (mD)
Citizen_Green_1	6,400	33	367.1	—
Citizen_Green_1	6,466	31.3	71.9	—
Citizen_Green_1	6,532	30.3	54.8	—
Citizen_Green_1	6,598	31.3	135.5	—
Citizen_Green_1	6,664	30.8	46.4	—
Citizen_Green_1	6,800	27.7	4.8	—
Whiskey_Slough_1A-E	5,442	29.3	16.8	14
Whiskey_Slough_1A-E	5,543.8	30.6	86.1	23.5
Whiskey_Slough_1A-E	5,446.1	30.3	43.5	24.3
Whiskey_Slough_1A-E	5,447.6	33.5	799.3	552.4
Whiskey_Slough_1A-E	5,449.8	34.2	1,126.8	1,056.8
Whiskey_Slough_1A-E	5,452.7	33.7	1,172	990
Whiskey_Slough_1A-E	5,455.6	34	1,765.1	1,221.1
Whiskey_Slough_1A-E	5,457.5	30.3	667.6	380.6
Whiskey_Slough_1A-E	5,460.2	33.7	1,089.2	991.5
Whiskey_Slough_1A-E	5,463.1	35	1,802.4	1,925.9
Whiskey_Slough_1A-E	5,466.1	35.4	1,156.5	1,125.1
Whiskey_Slough_1A-E	5,469.1	34.9	1,922.9	1,212.8
Whiskey_Slough_1A-E	5,472.1	35.5	1,565.9	891.1
Whiskey_Slough_1A-E	5,474.9	34	1,084.7	731.1
Whiskey_Slough_1A-E	5,476.5	34.5	1,397.4	1,108.8

Table 2.4-4. Core samples from the Lower Injection Zone

Well	Sample Depth (feet)	Porosity (%)	Permeability Horizontal (mD)
Citizen_Green_1	7,104	27.6	114.3
Citizen_Green_1	7,136	31.3	432.6
Citizen_Green_1	7,174	25.2	4.9
Citizen_Green_1	7,258	23.1	2.3
Citizen_Green_1	7,309	23	11.1

Table 2.4-5. Core Data for the Winters and Sacramento Shale

UWI	Well	Field	Formation	Depth (ft)	Porosity (%)	Permeability Horizontal (mD)	Permeability Vertical (mD)	Grain Density (g/cc)	Description
04067204850000	Lopes_Transamerica_1	Thornton	Winters	7848.3	19.3	0.75	NM	2.58	Mdst dgry slty fos no stn no flor
04067204850000	Lopes_Transamerica_1	Thornton	Winters	7926.4	28.2	2338.60	NM	2.65	Sd gry vf-fgr slslty mica calc incl no stn no flor
04067204850000	Lopes_Transamerica_1	Thornton	Winters	7928.4	18.2	1.98	NM	2.59	Mdst dgry slty no stn no flor
04067204850000	Lopes_Transamerica_1	Thornton	Winters	7929.15	NM	NM	0.12	NM	NM
04067204850000	Lopes_Transamerica_1	Thornton	Winters	7929.3	18.8	0.91	NM	2.59	Mdst dgry slty no stn no flor
04067204850000	Lopes_Transamerica_1	Thornton	Winters	7933	19.8	7.42	NM	2.59	Mdst dgry slty no stn no flor
04067204850000	Lopes_Transamerica_1	Thornton	Winters	7936.9	18.5	0.64	NM	2.56	Mdst dgry slty no stn no flor
04067204850000	Lopes_Transamerica_1	Thornton	Winters	7939.4	18.7	0.80	NM	2.60	Mdst dgry slty no stn no flor
04067204850000	Lopes_Transamerica_1	Thornton	Winters	7942.4	18.4	0.37	NM	2.58	Mdst dgry slty fos no stn no flor
04067204850000	Lopes_Transamerica_1	Thornton	Winters	7945.6	18.3	0.22	NM	2.57	Mdst dgry slty no stn no flor
04067204850000	Lopes_Transamerica_1	Thornton	Winters	7951.3	NM	NM	0.05	NM	NM
04067204850000	Lopes_Transamerica_1	Thornton	Winters	7951.6	19.0	0.78	NM	2.57	Mdst dgry slty no stn no flor
04067204850000	Lopes_Transamerica_1	Thornton	Winters	7953.5	18.8	0.61	NM	2.58	Mdst dgry slty fos no stn no flor
04067204850000	Lopes_Transamerica_1	Thornton	Winters	7960.4	18.7	2.66	NM	2.56	Mdst dgry slty no stn no flor
04067204850000	Lopes_Transamerica_1	Thornton	Winters	7962.5	18.9	2.11	NM	2.57	Mdst dgry slty no stn no flor
04067204850000	Lopes_Transamerica_1	Thornton	Winters	7965.8	18.4	3.31	NM	2.58	Mdst dgry slty no stn no flor
04067204850000	Lopes_Transamerica_1	Thornton	Winters	7968.7	20.5	2.60	NM	2.59	Mdst dgry slty no stn no flor
04067204850000	Lopes_Transamerica_1	Thornton	Winters	7971.7	17.7	0.24	NM	2.59	Mdst dgry slty no stn no flor
04067204850000	Lopes_Transamerica_1	Thornton	Winters	7974.2	16.9	1.08	NM	2.58	Mdst dgry slty no stn no flor
04067204850000	Lopes_Transamerica_1	Thornton	Winters	7977.3	16.6	0.03	NM	2.60	Mdst dgry slty no stn no flor
04067204850000	Lopes_Transamerica_1	Thornton	Winters	7979.9	17.2	0.43	NM	2.59	Mdst dgry slty fos no stn no flor
04067204850000	Lopes_Transamerica_1	Thornton	Winters	7981.3	16.6	0.18	NM	2.60	Mdst dgry slty fos no stn no flor
04067204850000	Lopes_Transamerica_1	Thornton	Winters	7987.4	17.6	2.27	NM	2.59	Mdst dgry slty no stn no flor
04067204850000	Lopes_Transamerica_1	Thornton	Winters	7990.8	17.6	0.66	NM	2.59	Mdst dgry slty fos no stn no flor
04067204850000	Lopes_Transamerica_1	Thornton	Sacramento Shale	8201.8	18.3	0.14	NM	2.57	Mdst dgry slty no stn no flor
04067204850000	Lopes_Transamerica_1	Thornton	Sacramento Shale	8204.6	18.4	0.22	NM	2.58	Mdst dgry slty no stn no flor
04067204850000	Lopes_Transamerica_1	Thornton	Sacramento Shale	8207.7	19.1	0.06	NM	2.59	Mdst dgry slty no stn no flor
04067204850000	Lopes_Transamerica_1	Thornton	Sacramento Shale	8209.9	19.3	1.27	NM	2.57	Mdst dgry slty no stn no flor
04067204850000	Lopes_Transamerica_1	Thornton	Sacramento Shale	8211.9	18.9	0.20	NM	2.55	Mdst dgry slty no stn no flor
04067204850000	Lopes_Transamerica_1	Thornton	Sacramento Shale	8214.6	18.7	0.06	NM	2.56	Mdst dgry slty no stn no flor
04067204850000	Lopes_Transamerica_1	Thornton	Sacramento Shale	8217.8	19.1	0.09	NM	2.55	Mdst dgry slty no stn no flor

UWI	Well	Field	Formation	Depth (ft)	Porosity (%)	Permeability Horizontal (mD)	Permeability Vertical (mD)	Grain Density (g/cc)	Description
04067204850000	Lopes_Transamerica_1	Thornton	Winters	7848.3	19.3	0.75	NM	2.58	Mdst dgry slty fos no stn no flor
04067204850000	Lopes_Transamerica_1	Thornton	Sacramento Shale	8219.5	19.3	0.21	NM	2.55	Mdst dgry slty no stn no flor
04067204850000	Lopes_Transamerica_1	Thornton	Sacramento Shale	8221.1	20.1	0.86	NM	2.53	Mdst dgry slty no stn no flor
04067204850000	Lopes_Transamerica_1	Thornton	Sacramento Shale	8207.35	NM	NM	0.13	NM	NM
04067204850000	Lopes_Transamerica_1	Thornton	Sacramento Shale	8220.8	NM	NM	0.59	NM	NM
04077205720100	GP_Dohrmann_1_RD1	McDonald Island	Winters	9752.8	2.5	0	NM	2.72	Sst gry vfgr v slty sl calc no vis stn gld flu
04077205720100	GP_Dohrmann_1_RD1	McDonald Island	Winters	9753.6	2.9	0	NM	2.72	Sst gry vfgr v slty sl calc no stn gld flu
04077205720100	GP_Dohrmann_1_RD1	McDonald Island	Winters	9754.3	3.8	0	NM	2.71	Sst gry vfgr v slty talc no stn gld flu
04077205720100	GP_Dohrmann_1_RD1	McDonald Island	Winters	9755.1	21.2	6.3	NM	2.73	Sst gry vfgr v slty no stn no flu
04077205720100	GP_Dohrmann_1_RD1	McDonald Island	Winters	9755.6	13.3	0.28	NM	2.63	Sh gry vfgr sdy lam v sity no stn no flu
04077205720100	GP_Dohrmann_1_RD1	McDonald Island	Winters	9756.4	12.6	0.06	NM	2.62	Sh gry vfgr ady str v slty no stn no flu
04077205720100	GP_Dohrmann_1_RD1	McDonald Island	Winters	9757.5	17.6	0.68	NM	2.66	Sst gry vfgr I slt lams shly f carb inc no stn no flu
04077205720100	GP_Dohrmann_1_RD1	McDonald Island	Winters	9758.5	24.3	36	NM	2.66	Sst gry vfgr shy mica no stn no flu
04077205720100	GP_Dohrmann_1_RD1	McDonald Island	Winters	9759.3	2.5	0	NM	2.77	Sst gry vfgr v slty v calc no stn dull gld flu
04077205720100	GP_Dohrmann_1_RD1	McDonald Island	Winters	9759.6	22.2	12	NM	2.66	Sst gry vfgr slty carb incl no stn no flu
04077205720100	GP_Dohrmann_1_RD1	McDonald Island	Winters	9760.5	13.1	0.07	NM	2.61	Sh gry vfgr sdy lass v slty no stn no flu
04077205720100	GP_Dohrmann_1_RD1	McDonald Island	Winters	9761.5	9.8	0.01	NM	2.59	Sh gry v shy no stn no flu
04077205720100	GP_Dohrmann_1_RD1	McDonald Island	Winters	9762.5	11.3	0.07	NM	2.61	Sh gry vfgr sdy strk v sity no stn no flu

NM = No measure

Table 2.4-6. Capay Shale, Mokelumne River Formation, H&T Shale, and Starkey Formation gross thickness and depth within the project AoR

Zone	Formation	Property	Low	High	Mean
Upper Confining Zone	Capay Shale	Thickness (feet)	73	1,353	723
		Depth (TVD)	4,483	5,228	4,880
Upper Injection Zone	Mokelumne River Formation	Thickness (feet)	100	1,490	774
		Depth (TVD)	4,427	6,975	5,590
Internal Barrier	H&T Shale	Thickness (feet)	75	179	121
		Depth (TVD)	6,086	6,634	6,367
Lower Injection Zone	Starkey Formation	Thickness (feet)	843	1,835	1,211
		Depth (TVD)	6,221	6,750	6,488

Table 2.5-1. Input Parameters used in the Mohr Circle Calculation

Parameter	Present-Day Conditions Mokelumne River Formation	Present-Day Conditions Starkey Formation
Reference Depth (ft TVD)	5500	7500
Pore Pressure (psi)	2260	3208
Overburden Stress Gradient (psi/ft)	0.893	0.918
Minimum Horizontal Stress Gradient (psi/ft)	0.76	0.76
Maximum Horizontal Stress Gradient (psi/ft)	0.98	1.02
Coefficient of Friction	0.6	0.6
Fault Cohesion (psi)	0	0

Table 2.5-2. Modeled Fault Orientations and Expected Pressure Increases for the Mokelumne River Formation

Fault	Strike	Dip (RHR)	Delta Pressure to Slip (psi)	Delta Pressure Average (psi)	Delta Pressure Maximum (psi)	Delta Pressure Maximum with Interference (psi)
1	350	45	1897	9	18	28
2	15	45	1688	18	28	44
3	170	60	1720	15	41	84
4	75	60	1569	50	79	140

Based on simulation modeling compared to the required pressure increase necessary to cause slip on the faults based on Mohr Coulomb analysis. The delta pressure to slip is the calculated pressure increase above present-day conditions from Mohr coulomb analysis that would cause each fault to slip. The delta pressure average and maximum are the actual pressure increases expected to be seen at each fault based on reservoir simulation. The interference case includes cumulative effects due to nearby Class VI projects.

Table 2.5-3. Modeled Fault Orientations and Expected Pressure Increases for the Starkey Formation

Fault	Strike	Dip (RHR)	Delta Pressure to Slip (psi)	Delta Pressure Average (psi)	Delta Pressure Maximum (psi)
1	350	45	2454	69	81
2	15	45	2116	98	103
3	170	60	2166	123	139
4	75	60	1922	113	132

Based on simulation modeling compared to the required pressure increase necessary to cause slip on the faults based on Mohr Coulomb analysis. The delta pressure to slip is the calculated pressure increase above present-day conditions from Mohr coulomb analysis that would cause each fault to slip. The delta pressure average and maximum are the actual pressure increases expected to be seen at each fault based on reservoir simulation.

Table 2.6-1. Data from USGS earthquake catalog for faults in the greater region of the project

Number	Date	Latitude	Longitude	Depth (km)	Magnitude	Last Updated	Location
1	10/4/2021	37.8718333	-121.6375	4.43	2.69	12/10/2021	0 km N of Byron, CA
2	11/15/2017	38.1125	-121.6463333	16.24	2.74	2/16/2018	6 km SE of Rio Vista, CA
3	11/26/2010	37.9956667	-121.6101667	11.664	2.52	7/22/2022	3 km SE of Bethel Island, California
4	11/26/2010	38.0023333	-121.5981667	11.434	2.95	7/22/2022	3 km ESE of Bethel Island, California
5	10/15/2010	37.8803333	-121.388	14.552	3.13	8/6/2022	9 km WSW of Taft Mosswood, California
6	5/28/2008	37.933	-121.5591667	14.132	2.64	1/18/2017	4 km NE of Discovery Bay, California
7	7/22/2005	38.0873333	-121.681	12.587	2.8	1/11/2017	8 km S of Rio Vista, California
8	6/15/2005	37.8893333	-121.7015	--	2.5	1/11/17	4 km S of Brentwood, California
9	6/28/20004	37.9943333	-121.6421667	10.927	2.66	1/7/2017	2 km S of Bethel Island, California
10	9/29/2002	37.8745	-121.611	4.312	3.42	6/18/2022	2 km ENE of Byron, California
11	8/28/1986	38.2353333	-121.4191667	4.958	3.24	12/6/2016	1 km NNE of Thornton, California
12	5/10/1982	37.938	-121.172	5.881	2.81	2/2/2016	6 km ESE of Garden Acres, CA
13	10/2/1981	37.925	-121.6533333	9.076	2.85	12/13/2016	3 km ESE of Brentwood, California
14	8/6/1979	37.8326667	-121.5105	6	4.31	4/1/2016	6 km NNE of Mountain House, CA
15	5/9/1975	37.9566667	-121.6493333	14.95	3.1	12/15/2016	2 km SE of Knightsen, California
16	2/2/1944	37.9251667	-121.4041667	6	3.79	1/28/2016	7 km SW of Country Club, CA
17	2/14/1909	38.1	-121.7	--	4.5	6/4/2018	7 km S of Rio Vista, California

Table 2.7-1. Stratigraphic Information

Aquifer	Formation Name	Geologic Age
Principal	Younger Alluvium and Modesto/Riverbank	Holocene-Pliocene
	Turlock Lake	Recent-Plio-Pleistocene
	Laguna	Plio-Pleistocene
	Mehrten	Mio-Pliocene
	Valley Springs	Miocene
	Ione	Eocene
	Undifferentiated Sediments	Eocene

Table 2.7-2 Water Well Information

Data Source	WCR Number	Wells from GAMA	Legacy Log Number	Planned Use or Former Use	LAT (DWR)	LONG (DWR)	LAT & LONG Accuracy (DWR)	LAT (GAMA)	LONG (GAMA)	T	R	S	APN	Date Work Ended	Total Completed Depth	Top Of Perforated Interval	Bottom of Perforated Interval	Static Water Level
DWR	WCR1996-002781	NA	468030	Water Supply Domestic	38.05097	-121.40647	Centroid of Section	NA	NA	02N	05E	3	71-140-3	1996-02-28	101	90	100	0
DWR	WCR2020-008437	T0607700310-MW10	NA	Monitoring	38.0553485	-121.4583184	Unknown	38.0553485	-121.4583184	02N	05E	6	NA	2020-06-16	28	0	0	0
DWR	WCR2017-011011	NA	E0354912	Monitoring	38.044166	-121.418333	Unknown	NA	NA	02N	05E	4	6605052	2017-09-21	20	4	19	0
DWR	WCR2017-011012	NA	E0354911	Monitoring	38.044444	-121.418333	Unknown	NA	NA	02N	05E	4	6605052	2017-09-22	24	5	20	0
DWR	WCR1992-009117	NA	498300	Water Supply Domestic	38.0652778	-121.3983333	NA	NA	NA	03N	05E	35	55-100-4	1992-08-28	145	88	108	0
DWR	WCR2020-008566	T0607700310-MW3	NA	Monitoring	38.0548721	-121.4581611	Unknown	38.0548721	-121.4581611	02N	05E	6	NA	2020-06-24	16	0	0	5
DWR	WCR1958-000256	NA	35778	Other Not Specified	38.0943	-121.37991	Centroid of Section	NA	NA	03N	05E	24	NA	1958-04-25	34	0	0	0
DWR	WCR1967-000270	NA	47155	Water Supply Domestic	38.06604	-121.45555	Centroid of Section	NA	NA	03N	05E	32	NA	1967-02-15	47	42	47	0
DWR	WCR2020-008562	T0607700310-MW1	NA	Remediation	38.0551148	-121.45775	Unknown	38.0551148	-121.45775	02N	05E	6	NA	2020-06-24	18	0	0	4
DWR	WCR1994-004295	NA	548779	Water Supply Domestic	38.0943	-121.37991	Centroid of Section	NA	NA	03N	05E	24	55-XX-XX	1994-09-15	220	100	140	0
DWR	WCR2007-004012	NA	e067373	Monitoring	38.0983333	-121.3933333	NA	NA	NA	03N	05E	11	55-32-25	2007-09-20	50	40	50	0
DWR	WCR2020-008560	T0607700310-MW13	NA	Monitoring	38.055104	-121.4583557	Unknown	38.055104	-121.4583557	02N	05E	6	NA	2020-06-19	62	0	0	0
DWR	WCR0034703	NA	NA	NA	38.05097	-121.40647	Centroid of Section	NA	NA	02N	05E	3	NA	NA	0	0	0	0
DWR	WCR1993-004251	NA	465226	Water Supply Irrigation - Agriculture	38.0652778	-121.3983333	NA	NA	NA	03N	05E	35	55-280-1	1993-07-09	260	208	238	0
DWR	WCR0100384	NA	NA	NA	38.06547	-121.41726	Centroid of Section	NA	NA	03N	05E	34	NA	NA	0	0	0	0
DWR	WCR1970-000033	NA	12463	Water Supply Irrigation - Agriculture	38.0941667	-121.38	NA	NA	NA	03N	05E	24	NA	1970-09-30	111	0	0	0
DWR	WCR1979-001555	NA	129569	Water Supply Domestic	38.0943	-121.37991	Centroid of Section	NA	NA	03N	05E	24	NA	1979-04-30	153	110	150	0
DWR	WCR2020-008467	T0607700310-MW12	NA	Monitoring	38.0549016	-121.4580016	Unknown	38.0549016	-121.4580016	02N	05E	6	NA	2020-06-23	53	0	0	10.25
DWR	WCR0192177	NA	NA	NA	38.03698	-121.44384	Centroid of Section	NA	NA	02N	05E	8	NA	NA	0	0	0	0
DWR	WCR1970-000029	NA	12455	Water Supply Public	38.0943	-121.37991	Centroid of Section	NA	NA	03N	05E	24	NA	1970-06-30	176	0	0	0
DWR	WCR1997-001626	NA	476403	Water Supply Domestic	38.07976	-121.3799	Centroid of Section	NA	NA	03N	05E	25	69-70-19	1997-08-26	84	40	60	0
DWR	WCR2020-008594	NA	NA	Remediation	38.0551481	-121.4583645	NA	NA	NA	02N	05E	6	NA	2020-06-19	30	0	0	13
DWR	WCR2021-013953	NA	NA	Monitoring	38.0475	-121.4080556	50 Ft	NA	NA	02N	05E	3	6605038	2021-10-20	16	11	16	15
DWR	WCR1994-004385	NA	547527	Water Supply Domestic	38.06547	-121.41726	Centroid of Section	NA	NA	03N	05E	34	NA	1994-08-05	102	40	60	0
DWR	WCR2020-008363	T0607700310-MW4R	NA	Monitoring	38.0551426	-121.4580451	Unknown	38.0551426	-121.4580451	02N	05E	6	NA	2020-06-15	18	0	0	0
DWR	WCR0047228	NA	NA	NA	38.07976	-121.3799	Centroid of Section	NA	NA	03N	05E	25	NA	NA	0	0	0	0
DWR	WCR0203653	NA	E078136	NA	38.05128	-121.42497	Centroid of Section	NA	NA	02N	05E	4	NA	NA	0	0	0	0
DWR	WCR2020-008436	T0607700310-MW9	NA	Monitoring	38.0555918	-121.458189	Unknown	38.0555918	-121.458189	02N	05E	6	NA	2020-06-15	20	0	0	0
DWR	WCR0263575	NA	NA	NA	38.05164	-121.44362	Centroid of Section	NA	NA	02N	05E	5	NA	NA	0	0	0	0
DWR	WCR0119376	NA	86664	Water Supply Domestic	38.05097	-121.40647	Centroid of Section	NA	NA	02N	05E	3	NA	1980-06-06	0	45	55	8
DWR	WCR0146854	NA	NA	NA	38.0943	-121.37991	Centroid of Section	NA	NA	03N	05E	24	NA	NA	0	0	0	0
DWR	WCR1967-000236	NA	44898	Water Supply Irrigation - Agriculture	38.0943	-121.37991	Centroid of Section	NA	NA	03N	05E	24	NA	1967-08-31	139	0	0	0
DWR	WCR1967-000254	NA	44089	Water Supply Public	38.0943	-121.37991	Centroid of Section	NA	NA	03N	05E	24	NA	1967-06-29	100	62	80	0
DWR	WCR1995-006612	NA	580216	Water Supply Domestic	38.05097	-121.40647	Centroid of Section	NA	NA	02N	05E	3	71-80-48	1995-09-19	90	73	85	0
DWR	WCR2020-008567	T0607700310-MW5	NA	Monitoring	38.055005	-121.458172	Unknown	38.055005	-121.458172	02N	05E	6	NA	2020-06-22	16	0	0	4
DWR	WCR2008-002219	NA	e0079937	Monitoring	38.07976	-121.3799	Centroid of Section	NA	NA	03N	05E	25	55-14-10	2008-08-28	28	8	28	17

Data Source	WCR Number	Wells from GAMA	Legacy Log Number	Planned Use or Former Use	LAT (DWR)	LONG (DWR)	LAT & LONG Accuracy (DWR)	LAT (GAMA)	LONG (GAMA)	T	R	S	APN	Date Work Ended	Total Completed Depth	Top Of Perforated Interval	Bottom of Perforated Interval	Static Water Level
DWR	WCR2022-005079	NA	NA	Destruction	38.100943	-121.388875	NA	NA	NA	03N	05E	24	Caltrans I-5 PM 38.41	2022-04-19	0	0	0	0
DWR	WCR1980-004105	NA	86664	Water Supply Domestic	38.05097	-121.40647	Centroid of Section	NA	NA	02N	05E	3	NA	1980-06-06	55	0	0	0
DWR	WCR0019926	NA	E0079936	NA	38.07976	-121.3799	Centroid of Section	NA	NA	03N	05E	25	NA	NA	0	0	0	0
DWR	WCR2020-008596	NA	NA	Remediation	38.0551798	-121.4583739	NA	NA	NA	02N	05E	6	NA	2020-06-19	31	0	0	13
DWR	WCR1986-004210	NA	187198	Water Supply Public	38.05164	-121.44362	Centroid of Section	NA	NA	02N	05E	5	NA	1986-11-25	142	0	0	0
DWR	WCR0134763	NA	39-270	Water Supply Domestic	38.05097	-121.40647	Centroid of Section	NA	NA	02N	05E	3	NA	NA	0	0	0	0
DWR	WCR0211384	NA	39-271	Monitoring	38.03698	-121.44384	Centroid of Section	NA	NA	02N	05E	8	NA	NA	930	0	0	0
DWR	WCR1986-007067	NA	256476	Water Supply Public	38.05097	-121.40647	Centroid of Section	NA	NA	02N	05E	3	NA	1986-01-23	76	0	0	0
DWR	WCR2017-009656	NA	E0370047	Monitoring	38.044166	-121.417777	Unknown	NA	NA	02N	05E	4	6605030	2017-09-21	20	4	19	0
DWR	WCR1986-003909	NA	197571	Water Supply Public	38.06604	-121.45555	Centroid of Section	NA	NA	03N	05E	32	NA	1986-05-16	75	0	0	0
DWR	WCR2012-000219	NA	955433	Water Supply Domestic	38.0877778	-121.3888889	NA	NA	NA	03N	05E	23	55-130-16	2012-01-20	240	100	220	17
DWR	WCR2008-002217	NA	e0079934	Monitoring	38.07976	-121.3799	Centroid of Section	NA	NA	03N	05E	25	55-13-1	2008-08-28	28	8	28	17
DWR	WCR2020-008528	T0607700310-MW14	NA	Monitoring	38.0548048	-121.457778	Unknown	38.0548048	-121.457778	02N	05E	6	NA	2020-06-24	121	0	0	13
DWR	WCR0242214	NA	E0079937	NA	38.07976	-121.3799	Centroid of Section	NA	NA	03N	05E	25	NA	NA	0	0	0	0
DWR	WCR2020-008565	T0607700310-MW2	NA	Monitoring	38.0549096	-121.4579195	Unknown	38.0549096	-121.4579195	02N	05E	6	NA	2020-06-24	17	0	0	6.8
DWR	WCR2018-009060	NA	NA	Water Supply Domestic	38.06207363	-121.4664987	>50 FT	NA	NA	03N	05E	31	069-080-06	2018-09-19	100	80	100	10
DWR	WCR2012-000218	NA	955432	Water Supply Industrial	38.0894444	-121.3855556	NA	NA	NA	03N	05E	24	55-130-16	2012-02-02	240	40	220	20
DWR	WCR2017-009654	NA	E0370048	Monitoring	38.044444	-121.417777	Unknown	NA	NA	02N	05E	4	6605052	2017-09-22	20	4	19	0
DWR	WCR0233444	NA	NA	NA	38.06524	-121.3982	Centroid of Section	NA	NA	03N	05E	35	NA	NA	0	0	0	0
DWR	WCR2008-002218	NA	e0079936	Monitoring	38.07976	-121.3799	Centroid of Section	NA	NA	03N	05E	25	55-13-1	2008-08-28	28	8	28	17
DWR	WCR2020-008599	T0607700310-MW6	NA	Monitoring	38.0552898	-121.4579866	Unknown	38.0552898	-121.4579866	02N	05E	6	NA	2020-06-15	18	0	0	0
DWR	WCR0288639	NA	61314	Water Supply Domestic	38.05164	-121.44362	Centroid of Section	NA	NA	02N	05E	5	NA	1979-03-02	120	100	120	14
DWR	WCR0059456	NA	142004	Water Supply Domestic	38.05097	-121.40647	Centroid of Section	NA	NA	02N	05E	3	NA	1976-04-14	74	69	74	0
DWR	WCR0212947	NA	E0079934	NA	38.07976	-121.3799	Centroid of Section	NA	NA	03N	05E	25	NA	NA	0	0	0	0
DWR	WCR2020-008586	NA	NA	Remediation	38.0550763	-121.4583678	Unknown	NA	NA	02N	05E	6	NA	2020-06-19	30	0	0	14
DWR	WCR2017-009657	NA	E0370046	Monitoring	38.043611	-121.418333	Unknown	NA	NA	02N	05E	9	6605052	2017-09-21	20	4	19	0
DWR	WCR2014-015527	NA	805276	Water Supply Domestic	38.076111	-121.404722	Unknown	NA	NA	03N	05E	26	NA	NA	130	64	34	0
DWR	WCR2020-008438	T0607700310-MW11	NA	Monitoring	38.0553084	-121.4579978	Unknown	38.0553084	-121.4579978	02N	05E	6	NA	2020-06-16	52	0	0	0
DWR	WCR2020-008568	T0607700310-MW7	NA	Monitoring	38.0551168	-121.4583378	Unknown	38.0551168	-121.4583378	02N	05E	6	NA	2020-06-17	30	0	0	0
DWR	WCR2020-008435	T0607700310-MW8	NA	Monitoring	38.0553161	-121.4576997	Unknown	38.0553161	-121.4576997	02N	05E	6	NA	2020-06-15	15	0	0	0
DWR	WCR0300302	NA	NA	NA	38.06604	-121.45555	Centroid of Section	NA	NA	03N	05E	32	NA	NA	0	0	0	0
GAMA	AGW080017565-120	NA	NA	DOMESTIC	NA	NA	NA	38.0785103	-121.434455	03N	05E	28	NA	NA	NA	NA	NA	NA
GAMA	AGW080018293-KING	NA	NA	DOMESTIC	NA	NA	NA	38.069911	-121.4321661	03N	05E	33	NA	NA	NA	NA	NA	NA
GAMA	CA3901114_001_001	NA	NA	MUNICIPAL	NA	NA	NA	38.056709	-121.455957	02N	05E	5	NA	NA	NA	0	0	NA
GAMA	CA3901130_001_001	NA	NA	MUNICIPAL	NA	NA	NA	38.05	-121.44	02N	05E	4	NA	NA	NA	NA	NA	NA
GAMA	CA3400433_003_003	NA	NA	MUNICIPAL	NA	NA	NA	38.043067	-121.451046	02N	05E	8	NA	NA	NA	NA	NA	NA
GAMA	CA3900637_002_002	NA	NA	MUNICIPAL	NA	NA	NA	38.054694	-121.457667	02N	05E	5	NA	NA	NA	0	0	NA
GAMA	CA3900701_001_001	NA	NA	MUNICIPAL	NA	NA	NA	38.057889	-121.457694	02N	05E	5	NA	NA	NA	0	0	NA

Data Source	WCR Number	Wells from GAMA	Legacy Log Number	Planned Use or Former Use	LAT (DWR)	LONG (DWR)	LAT & LONG Accuracy (DWR)	LAT (GAMA)	LONG (GAMA)	T	R	S	APN	Date Work Ended	Total Completed Depth	Top Of Perforated Interval	Bottom of Perforated Interval	Static Water Level
GAMA	CA3900666_001_001	NA	NA	MUNICIPAL	NA	NA	NA	38.057888	-121.457694	02N	05E	5	NA	NA	NA	0	0	NA
GAMA	CA3901360_008_008	NA	NA	MUNICIPAL	NA	NA	NA	38.054716	-121.457736	02N	05E	5	NA	NA	NA	NA	NA	NA
GAMA	CA3900666_002_002	NA	NA	MUNICIPAL	NA	NA	NA	38.054694	-121.457666	02N	05E	5	NA	NA	NA	100	120	NA
GAMA	77694	NA	NA	IRRIGATION / INDUSTRIAL	NA	NA	NA	38.052983	-121.422609	03N	05E	4	NA	NA	NA	NA	NA	NA
GAMA	78503	NA	NA	DOMESTIC	NA	NA	NA	38.057077	-121.443917	03N	05E	5	NA	NA	NA	NA	NA	NA
GAMA	03N05E26Q001M	NA	NA	WATER SUPPLY, OTHER	NA	NA	NA	38.0711	-121.3924	03N	05E	35	NA	NA	NA	NA	NA	NA
GAMA	03N05E27P002M	NA	NA	WATER SUPPLY, OTHER	NA	NA	NA	38.0711	-121.4153	03N	05E	34	NA	NA	NA	NA	NA	NA
GAMA	03N05E26C008M	NA	NA	WATER SUPPLY, OTHER	NA	NA	NA	38.0819	-121.397	03N	05E	26	NA	NA	NA	NA	NA	NA
GAMA	02N05E05C001M	NA	NA	WATER SUPPLY, OTHER	NA	NA	NA	38.053	-121.4519	02N	05E	5	NA	NA	NA	NA	NA	NA
GAMA	03N05E26R001M	NA	NA	WATER SUPPLY, OTHER	NA	NA	NA	38.0711	-121.3878	03N	05E	36	NA	NA	NA	NA	NA	NA
GAMA	03N05E21L002M	NA	NA	WATER SUPPLY, OTHER	NA	NA	NA	38.0891	-121.4336	03N	05E	21	NA	NA	NA	NA	NA	NA
GAMA	03N05E26N001M	NA	NA	WATER SUPPLY, OTHER	NA	NA	NA	38.0711	-121.4016	03N	05E	35	NA	NA	NA	NA	NA	NA
GAMA	03N05E27P001M	NA	NA	WATER SUPPLY, OTHER	NA	NA	NA	38.0711	-121.4153	03N	05E	34	NA	NA	NA	NA	NA	NA
GAMA	03N05E23N002M	NA	NA	WATER SUPPLY, OTHER	NA	NA	NA	38.0855	-121.4016	03N	05E	26	NA	NA	NA	NA	NA	NA
GAMA	03N05E26K003M	NA	NA	WATER SUPPLY, OTHER	NA	NA	NA	38.0747	-121.3924	03N	05E	26	NA	NA	NA	NA	NA	NA
GAMA	03N05E29P001M	NA	NA	WATER SUPPLY, OTHER	NA	NA	NA	38.0711	-121.4519	03N	05E	32	NA	NA	NA	NA	NA	NA
GAMA	03N05E32N003M	NA	NA	WATER SUPPLY, OTHER	NA	NA	NA	38.0566	-121.4565	02N	05E	5	NA	NA	NA	NA	NA	NA
GAMA	03N05E25N002M	NA	NA	WATER SUPPLY, OTHER	NA	NA	NA	38.0711	-121.3833	03N	05E	36	NA	NA	NA	NA	NA	NA
GAMA	03N05E32N001M	NA	NA	WATER SUPPLY, OTHER	NA	NA	NA	38.0566	-121.4565	02N	05E	5	NA	NA	NA	NA	NA	NA
GAMA	03N05E36D002M	NA	NA	WATER SUPPLY, OTHER	NA	NA	NA	38.0674	-121.3833	03N	05E	36	NA	NA	NA	NA	NA	NA
GAMA	03N05E24P001M	NA	NA	WATER SUPPLY, OTHER	NA	NA	NA	38.0855	-121.3787	03N	05E	25	NA	NA	NA	NA	NA	NA
GAMA	03N05E26H003M	NA	NA	WATER SUPPLY, OTHER	NA	NA	NA	38.0783	-121.3878	03N	05E	25	NA	NA	NA	NA	NA	NA
GAMA	03N05E27G001M	NA	NA	WATER SUPPLY, OTHER	NA	NA	NA	38.0783	-121.4107	03N	05E	27	NA	NA	NA	NA	NA	NA
GAMA	03N05E29L001M	NA	NA	WATER SUPPLY, OTHER	NA	NA	NA	38.0747	-121.4519	03N	05E	29	NA	NA	NA	NA	NA	NA
GAMA	03N05E23D002M	NA	NA	WATER SUPPLY, OTHER	NA	NA	NA	38.0963	-121.4016	03N	05E	23	NA	NA	NA	NA	NA	NA
GAMA	03N05E36D001M	NA	NA	WATER SUPPLY, OTHER	NA	NA	NA	38.0674	-121.3833	03N	05E	36	NA	NA	NA	NA	NA	NA
GAMA	03N05E26R006M	NA	NA	WATER SUPPLY, OTHER	NA	NA	NA	38.0711	-121.3878	03N	05E	36	NA	NA	NA	NA	NA	NA
GAMA	03N05E27K001M	NA	NA	WATER SUPPLY, OTHER	NA	NA	NA	38.0747	-121.4107	03N	05E	27	NA	NA	NA	NA	NA	NA
GAMA	03N05E23D001M	NA	NA	WATER SUPPLY, OTHER	NA	NA	NA	38.0963	-121.4016	03N	05E	23	NA	NA	NA	NA	NA	NA
GAMA	03N05E27N001M	NA	NA	WATER SUPPLY, OTHER	NA	NA	NA	38.0711	-121.4199	03N	05E	34	NA	NA	NA	NA	NA	NA
GAMA	03N05E32N002M	NA	NA	WATER SUPPLY, OTHER	NA	NA	NA	38.0566	-121.4565	02N	05E	5	NA	NA	NA	NA	NA	NA
GAMA	03N05E23E002M	NA	NA	WATER SUPPLY, OTHER	NA	NA	NA	38.0927	-121.4016	03N	05E	23	NA	NA	NA	NA	NA	NA
GAMA	03N05E34L001M	NA	NA	WATER SUPPLY, OTHER	NA	NA	NA	38.0602	-121.4153	03N	05E	34	NA	NA	NA	NA	NA	NA
GAMA	03N05E26A002M	NA	NA	WATER SUPPLY, OTHER	NA	NA	NA	38.0819	-121.3878	03N	05E	25	NA	NA	NA	NA	NA	NA
GAMA	03N05E32M001M	NA	NA	WATER SUPPLY, OTHER	NA	NA	NA	38.0602	-121.4565	03N	05E	32	NA	NA	NA	NA	NA	NA
GAMA	03N05E23P002M	NA	NA	WATER SUPPLY, OTHER	NA	NA	NA	38.0855	-121.397	03N	05E	26	NA	NA	NA	NA	NA	NA
GAMA	03N05E33P001M	NA	NA	WATER SUPPLY, OTHER	NA	NA	NA	38.0566	-121.4336	02N	05E	4	NA	NA	NA	NA	NA	NA
GAMA	03N05E23L001M	NA	NA	WATER SUPPLY, OTHER	NA	NA	NA	38.0891	-121.397	03N	05E	23	NA	NA	NA	NA	NA	NA

Data Source	WCR Number	Wells from GAMA	Legacy Log Number	Planned Use or Former Use	LAT (DWR)	LONG (DWR)	LAT & LONG Accuracy (DWR)	LAT (GAMA)	LONG (GAMA)	T	R	S	APN	Date Work Ended	Total Completed Depth	Top Of Perforated Interval	Bottom of Perforated Interval	Static Water Level
GAMA	03N05E26K001M	NA	NA	WATER SUPPLY, OTHER	NA	NA	NA	38.0747	-121.3924	03N	05E	26	NA	NA	NA	NA	NA	NA
GAMA	T0607700310-MW2	NA	NA	MONITORING	NA	NA	NA	38.0549096	-121.4579195	02N	05E	5	NA	NA	NA	NA	NA	NA
GAMA	T0607700310-MW3	NA	NA	MONITORING	NA	NA	NA	38.0548721	-121.4581611	02N	05E	5	NA	NA	15.94	NA	NA	NA
GAMA	T0607700310-MW14	NA	NA	MONITORING	NA	NA	NA	38.0548048	-121.457778	02N	05E	5	NA	NA	120	NA	NA	NA
GAMA	T10000007741-MWP-10	NA	NA	MONITORING	NA	NA	NA	38.0446683	-121.417976	02N	05E	3	NA	NA	NA	7	17	NA
GAMA	T0607700310-MW10	NA	NA	MONITORING	NA	NA	NA	38.0553485	-121.4583184	02N	05E	5	NA	NA	27.5	NA	NA	NA
GAMA	T0607700310-MW5	NA	NA	MONITORING	NA	NA	NA	38.055005	-121.458172	02N	05E	5	NA	NA	15.8	NA	NA	NA
GAMA	T10000007741-MWP-4	NA	NA	MONITORING	NA	NA	NA	38.0440744	-121.418667	02N	05E	3	NA	NA	NA	9	19	NA
GAMA	T0607700310-MW11	NA	NA	MONITORING	NA	NA	NA	38.0553084	-121.4579978	02N	05E	5	NA	NA	51.21	NA	NA	NA
GAMA	T0607700310-MW13	NA	NA	MONITORING	NA	NA	NA	38.055104	-121.4583557	02N	05E	5	NA	NA	60.77	NA	NA	NA
GAMA	T0607700310-MW6	NA	NA	MONITORING	NA	NA	NA	38.0552898	-121.4579866	02N	05E	5	NA	NA	17.47	NA	NA	NA
GAMA	T10000007741-MWP-11	NA	NA	MONITORING	NA	NA	NA	38.0446808	-121.418507	02N	05E	3	NA	NA	NA	10	20	NA
GAMA	T10000007741-MWP-3	NA	NA	MONITORING	NA	NA	NA	38.0441066	-121.4182196	02N	05E	3	NA	NA	NA	9	19	NA
GAMA	T10000007741-MWP-6	NA	NA	MONITORING	NA	NA	NA	38.0438994	-121.4180116	02N	05E	3	NA	NA	NA	9	19	NA
GAMA	T0607700310-AFW	NA	NA	MONITORING	NA	NA	NA	38.0547139	-121.4576818	02N	05E	5	NA	NA	NA	NA	NA	NA
GAMA	T0607700310-MW1	NA	NA	MONITORING	NA	NA	NA	38.0551148	-121.45775	02N	05E	5	NA	NA	17.71	NA	NA	NA
GAMA	T0607700310-MW12	NA	NA	MONITORING	NA	NA	NA	38.0549016	-121.4580016	02N	05E	5	NA	NA	51.89	NA	NA	NA
GAMA	T0607700310-MW4R	NA	NA	MONITORING	NA	NA	NA	38.0551426	-121.4580451	02N	05E	5	NA	NA	17.45	NA	NA	NA
GAMA	T0607700310-MW7	NA	NA	MONITORING	NA	NA	NA	38.0551168	-121.4583378	02N	05E	5	NA	NA	29.94	NA	NA	NA
GAMA	T0607700310-MW8	NA	NA	MONITORING	NA	NA	NA	38.0553161	-121.4576997	02N	05E	5	NA	NA	15.18	NA	NA	NA
GAMA	T10000007741-MWP-1	NA	NA	MONITORING	NA	NA	NA	38.0444857	-121.4184426	02N	05E	3	NA	NA	NA	9	19	NA
GAMA	T10000007741-MWP-2	NA	NA	MONITORING	NA	NA	NA	38.0445234	-121.4175421	02N	05E	3	NA	NA	NA	9	19	NA
GAMA	T10000007741-MWP-5	NA	NA	MONITORING	NA	NA	NA	38.0440036	-121.4179185	02N	05E	3	NA	NA	NA	9	19	NA
GAMA	T10000007741-MWP-9	NA	NA	MONITORING	NA	NA	NA	38.0438859	-121.418385	02N	05E	3	NA	NA	NA	9	19	NA
GAMA	T0607700310-MW9	NA	NA	MONITORING	NA	NA	NA	38.0555918	-121.458189	02N	05E	5	NA	NA	20.2	NA	NA	NA
GAMA	T10000007741-MWP-8	NA	NA	MONITORING	NA	NA	NA	38.0442643	-121.4183843	02N	05E	3	NA	NA	NA	9	19	NA
GAMA	380518121230201	NA	NA	WATER SUPPLY, OTHER	NA	NA	NA	38.0883333	-121.384111	03N	05E	24	NA	NA	NA	NA	NA	NA
GAMA	380336121273501	NA	NA	WATER SUPPLY, OTHER	NA	NA	NA	38.0599207	-121.4607843	03N	05E	32	NA	NA	42	NA	NA	NA
GAMA	380517121225801	NA	NA	WATER SUPPLY, OTHER	NA	NA	NA	38.0879756	-121.3838384	03N	05E	24	NA	NA	142	NA	NA	NA

All depths are based on feet below ground surface
WCR= Department of Water Resources Well Completion Report
LAT= Latitide
LONG= Longitude
T= Township
R= Range
S= Section
APN= Assessor Parcel Number
NA= Data not available or not applicable

GAMA= State Water Board's GAMA website
WCR2020-008437 Well is included in both the GAMMA and DWR database

Table 2.10-1. Approximate Capay Shale thickness at injection well locations

Injection Well	Approximate Capay Shale Thickness (feet)
KI-I-M1	455
KI-I-M2	1,285
KI-I-M3	625
KI-I-S1	350
KI-I-S2	955
KI-I-S3	540

Table 7.2-1. Injectate compositions

Component	Injectate 1 (Mass %)	Injectate 2 (Mass %)
CO_2	99.21%	99.88%
H_2	0.05%	0.01%
N_2	0.64%	0.00%
H_2O	0.02%	0.00%
CO	0.03%	0.00%
Ar	0.03%	0.00%
O_2	0.00%	0.00%
SO_2+SO_3	0.00%	0.00%
H_2S	0.00%	0.01%
CH_4	0.00%	0.04%
NOx	0.00%	0.00%
NH_3	0.00%	0.00%
C_2H_6	0.00%	0.05%
Ethylene	0.00%	0.00%
Total	100.00%	100.00%

Table 7.2-2. Simplified four component composition for Injectate 1 and Injectate 2

Injectate 1	
Component	Mass %
CO_2	99.213%
N_2	0.643%
SO_2+SO_3	0.003%
H_2S	0.001%

Injectate 2	
Component	Mass %
CO_2	99.884%
CH_4	0.039%
C_2H_6	0.053%
H_2S	0.014%

Table 7.2-3. Injectate properties range over project life at downhole conditions for Injectate 1 and Injectate 2

Injectate property at downhole conditions	Injectate 1	Injectate 2
Viscosity, cp	0.022 – 0.054	0.022 – 0.056
Density, lb/ft^3	9.1 - 40.6	9.1 – 41.5
Compressibility factor, Z	0.81 - 0.67	0.80 – 0.66